



Dipl.-Ing. Bianca Grabner BSc.

Novel Concepts of Heterogeneous (Bio-)Catalysis for the Synthesis of Active Pharmaceutical Ingredients

DISSERTATION

to achieve the university degree of
Doktorin der technischen Wissenschaften

submitted to

Graz University of Technology

Supervisor

Assoc.Prof. Dipl.-Ing. Dr. techn. Heidrun Gruber-Wölfler
Institute of Process and Particle Engineering

Graz, January 2020

AFFIDAVIT

I declare that I have authored this thesis independently, that I have not used other than the declared sources/recourses, and that I have explicitly indicated all material which has been quoted either literally or by content from the sources used. The text document uploaded to TUGRAZonline is identical to the present dissertation.

Date

Signature

Liebe vergeht, Paper besteht.

Prof. Khinast, IPPT Weihnachtsfeier 2018

Für alle Menschen, die ich liebe!

Danksagung

Zu Beginn möchte ich mich bei den Menschen bedanken, die mich in den letzten vier bzw. fast zehn Jahren durch mein Studium und mein Leben begleitet haben.

Ein großes Dankeschön geht an meine Betreuer Prof. Johannes Khinast und Assoc.Prof. Heidrun Gruber-Wölfli, für die einmalige Möglichkeit meine Dissertation am Institut für Prozess- und Partikeltechnik zu verfassen. Die Jahre hier waren äußerst lehrreich und ich bin euch sehr dankbar, dass ich mich hier entfalten und entwickeln durfte.

Ganz herzlicher Dank geht an den Rest der Institutsmitarbeiter, sowohl an jene, die schon vor mir den Schritt aus der Uni-Blase getan haben, als auch an jene, die noch etwas länger bleiben. Liebsten Dank an Adela, Michaela und Silvie für die offenen Ohren, wenn ich euch mein Herz ausgeschüttet habe und für die lustigen Mittagspausen und Ausflüge. Vielen Dank auch für die tolle Unterstützung, wenn es was zu organisieren gab.

Liebe CoSy Bros, es war mir eine große Freude mit euch im Team zu arbeiten. Ich freue mich, dass ich dabei sein durfte, als diese Arbeitsgruppe gewachsen und zu einer kleinen Familie geworden ist. Danke Katharina, Manuel, Peter und vor allem Christoph für die fachliche und persönliche Zusammenarbeit.

Ein ganz herzliches Dankeschön geht auch an meine DiplomandInnen Katja, Kristian, Markus und Peter. Ohne euch wäre der Output nach vier Jahren Laborarbeit wohl etwas geringer ausgefallen. Vielen Dank für eure Unterstützung. Daneben möchte ich mich auch bei allen anderen StudentInnen der Arbeitsgruppe bedanken. Es war immer ein riesen Spaß mit euch.

Vielen liebsten Dank an meine best-of-CPE Studienkollegen Martin und Ioannis, sowie meine BORG-Mädels und meine exzellenten Freunde im Circle, allen voran dem Vorstand 2019. Ihr seid alle miteinander wunderbare Menschen, Raritäten möchte ich fast sagen. Ich will keinen von euch missen.

Überaus dankbar bin ich meinem Allerliebsten Albin dafür, dass er mich auch als Studentin genommen hat. Danke, dass du in diesen Jahren immer unterstützend hinter mir gestanden bist und mir all die Zeit und den Raum gegeben hast, den ich gebraucht habe. Ich schätze deine Freundschaft, deine Liebe und deine großartige Persönlichkeit!

Ganz lieb bedanken möchte ich mich auch bei meiner ganzen Familie, insbesondere bei meiner wundervollen Mama, aber natürlich auch bei Erwin, meinen Geschwistern, Schwiegereltern und SchwägerInnen.

Ihr alle zeigt mir immer wieder, worauf es im Leben wirklich ankommt, nämlich doch nicht auf das Paper.

Abstract

Process intensification, continuous flow synthesis and green chemistry come to the scientist's mind, when she/he is asked for sustainable industrial processes in a time where environmental protection and emission reduction are more demanded than ever before. Besides optimizing established processes, the emergence of novel concepts in process development is crucial, as these can be the wrecking ball for the wall representing the limits of conventional chemistry. In this work, three novel approaches for chemical and pharmaceutical synthesis are presented.

The first chapter shows the application of enzymes (ω -transaminases) in conventional organic solvents. Co-lyophilization of the biocatalyst with RTSPIL (room-temperature solid phase ionic liquid) increased the long term stability of enzyme and cofactor as well as the enzymes activity up to a factor of eight in comparison to the non-coated system (no RTSPIL included in catalyst preparation). In addition, the co-lyophilized enzyme showed excellent recyclability and was stable for 27 days.

Secondly, a flow process for the continuous synthesis of a statin side chain precursor was developed by a DoE (Design of Experiments) approach. Starting off with the identification of the ideal reaction conditions regarding temperature and pH value, at 32.5 °C and a pH of 7.5 DERA (deoxyribose-5-phosphate aldolase) mutant C47M showed the highest activity and long term stability. Additionally, an immobilization of the biocatalyst in alginate-luffa matrix (ALM) turned out to be a fast, inexpensive and ecological method to prepare the enzyme for its application in continuous flow. Lastly, the flow process was optimized to a flow rate of 0.1 mL min⁻¹ and a substrate concentration of 0.25 M for chloroacetaldehyde. The final process was operated stably for 4 h without any loss of activity and could produce up to 4.5 g of product per day.

The third chapter discusses the combination of biocatalysis (*Bs*PAD catalyzed decarboxylation) with metal catalysis (Pd-catalyzed Heck coupling using a Pd-substituted Ce-Sn-Oxide) in an integrated two-step flow process. Utilization of a deep eutectic solvent (DES) proofed to be a solution to overcome the obstacle of solvent compatibility of these two particularly difference reactions. DES also turned out to be crucial for the solubility of the substrate (*p*-coumaric acid), which could be increased to more than 5-fold by switching from neat buffer to a DES-buffer mixture. The final continuous flow process ran stable for more than 16 h and could produce more than 4.8 g L⁻¹ h⁻¹ of decarboxylation product (4-vinylphenol) and 0.52 g L⁻¹ h⁻¹ of the Heck coupling product (4-hydroxystilbene) in a benchtop reactor.

All these concepts prove that it requires curiosity, creativity and the courage to think outside the box, in order to lay foundation stones for potentially novel processes in an age where it seems that everything has already been invented.

Kurzfassung

Prozessintensivierung, kontinuierliche Synthese und grüne Chemie sind die Schlagwörter, die einer Wissenschaftlerin / einem Wissenschaftler in den Sinn kommen, wenn von nachhaltigen industriellen Prozessen die Rede ist. In einer Zeit, in der Umweltschutz und die Reduktion von Emissionen gefragter ist, als je zuvor, ist neben der Optimierung von etablierten Prozessen, die Erarbeitung neuer Konzepte in der Prozessentwicklung entscheidend, da diese Ansätze, jene sein könnten, die die Grenzen der konventionellen Chemie sprengen. In dieser Arbeit werden drei alternative Ansätze für die chemische und pharmazeutische Chemie präsentiert.

Im ersten Kapitel wird die Anwendung von Enzymen (ω -Transaminasen) in konventionellen organischen Lösungsmittel behandelt. Der Biokatalysator wurde durch Co-Lyophilisation mit einer ionischen Flüssigkeit mit Schmelzpunkt über Raumtemperatur (room-temperature solid phase ionic liquid, RTSPIL) stabilisiert. Diese Präparation des Enzyms führte zu einer Erhöhung der Aktivität um den Faktor acht, verglichen mit dem freien Enzym. (keine ionische Flüssigkeit im Herstellungsprozess). Zusätzlich war das präparierte Enzym über 27 Tage stabil und besaß ausgezeichnete Rezyklierbarkeit.

Als zweites wird ein Prozess für die kontinuierliche Synthese einer Vorstufe der Seitenkette von Statinen beschrieben, welcher mit Hilfe von statistische Versuchsplanung (Design of Experiments, DoE) optimiert wurde. Im ersten Schritt konnten eine Temperatur von 32,5 °C und ein pH-Wert von 7.5 als jene Prozessbedingungen identifiziert werden, bei denen der DERA (deoxyribose-5-phosphate aldolase) Mutant C47M die höchste Aktivität und Langzeitstabilität zeigte. Anschließend erfolgte mittels Alginat-Luffa Matrix (ALM) eine schnelle, günstige und ökologische Immobilisierung des Enzyms, um es im kontinuierlichen Durchflussreaktor einzusetzen. Zuletzt, wurde der kontinuierliche Prozess optimiert und eine Flussgeschwindigkeit von 0,1 mL min⁻¹ und einer Substratkonzentration von 0,25 M für Chloroacetaldehyd als ideal identifiziert. Der entwickelte Prozess konnte für 4 h ohne Aktivitätsverluste stabil betrieben werden und könnte pro Tag bis zu 4,5 g Produkt herstellen.

Das dritte Kapitel diskutiert die Kombination von Biokatalyse (BsPAD-katalysierte Decarboxylierung) mit Metallkatalyse (Pd-katalysierte Heck Kupplung mittels Pd-substituiertem Ce-Sn-Oxid) in einem zweistufigen kontinuierlichen Prozess. Die Nutzung von stark eutektischen Lösungsmittel (deep eutectic solvents, DES) war entscheidend für die Kompatibilität des Lösungsmittels mit beiden doch sehr unterschiedlichen Reaktionen. Das Substrat (*p*-Coumarsäure) zeigte zudem eine 5-fach erhöhte Löslichkeit im der verwendeten DES-Puffer Mischung, verglichen mit reinem Puffer. Der finale kontinuierliche Prozess lief stabil für über 16 h mit einer Produktivität von 4,8 g L⁻¹ h⁻¹ für die Decarboxylierung

(4-Vinylphenol) und $0,52 \text{ g L}^{-1} \text{ h}^{-1}$ für die Heck Kupplung (4-Hydroxystilben) in einem Benchtop-Reaktor.

Die vorgestellten Konzepte zeigen, dass mit Neugierde, Kreativität und Mut über den Tellerrand hinauszublicken, der Grundstein für mögliche neue Prozesse gelegt werden kann; auch in einer Zeit, in der es scheinbar schon alle gibt.

Table of Contents

A. Introduction	9
1 Biocatalysis	10
2 Continuous manufacturing	12
3 Heterogeneous catalysis	14
4 Chemo-enzymatic tandem-reactions in flow	15
5 References	17
B. Room-Temperature Solid Phase Ionic Liquid (RTSPIL) Coated ω -Transaminases: Development and Application in Organic Solvents*	20
1 Introduction.....	21
2 Results	22
3 Conclusion.....	32
4 Experimental	32
5 References.....	36
C. DERA in flow: Synthesis of a statin side chain precursor in continuous flow employing DERA immobilized in alginate-luffa matrix*.....	39
1 Introduction.....	40
2 Results	42
3 Conclusion.....	51
4 Experimental	51
5 References.....	54
6 Appendix.....	56
D. A chemo-enzymatic tandem reaction in a mixture of deep eutectic solvent and water in continuous flow*	70
1 Introduction.....	71
2 Results	73
3 Conclusion.....	79
4 Experimental	79
5 References	88
E. Outlook.....	90

A. Introduction

Sustainability and environmental friendly products have never been a bigger topic than they are today. A global movement demand the switch to an emission neutral future. This trend also affects industries. Especially wasteful branches, such as pharmaceutical industry where often more than 100 kg of waste are generated during the production of 1 kg of product, are in demand for “greener” chemistry.^{1,2} Passion and creativity of scientists is required to rethink and redesign established processes.^{3,4} The 12 principles of green chemistry are a guide for chemists to help in the development of more sustainable synthetic routes. The 12 principles of green chemistry are:^{5,6}

1. **P** – Prevent wastes
2. **R** – Renewable materials
3. **O** – Omit derivatization
4. **D** – Degradable chemical products
5. **U** – Use safe synthetic methods
6. **C** – Catalytic reagents
7. **T** – Temperature, Pressure ambient
8. **I** – In-Process Monitoring
9. **V** – Very few auxiliary substances
10. **E** – E-factor, maximise feed in product
11. **L** – Low toxicity of chemical products
12. **Y** – Yes, it is safe

In addition to the 12 principles of green chemistry, Anastas and Zimmermann developed the 12 principles of green engineering:^{7,8}

1. **I** – Inherently non-hazardous and safe
2. **M** – Minimize material diversity
3. **P** – Prevention instead of treatment
4. **R** – Renewable material and energy inputs
5. **O** – Output-led design
6. **V** – Very simple
7. **E** – Efficient use of mass, energy, space & time
8. **M** – Meet the need
9. **E** – Easy to separate by design
10. **N** – Networks for exchange of local mass & energy
11. **T** – Test the life cycle of the design
12. **S** – Sustainable throughout product life cycle

One technology which includes a series of these principles is biocatalysis. Biocatalysis uses highly selective catalysts, which are usually prepared from a renewable feedstock (overexpression in microorganisms). In addition to that, biocatalysts are biodegradable and operate under moderate reaction conditions.⁹

1 Biocatalysis

Biocatalysis utilizes enzymes for the biotransformation of inexpensive substrates to valuable products in high purity.^{10,11} Almost all industries employ biocatalysis in their processes today, including fine chemical industry and pharmaceutical industry.¹² These branches benefit from the high selectivity of biocatalysts and mild reactions conditions, which spare potentially sensitive functional groups on the molecule prone to thermal or chemical alteration.^{13,14}

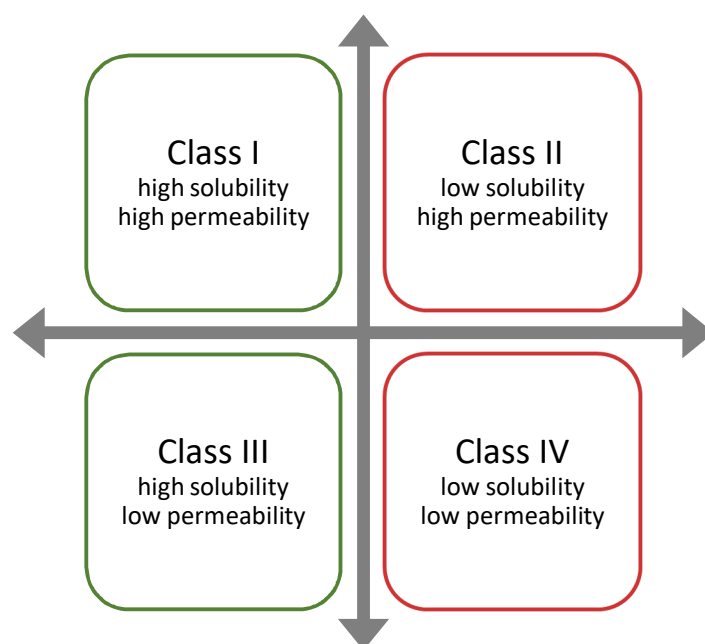
Biocatalysts are produced by overexpression in microorganisms and can either be utilized by employing the whole hosting cell (fresh or lyophilized) or by isolating the enzyme of interest by disrupting the cells membrane (cell free extract or chromatographically purified enzyme). Each of the mentioned methods has its advantages and drawbacks (Table A-1). Which mode is the most beneficial for a certain application needs to be evaluated individually for each process.

Table A-1. Comparison of general advantages and disadvantages of isolated enzymes and whole cell biocatalysis^{11,15}

Isolated enzyme		Whole cells	
Advantages	Disadvantages	Advantages	Disadvantages
<ul style="list-style-type: none"> Higher reactant specificity Better tolerance for co-solvents 	<ul style="list-style-type: none"> Not-suitable for multi-enzymatic reactions (complex) Less active than whole cells 	<ul style="list-style-type: none"> Simplicity of handling Minimal activity loss (cell membrane protection) Suitable for multi-enzymatic reactions 	<ul style="list-style-type: none"> Substrate/product inhibition Metabolic by-product formation Cell membrane is a mass transport barrier

One crucial factor in biocatalysis, whole cells or isolated enzymes, is the solubility of substrates in aqueous buffer systems.¹⁶ Most enzymes show their highest activity in an environment similar to their natural habitat where substrates are present in low concentrations in mild buffer systems.¹⁵ In contrast to this preference of biocatalysts, pharmaceutical industry is developing in the opposite direction. In order to make an enzymatic process economically feasible, high throughput and high concentrations are required.¹⁷ Molecular engineering enables the modification of wild-type (WT) enzymes to more resistant, more selective and more productive

mutants. Thanks to these directed mutations, enzymes can withstand high substrate concentrations in buffer systems.¹⁸ However, today, 40 % of all active pharmaceutical ingredients (APIs) possess solubility in the lower $\mu\text{g/mL}$ range in water.¹⁹ In general, APIs are classified in four categories in the biopharmaceutical classification system (BCS), of which Class II and Class IV include those of low solubility (Scheme A-1).^{20,21} Taking a look at the current product pipeline of pharmaceutical companies this trend towards low solubility is growing. In fact, about 90 % of pipeline drugs are poorly water soluble drugs.^{22,23}



Scheme A-1. Biopharmaceutical Classification System (BCS)

The utilization of biocatalysis for the synthesis of APIs belonging to Class II and Class IV of the BCS can be challenging. The necessity of large amounts of water and low space-time yields due to low substrate concentration make biocatalytic processes in conventional buffer systems economically and ecologically unfavourable.¹⁶ Alternative solvents, the application of novel immobilization methods and innovative process management are in demand in order to solve future challenges in fine chemical and pharmaceutical synthesis.

Alternative solvents in the field of biocatalysis are all non-aqueous systems, traditional organic solvents as well as green solvents. Traditional organic solvents have on the one hand the advantage of high solubility of substrates and low viscosity, which is beneficial for heat and mass transfer in the reaction mixture. On the other hand, most enzymes show low activity in organic solvents because they lack the necessary aqueous boundary layer on the enzyme surface.²⁴ Furthermore, these traditional solvents are volatile organic compounds (VOC) and should be avoided in terms of sustainability. An alternative to VOCs are so-called green solvents.

Green solvents became an innovative field in the past decades.²⁵ While the first generation of green solvents were supercritical fluids,^{26,27} ionic liquids (ILs) were the driving force for the second generation of green solvents and were also investigated for application in biocatalysis.^{28–31} The latest generation of alternative solvents are deep eutectic solvents (DESs).^{32–35} DESs compose of at least two components, which reach a eutectic point at a certain mixing ratio. At this eutectic point the melting point of the mixture is significantly lower in comparison to the individual components. The reduction in the melting point is caused by hydrogen bond interactions between the hydrogen bond donor (e.g. amine or alcohol group) and the acceptor (e.g. halide salts). DESs suffer from some similar drawbacks as ILs, e.g. high viscosity. However, these disadvantages are cancelled out by numerous advantages, such as non-flammability, biodegradability, low toxicity and simple preparation from inexpensive starting materials. Another positive aspect of DESs is their compatibility with enzymes.^{36–38} Furthermore, DESs are under investigation to serve as solvents for the application of drugs with low water solubility.³⁹

Green solvents are just one step of the evolution towards more sustainable and green chemistry. Continuous manufacturing is another option to develop a more environmentally friendly process.

2 Continuous manufacturing

Unit operations in synthesis and manufacturing processes can be classified into four modes, batch, semi-batch, semi-continuous, and continuous.⁴⁰

The advantages of continuous processes over batch include reduction of equipment and facility size, less energy consumption and easy automation, what leads to a smaller ecological footprint. Furthermore, the issue of batch-to-batch variation can be overcome with continuous manufacturing. In addition, the overall manufacturing time can be reduced and end-to-end manufacturing can minimize costs for storage and transportation.⁴⁰ The introduction of in-line monitoring together with feed-forward and feed-back control enables real-time release (RTR) in continuous manufacturing.⁴¹ An overview of general characteristics of batch and continuous operation are shown in Table A-2.

Although, continuous manufacturing brings along a series of advantages, batch processes are state of the art in pharmaceutical industry. High flexibility of batch plants, the low annual market demand for pharmaceuticals and high investment costs for the transformation of an established batch process to a continuous process are the main reasons for companies for sticking to well-established batch process.⁴²

Table A-2. General comparison of batch and continuous operation

Batch operation		Continuous operation	
Advantages	Disadvantages	Advantages	Disadvantages
<ul style="list-style-type: none"> • Simple and flexible equipment • Established in pharmaceutical industry 	<ul style="list-style-type: none"> • Labour intensive • High energy consumption • Difficult to scale up • Varying product quality • Difficult to automate 	<ul style="list-style-type: none"> • Constant product quality • Reduction of equipment/facility size • Low personal costs • Decrease of potential danger (hazardous reactions) • Smaller ecological footprint • Allows faster response to changes in demand • Scale-up is easier (numbering up) • Automation and inline-monitoring and control of product quality in real-time 	<ul style="list-style-type: none"> • Low flexibility in changing products • High financial investment • Interdependence of individual process steps

A lack of equipment, especially in downstream processes, and personnel with adequate knowledge as well as gaps of technology display obstacles for those companies that are willing to change their operation mode. Regulatory agencies support the intentions of these companies with the provision of guidelines and cooperation for re-approving the redesigned processes.⁴¹

Examples for continuous manufacturing in pharmaceutical industry are rare, but a small number of processes was developed and also approved by the Food and Drug Administration (FDA) or the European Medicines Agency (EMA). An overview of pharmaceutical products which are currently manufactured using continuous manufacturing are listed in Table A-3.

In order to run secondary manufacturing continuously, a continuous supply of API from the primary manufacturing is desirable. Industry and academics have switched their focus in research on continuous synthesis in order to be prepared for the shift towards continuous manufacturing. Guidelines and a long list of examples for the successful implementation of API synthesis in continuous flow are available.^{43–46}

For the application of (bio-)catalysts in continuous processes, heterogeneous catalysts can be of major advantage because the utilization of the catalyst in a packed-bed eliminates the step of catalyst removal from the product stream and enables long-term usage of expensive catalysts. In order to bring enzymes and other soluble catalysts, such as metal complexes, onto an additional solid support immobilization is required.

Table A-3. List of FDA approved products manufactured using continuous manufacturing

No.	Product Name	Indication	Company	Approval Year	Ref.
1	Orkambi (lumacaftor / ivacaftor)	Cystic fibrosis	Vertex Pharmaceutical	2015	47
2	Prezista (darunavir)	HIV-1 infection	Janssen Pharmaceuticals	2016	48
3	Verzenio (abemaciclib)	Breast cancer	Eli Lilly and Company	2018	49
4	Symdeko (tezacaftor/ivacaftor and ivacaftor)	Cyctic fibrosis	Vertex Pharmaceuticals	2018	50
5	Daurismo (glasdegib)	Acute myeloid leukemia	Pfizer	2018	50

3 Heterogeneous catalysis

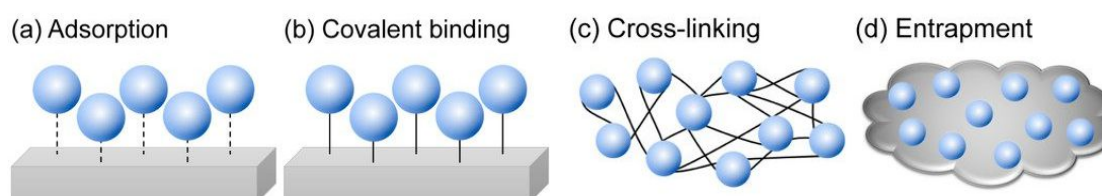
While batch processes in many cases utilize homogeneous catalysts, especially for the application in continuous flow synthesis, heterogeneous catalysts bring along a number of advantages. Benefits of heterogeneous catalysis include but are not limited to easy separation and recycling of the catalyst and increased stability.⁵¹ Table A-4 shows an overview of advantages and drawbacks of homogeneous and heterogeneous catalysis.

In general, immobilization techniques can be classified in 4 categories: covalent binding, adsorption, entrapment, and self-immobilization (Scheme A-2).⁵² Adsorption by Van-der-Waals forces, hydrogen bonds or electrostatic interaction binds the catalyst often insufficiently to the solid support, which can lead to catalyst leaching into the product stream. Covalent binding and cross-linking (self-immobilization) with covalent binding require modifications in the catalyst and can alter the structure and thus the performance of the catalyst. An advantage of this method is the strong binding of the catalyst preventing catalyst leaching. Entrapment, however, does not require additional bond formation on the catalyst. Furthermore, entrapment is a simple, fast and inexpensive method for catalyst immobilization.⁵³

Heterogeneous bulk catalysts, such as zeolites or metal oxides can directly be utilized in suspensions in stirred tanks or in a fixed-bed reactor.⁵⁴

Table A-4. General comparison of homogeneous and heterogeneous catalysis⁵⁵

Homogeneous catalysis	Heterogeneous catalysis
+ Well known reaction mechanisms	+ Easy separation and recycling
+ No influence of solid support	+ Prevention of leaching
+ No transport limitations	+ High stability
- Separation and recycling is demanding	+ Allow continuous flow processes
- Continuous processes only possible with post reaction zone	- Influence of solid support on reaction rate and selectivity
- Difficult handling	- Transport limitations
- Metal carry over/leaching	- Poor understanding of the non-uniform surface

**Scheme A-2:** Overview of 4 general immobilization techniques⁵⁶

4 Chemo-enzymatic tandem-reactions in flow

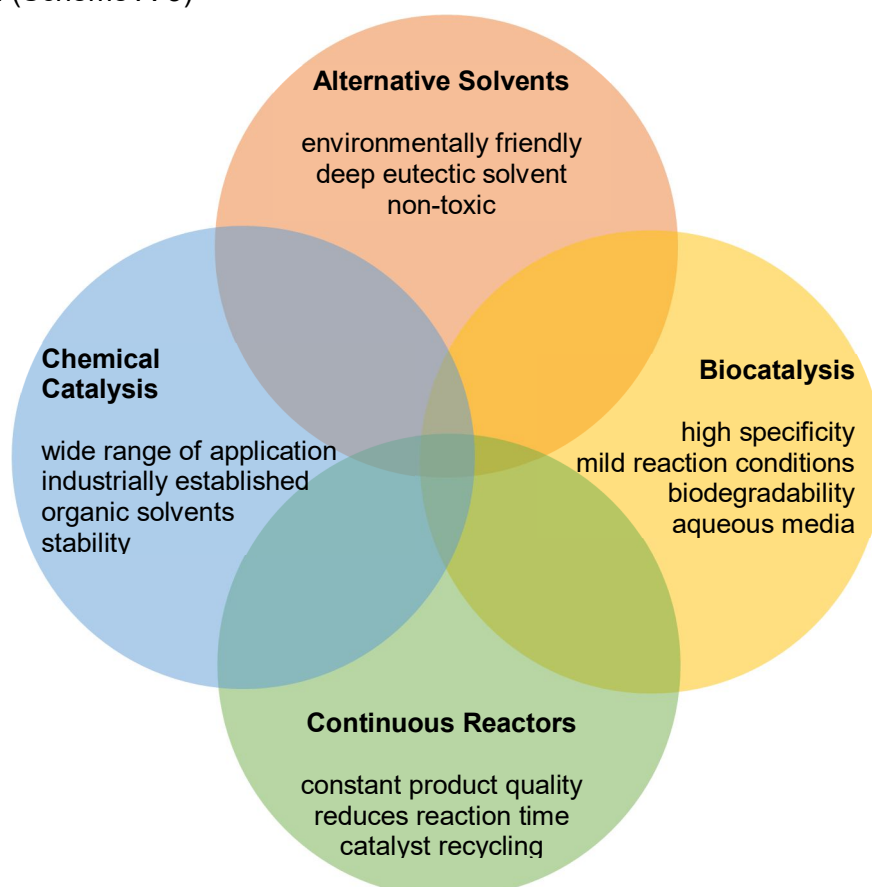
Biocatalysts convince by their high selectivity and mild reaction conditions. However, the saying “A herb grows for everything” is not true in this case. Chemical catalysis, including acid-base and metal-catalysis, covers a range of applications biocatalysis cannot reach. Each branch of catalysis has its benefits and drawbacks (Table A-5).

Table A-5. General comparison of biocatalysis and chemical catalysis

Biocatalysis	Chemical catalysis
• High selectivity	• Established in industry
• “Green”	• High stability towards organic solvents
• Biodegradable	• Broad range of application and reactions
• Renewable feedstock	• Complex and costly synthesis
• Often limited to natural substrates	• Often expensive
• Inhibited by high substrate concentration	
• Moderate reaction conditions	
• Long development and production times	
• Resource intense production	

The combination of bio- and chemical catalysis is for multiple reasons favourable.^{57,58} One major advantage is the elimination of the isolation of the often highly reactive intermediates.⁵⁹ Flow set-ups enable spatial separation of both steps and conduct each reaction at optimal reaction conditions. Challenges that occur with the combination of chemo-enzymatic tandem reactions include issues regarding solvent selection, which can be tackled by the utilization of alternative solvents.^{60,61} Catalyst or enzyme leaching from the first step can lead to catalyst poisoning and unreacted starting material or side products can inhibit the subsequent reaction.⁶² Overall, chemo-enzymatic tandem reaction benefit from their simple set-up and reduced financial and labour effort. A large number of leading examples for the successful application of enzymes and chemical catalysts in one reaction set-up was collected in literature over the past decades.^{63,64}

The aim of this thesis is the development and application of novel concepts for biocatalysis including the use of alternative solvents and the combination of enzymes with chemical catalysis with the overall goal of transforming batch processes into continuous flow applications. (Scheme A-3)



Scheme A-3. Synergy of biocatalysis and chemical catalysis via continuous reactors and alternative solvents

The concepts described in this thesis are still in their infancy, but each of them can be a first step on the path to alternative processes in API synthesis.

5 References

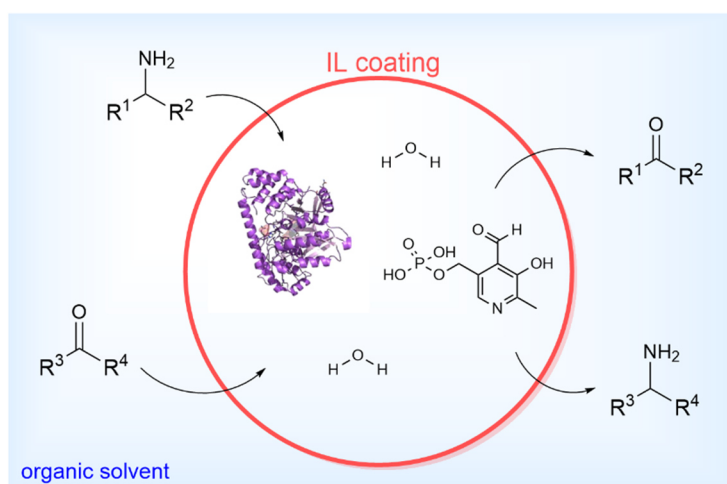
1. C. Jiménez-González, P. Poechlauer, Q. B. Broxterman, B.-S. Yang, D. Am Ende, J. Baird, C. Bertsch, R. E. Hannah, P. Dell'Orco, H. Noorman, S. Yee, R. Reintjens, A. Wells, V. Massonneau and J. Manley, *Org. Process Res. Dev.*, 2011, **15**(4), 900.
2. R. A. Sheldon, *Green Chem.*, 2017, **19**(1), 18.
3. R. A. Sheldon, *Green Chem.*, 2016, **18**(11), 3180.
4. R. S. Varma, *ACS Sustainable Chem. Eng.*, 2016, **4**(11), 5866.
5. S. L. Y. Tang, R. L. Smith and M. Poliakoff, *Green Chem.*, 2005, **7**(11), 761.
6. P. T. Anastas and J. C. Warner, *Green Chemistry: Theory and Practice*, Oxford University Press, 1998.
7. P. T. Anastas and J. B. Zimmermann, *Environ. Sci. Technol.*, 2003, **37**(94A).
8. S. Y. Tang, R. A. Bourne, R. L. Smith and M. Poliakoff, *Green Chem.*, 2008, **10**(3), 268.
9. R. A. Sheldon and J. M. Woodley, *Chem. Rev.*, 2018, **118**(2), 801.
10. G. Torrelo, U. Hanefeld and F. Hollmann, *Catal. Lett.*, 2015, **145**(1), 309.
11. P. Grunwald, *Biocatalysis - Biochemical Fundamentals and Application*, World Scientific Publishing Europe Ltd., New Jersey, 2018.
12. J.-M. Choi, S.-S. Han and H.-S. Kim, *Biotechnol. Adv.*, 2015, **33**(7), 1443.
13. R. N. Patel, *Bioorg. Med. Chem.*, 2018, **26**(7), 1252.
14. M. D. Truppo, *ACS Med. Chem. Lett.*, 2017, **8**(5), 476.
15. K. Faber, *Biotransformations in Organic Chemistry: A Textbook*, Springer, Heidelberg, 2011.
16. F. Hollmann and S. Kara, *Biospektrum*, 2014, **20**, 100.
17. G. W. Huisman and S. J. Collier, *Curr. Opin. Chem. Biol.*, 2013, **17**(2), 284.
18. U. T. Bornscheuer, G. W. Huisman, R. J. Kazlauskas, S. Lutz, J. C. Moore and K. Robins, *Nature*, 2012, **485**(7397), 185.
19. B. J. Boyd, C. A. S. Bergström, Z. Vinarov, M. Kuentz, J. Brouwers, P. Augustijns, M. Brandl, A. Bernkop-Schnürch, N. Shrestha, V. Préat, A. Müllertz, A. Bauer-Brandl and V. Jannin, *Eur. J. Pharm. Sci.*, 2019, **137**, 104967.
20. A. K. Nair, O. Anand, N. Chun, D. P. Conner, M. U. Mehta, D. T. Nhu, J. E. Polli, L. X. Yu and B. M. Davit, *AAPS J.*, 2012, **14**(4), 664.
21. PharmaQuestT. BCS, it's significance and application, available online: <http://pharmaquest.weebly.com/uploads/9/9/4/2/9942916/bcs.pdf> (last accessed September 2019).
22. S. Kalepu and V. Nekkanti, *Acta Pharm. Sin. B*, 2015, **5**(5), 442.
23. R. Lipp, *Am. Pharmac. Rev.*, 2013, **16**(3).
24. A. Goswami and J. D. Stewart, eds., *Organic Synthesis Using Biocatalysis: Biocatalysis in Organic Solvents, Supercritical Fluids and Ionic Liquids*, Elsevier, USA, 2016.
25. C. J. Clarke, W.-C. Tu, O. Levers, A. Bröhl and J. P. Hallett, *Chem. Rev.*, 2018, **118**(2), 747.
26. Ž. Knez, *J. Supercrit. Fluid.*, 2018, **134**, 133.
27. A. J. Mesiano, E. J. Beckman and A. J. Russell, *Chem. Rev.*, 1999, **99**(2), 623.
28. F. van Rantwijk and R. A. Sheldon, *Chem. Rev.*, 2007, **107**(6), 2757.
29. Kadokawa J., ed., *Ionic Liquids - New Aspects for the Future*, InTech, Croatia, 2013.
30. R. A. Sheldon, R. M. Lau, M. J. Sorgedragar, F. van Rantwijk and K. R. Seddon, *Green Chem.*, 2002, **4**(2), 147.
31. J. M. Sperl, J. M. Carsten, J.-K. Güterl, P. Lommès and V. Sieber, *ACS Catal.*, 2016, **6**(10), 6329.

32. D. A. Alonso, A. Baeza, R. Chinchilla, G. Guillena, I. M. Pastor and D. J. Ramón, *Eur. J. Org. Chem.*, 2016, **2016**(4), 612.
33. I. Wazeer, M. Hayyan and M. K. Hadj-Kali, *J. Chem. Technol. Biotechnol.*, 2018, **93**(4), 945.
34. Z. Maugeri and P. Domínguez de María, *ChemCatChem*, 2014, **6**(6), 1535.
35. M. Pätzold, S. Siebenhaller, S. Kara, A. Liese, C. Syldatk and D. Holtmann, *Trends Biotechnol.*, 2019, **37**(9), 943.
36. Z.-L. Huang, B.-P. Wu, Q. Wen, T.-X. Yang and Z. Yang, *J. Chem. Technol. Biotechnol.*, 2014, **89**(12), 1975.
37. P. Xu, G.-W. Zheng, M.-H. Zong, N. Li and W.-Y. Lou, *Bioresour. Bioprocess.*, 2017, **4**(1), 34.
38. A. K. Schweiger, N. Ríos-Lombardía, C. K. Winkler, S. Schmidt, F. Morís, W. Kroutil, J. González-Sabín and R. Kourist, *ACS Sustainable Chem. Eng.*, 2019, **7**(19), 16364.
39. S. N. Pedro, M. G. Freire, C. S. R. Freire and A. J. D. Silvestre, *Expert Opin. Drug Deliv.*, 2019, **16**(5), 497.
40. S. L. Lee, T. F. O'Connor, X. Yang, C. N. Cruz, S. Chatterjee, R. D. Madurawe, C. M. V. Moore, L. X. Yu and J. Woodcock, *J. Pharm. Innov.*, 2015, **10**(3), 191.
41. Food and Drug Administration, *Guidance for Industry PAT - A Framework for Innovative Pharmaceutical Development, manufacturing, and Quality Assurance*, 2004.
42. P. Poehlauer, J. Manley, R. Broxterman, B. Gregertsen and M. Ridemark, *Org. Process Res. Dev.*, 2012, **16**(10), 1586.
43. M. B. Plutschack, B. Pieber, K. Gilmore and P. H. Seeberger, *Chem. Rev.*, 2017, **117**(18), 11796.
44. S. A. May, *J. Flow Chem.*, 2017, **7**(3–4), 137.
45. R. Porta, M. Benaglia and A. Puglisi, *Org. Process Res. Dev.*, 2016, **20**(1), 2.
46. B. Gutmann, D. Cantillo and C. O. Kappe, *Angew. Chem. Int. Ed.*, 2015, **54**(23), 6688.
47. European Medical Agency, *Assesment Report - Orkambi*, United Kingdom, 2015.
48. PharmTech.com - Advancing Development and Manufacturing. FDA approves tablet production on Janssen continuous manufacturing line, available online: <http://www.pharmtech.com/fda-approves-tablet-production-janssen-continuous-manufacturing-line> (last accessed December 2019).
49. C. Badman, C. L. Cooney, A. Florence, K. Konstantinov, M. Krumme, S. Mascia, M. Nasr and B. L. Trout, *J. Pharm. Sci.*, 2019, **108**(11), 3521.
50. C. Hu, C. Testa, W. Wu, K. Shvedova, D. E. Shen, R. Sayin, B. Halkude, F. Casati, P. Hermant, A. Ramnath, S. Born, B. Takizawa, T. O'Connor, B. Yang, S. Ramanujam and S. Mascia, *Chem. Commun.*, 2019, accepted on 09 Dec.
51. J. Heveling, *J. Chem. Educ.*, 2012, **89**(12), 1530.
52. M. P. Thompson, I. Peñafiel, S. C. Cosgrove and N. J. Turner, *Org. Process Res. Dev.*, 2018, **23**(1), 9.
53. A. Dwevedi, ed., *Basics of Enzyme Immobilization. In: Enzyme Immobilization*, Springer, Cham, 2016.
54. J. Hagen, *Industrial catalysis: A practical approach*, Wiley-VCH, Weinheim, 2006.
55. P. K. Robinson, *Essays Biochem.*, 2015, **59**, 1.
56. C. Lee, S.-H. Jang and H.-S. Chung, *Catalysts*, 2017, **7**(12), 112.
57. H. Gröger and W. Hummel, *Curr. Opin. Chem. Biol.*, 2014, **19**, 171.
58. C. Simons, U. Hanefeld, I. W. C. E. Arends, T. Maschmeyer and R. A. Sheldon, *Top Catal*, 2006, **40**(1-4), 35.
59. Á. Gómez Baraibar, D. Reichert, C. Mügge, S. Seger, H. Gröger and R. Kourist, *Angew. Chem. Int. Ed.*, 2016, **55**(47), 14823.

60. L. Cicco, N. Ríos-Lombardía, M. J. Rodríguez-Álvarez, F. Morís, F. M. Perna, V. Capriati, J. García-Álvarez and J. González-Sabín, *Green Chem.*, 2018, **20**(15), 3468.
61. S. Schmidt, K. Castiglione and R. Kourist, *Chem. Eur. J.*, 2018, **24**(8), 1755.
62. G. J. Lichtenegger and H. Gruber-Woelfler, *Chimica Oggi*, 2015, **33**(4), 12.
63. J. Paris, N. Ríos-Lombardía, F. Morís, H. Gröger and J. González-Sabín, *ChemCatChem*, 2018, **10**(19), 4417.
64. J. Enoki, C. Mügge, D. Tischler, K. Miyamoto and R. Kourist, *Chemistry*, 2019, **25**(19), 5071.

B. Room-Temperature Solid Phase Ionic Liquid (RTSPIL) Coated ω -Transaminases: Development and Application in Organic Solvents*

ω -Transaminases ATA-40, ATA-47 and ATA-82P were coated with room-temperature solid phase ionic liquids (RTSPILs) by means of three methods, melt coating, precipitation coating, and co-lyophilization, and showed increased stability in all of the five tested organic solvents. Co-lyophilization and melt coating were further found to have an activating effect on the enzymes. The former led to an up to 8-fold increase of reaction rate and excellent recyclability. The coating also protected the cofactor pyridoxal 5'-phosphate (PLP), which is essential for transaminase activity, from degradation, leading to a reaction proceeding for 27 days. With this method the sparingly water soluble substrate 5-bromo-1-indenone could be processed enzymatically in cyclohexane as solvent.



*The following chapter is taken from the journal article by Grabner *et al.*, published in *Molecular Catalysis* (Grabner, B., Nazario, M. A., Gundersen, M. T., Lois, S., Fantini, S., Bartsch, S., Woodley, J. M., Gruber-Woelfler, H., (2018). "Room-temperature solid phase ionic liquid (RTSPIL) coated omega-transaminase: Development and application in organic solvents". *Molecular Catalysis*, 452, 11-19)

1 Introduction

Transaminases are highly potential enzymes to assist in the synthesis of molecules of interest to both the chemical and pharmaceutical industry.^{1–4} Their products, chiral amines, are of high value and possess a wide range of applications such as intermediates for fine chemicals and resolving agents for enantiomeric resolution.⁵ Since 40% of active pharmaceutical ingredients (APIs) are estimated to contain a chiral amine, enantiomerically pure amines take a remarkable position in pharmaceutical industry.^{6,7} An exemplary biocatalytic industrial process employing an ω -transaminase (EC 2.6.1.X) is the total synthesis of Sitagliptin, the API of Januvia®.⁸ Sitagliptin is according to the BCS (Biopharmaceutics Classifications System) a Class III (high solubility / low permeability) / borderline Class I compound used to treat Type 2 diabetes mellitus.⁹ In this case, the high water solubility of the compound makes a biocatalytic process in aqueous solution feasible.

However, not all APIs belong to this class. In fact, almost half of the drugs on the market contain a poorly water soluble API and 80-90% of pipeline drugs are poorly water soluble.^{10–12} Combining Class II (low solubility / high permeability) and Class IV (low solubility / low permeability) compounds with biocatalysts in aqueous systems is therefore challenging. Such systems are limited to low concentrations of hydrophobic substrate, generate large quantities of waste and make downstream processing (DSP) more difficult.¹³ In this case, the use of organic solvents as an alternative reaction media can make a process economically viable.¹⁴ On the other hand, enzymes often are inactivated by organic solvents, resulting in poor reaction rates, relative to those observed in aqueous media. To overcome this problem, various techniques for immobilization and stabilization of enzymes in organic solvents have been investigated in the past decade.^{15,16} One of the approaches includes the coating with ionic liquids (ILs). In 2002, Lee and Kim were the first to coat an enzyme with an ionic liquid.¹⁷ Applying RTSPIL (room-temperature solid phase ionic liquids) with a melting point slightly above room-temperature enabled the use of enzymes as a heterogeneous catalyst in a solid/liquid system. These ionic liquid-coated enzymes (ILCE) showed increased enantioselectivity. This technique for immobilizing enzymes in ionic liquids was investigated by various researchers in the past decade. Mostly lipases were coated with various ILs or pre-incubated in ILs prior the reaction, resulting in excellent enantioselectivity and increased reaction rate.^{18–30} Coating enzymes with RTSPIL is an excellent supplement to biocatalysis in RTIL (room-temperature ionic liquids) where the ILs are used as a solvent.^{31–41} In 2010, Lee and Kim, reported an alternative method to stabilize enzymes in organic solvents – ionic liquid co-lyophilized enzymes were found to be enantioselective and up to 660-fold

more active than their free counterpart.⁴² Since then, co-lyophilized enzymes (mostly lipases) with ILs have been investigated only by few researchers.^{43,44}

We present here a novel approach to coat Transaminases with ILs. To the best of our knowledge transaminases have so far not been tested in combination with IL coating, but were already applied in organic media and two-phase systems.^{3,14,45,46} This article will show the applicability of ionic liquid coating on cofactor dependent transaminase. The coated enzymes showed extended stability in various organic solvents, especially in cyclohexane. Enzyme coated by co-lyophilization additionally showed increased reaction rate compared to the free enzyme.

2 Results

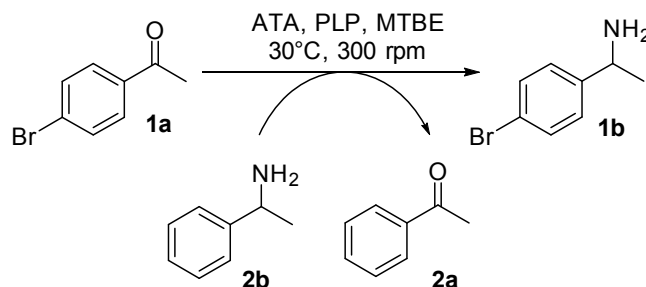
2.1 Preliminary studies

In preliminary studies two coating methods were tested and the activity of the coated and the free enzymes were compared using methyl-*t*-butyl-ether (MTBE) as organic solvent. After defining the requirements of ILs for coating enzymes that require water in their reaction mechanism, namely (i) a melting point above room and operation temperature, (ii) a melting point low enough to not inactivate the enzyme during the melt coating process, (iii) water miscibility or at least insensitivity to water, and (iv) insolubility in the used solvent, a list of potential ILs was compiled. Amongst others, 1-ethyl-3-methyl-imidazolium bromide [Emim]Br (EB) meets these requirements and was chosen for coating transaminase ATA-40 applying two different methods, melt coating and precipitation coating. The melt-coated enzyme was produced by heating the IL above its melting point and mixing the melt with the enzyme and cofactor. For the precipitation-coated enzyme, the IL was precipitated out of a concentrated aqueous solution of the IL, enzyme and cofactor.

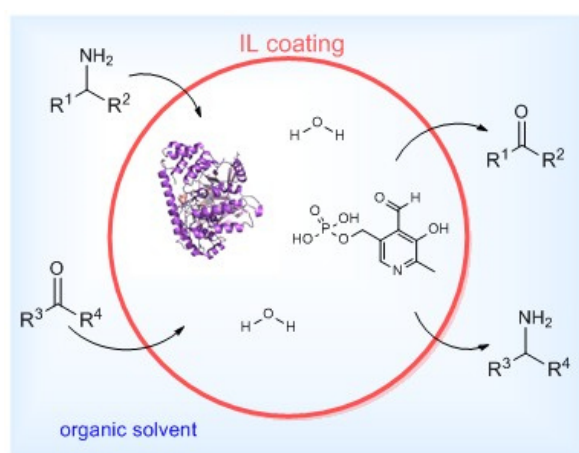
The two prepared solid phases were then used for the enzymatic reductive amination of 4'-bromoacetophenone **1a** with methylbenzylamine **2b** as amine donor forming the product 1-(4-bromophenyl)ethanamine **1b** and the co-product acetophenone **2a**. (Scheme B-1)

The reaction system is assumed to work as shown in Scheme B-2. The IL coating encloses the catalytic system consisting of the enzyme, PLP and water, protecting it from the organic solvent. The substrates dissolved in the organic phase need to pass the IL barrier in order to reach the active site and undergo a reaction. Afterwards, the formed products diffuse back into the organic solvent. As a reference, a reaction with soluble free enzyme was also carried out. Samples were taken over time and analyzed by means of GC. Because of its low volatility the

product could hardly be analyzed by means of GC. Therefore, the co-product (**2a**, acetophenone) concentration was observed over time. (Figure B-1)



Scheme B-1. Enzymatic amination of **1a** employing ATA-40 in MTBE using **2a** as donor resulting in product **1b** and co-product **2b**.



Scheme B-2. Scheme of the reaction system. Enzyme, PLP and water are enclosed in the IL coating. The substrates need to diffuse through the coating to reach the active site. The products diffuse back into the surrounding organic.

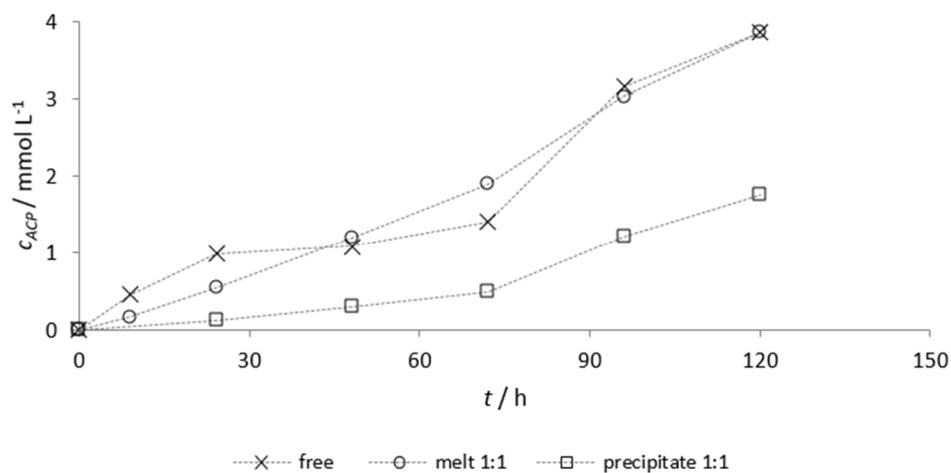


Figure B-1. Co-product concentration in the reaction system over time for free enzyme (X), melt coated enzyme (□) and precipitate coated enzyme (O). The amount of coating material was 1:1 (mass enzyme:mass coating material) for both melt and precipitation coated.

At the beginning of the reaction, the soluble free enzyme run fastest with an initial rate of $50.8 \mu\text{mol L}^{-1} \text{h}^{-1}$ (X in Figure B-1), but it slows down and finally stops after less than 30 h of reaction. Addition of further cofactor restarted the reaction for 50 h, but after 120 h the reaction rate decreased again and the reaction subsequently stopped. In contrast, coating the enzyme and the cofactor with IL melt (O in Figure B-1) stabilized the reaction over 120 h indicated by the constant slope (Figure B-1).

The reaction rate of the melt coated enzyme is with $18.2 \mu\text{mol L}^{-1} \text{h}^{-1}$ lower than that of the initial reaction rate of the soluble free enzyme. This might be due to the additional barrier the substrate needs to overcome to reach the active site of the enzyme or potentially due to reduced activity caused by the coating process itself. The behaviour of the precipitate coated enzyme (\square in Figure B-1) is almost the same as for the melt coated catalyst. The reaction rate of $4.9 \mu\text{mol L}^{-1} \text{h}^{-1}$ is approximately constant during the entire experiment. As with the melt-coated catalyst, the reaction proceeds over 120 h.

However, compared to the melt-coated enzyme, the reaction runs at a lower rate. This reduction in reaction rate was thought to be caused by the coating process and/or the added acetone for the precipitation. Therefore, acetonitrile was used as anti-solvent in the later experiments because residuals of acetone can participate in the reaction and act as amino acceptor. However, later experiments showed, that the coating method itself is less efficient, independent from the used anti-solvent. Another possibility for the loss of activity is the way enzyme and cofactor are immobilized on/in the IL crystals. If the cofactor is too far from the enzyme and cannot diffuse to the active site, less active enzyme-PLP complexes can form and less turnover per time unit can happen.

To find out how the coating thickness affects the reaction rate, enzymes were coated with various amounts of IL (1:1, 1:2, 1:5, and 1:10 in terms of enzyme mass).

Using 1:2 of IL for the melt-coating process decreases the reaction rate compared to the 1:1 coating. It is likely that this effect is due to a hindered mass transport through the coating. For all higher amounts of coating material almost no conversion was observed. Indeed, the coating may get too thick for the substrate to permeate.

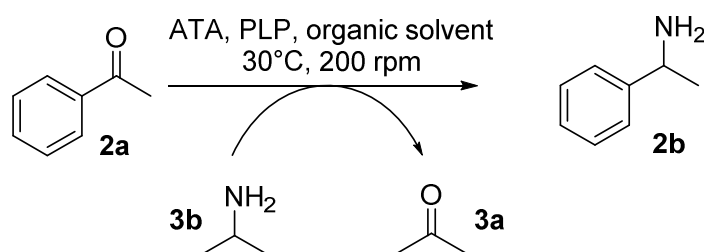
Coating the enzyme with double the amount of IL with the precipitation method hardly affects the initial reaction rate. However, thicker coatings (1:5 and 1:10) result in very low catalytic activity.

Interestingly, coating only the enzyme, by melt or precipitation coating, and adding the cofactor in solution with the substrate did not result in any reaction. This observation can either be caused by the inability of the cofactor to permeate through the coating or the low probability of a substrate and PLP molecule to permeate and bind to the enzyme simultaneously.

2.2 Solvent Stability

Starting from this point, and knowing about the stabilizing effect of the coating, we decided to investigate the method of coating enzymes with ILs more intensively drawing more attention to the stabilizing effect of different coating methods and the influence of the used organic solvent. In addition, two other enzymes, kindly provided by c-LEcta GmbH, and two ILs, contributed by Solvionic, were tested.

Two ILs, 1-allyl-3-methyl-imidazolium chloride [Amim]Cl (AC) and 1-ethyl-3-methyl-imidazolium bromide [Emim]Br (EB) were available as coating material. In the first step, five frequently used organic solvents were tested concerning their effect on the enzyme stability. Two solvents of low polarity (cyclohexane [chex] ($\log P = 3.44$) and toluene [tol] ($\log P = 2.73$)) were chosen because enzymes are generally more stable in solvents with high $\log P$. This observation was mostly made with lipases.¹⁹ However, we wanted to see whether the stability of the enzyme could be further increased by the IL coating. Furthermore, three solvents of higher polarity (ethyl acetate [EtOAc] ($\log P = 0.73$), diethyl ether [Et₂O] ($\log P = 0.83$) and MTBE ($\log P = 0.93$)) were chosen because solvents in this polarity range have already been used successfully as reaction media for ω -transaminases.^{14,46} Both enzymes tested, ATA-47 and ATA-82P, were coated by means of three different methods, melt coating, precipitation coating, and co-lyophilization using one mass equivalent of IL with regard to enzyme. For co-lyophilization all necessary components for the coating (enzyme, cofactor and IL) were dissolved in a suitable buffer and freeze-dried. The solid residue can be used as catalyst in a grinded form or without further treatment.⁴² A reference reaction employing free enzymes was run. Each enzyme was tested in five solvents cyclohexane, ethyl acetate, diethyl ether, MTBE, and toluene, all three coating methods and both ILs in a standard reaction system containing substrate **2a** and donor **3b** (Scheme B-3).



Scheme B-3. Standard reaction: ω -TA-catalysed formation of methylbenzylamine **2b** from acetophenone **2a** using iso-propyl amine **3b** as amino donor.

The analysis of the formed amine **2b** was done by means of RP-HPLC. The results of the screening are shown in Table B-1.

Table B-1. Yield of 2b after 10 days for all screening reactions

#	method	enzyme	IL	yield [%] in various solvents				
				chex	EtOAc	Et ₂ O	MTBE	tol
1	free	47	-	11.2	6.2	3.2	1.6	3.6
2		82P	-	7.6	4.6	4.0	2.4	3.8
3	free lyo	47	-	40.8	17.0	5.4	3.0	12.6
4		82P	-	26.2	8.6	5.4	5.6	7.2
5	L	47	AC	60.6	14.0	38.4	27.2	12.2
6			EB	77.6	22.6	35.4	18.2	18.8
7		82P	AC	43.2	14.8	24.4	20.0	14.2
8			EB	53.8	21.2	33.6	24.2	22.8
9	M	47	EB	35.8	7.2	11.2	16.0	12.8
10		82P	EB	29.6	16.4	14.2	19.4	12.2
11	P	47	AC	8.0	2.2	5.4	6.2	2.0
12			EB	18.8	3.0	3.2	6.0	4.4
13		82P	AC	2.0	1.8	4.2	1.8	4.4
14			EB	14.2	2.4	5.0	2.6	2.8

free = untreated enzyme, free lyo = lyophilized from buffer, L = co-lyophilized, M = melt coated, P = precipitation coated, 47 = ATA-47, 82P = ATA-82P, AC = 1 allyl 3 methyl imidazolium chloride, EB = 1-ethyl-3-methyl-imidazolium bromide chex = cyclohexane, EtOAc = ethyl acetate, Et₂O = diethylether, MTBE = methyl-t-butyl ether, tol = toluene

Although cyclohexane and the co-lyophilized ATA-47 led to the fastest reaction in this screening, the almost 40 mmol L⁻¹ of product after 10 days appear trivial in comparison to the reaction rate in an aqueous system. However, for the same reaction in 50 mM Tris/HCl buffer

(pH 7.0) a product concentration of 10 mmol L⁻¹ was achieved within 2 h. In the same time the co-lyophilized ATA-47 reaches a product concentration of 0.33 mmol L⁻¹.

Co-lyophilized enzymes show outstanding productivity compared to the other coating methods, they are eight-fold more active than the soluble enzymes. By comparison, precipitation coating showed little improvement over the untreated enzyme. Melt coated enzymes showed approximately a four-fold improvement in activity. Furthermore, ATA-47 appeared to be overall more active for the chosen reaction than ATA-82P. Additionally, EB as coating material led to better activation than AC for both enzymes ATA-47 and ATA-82P.

For all tested combinations for enzyme and coating method cyclohexane appeared to be the most suitable solvent. At first sight one might think that this is because cyclohexane is the least polar solvent in this list and it is well known, that enzymes are more stable in non-polar organic solvents because the tightly bound water on the enzyme surface is not withdrawn. Consequently, this idea leads to the conclusion, that toluene would be the second best solvent. However, toluene turned out to be only an average (or less than average) solvent. For the polar solvents the activity strongly depends on the combination of coating and solvent. The highest activity for the soluble enzyme could be found in ethyl acetate. However, diethyl ether was the most suitable solvent in combination with co-lyophilization. MTBE is the best solvent in the case of melt coating.

The samples of the free enzyme and the co-lyophilized enzymes were not only analyzed by means of RP-HPLC, but also by means of chiral HPLC to identify the effect of the organic solvent and the coating on the enantioselectivity.

Figure B-2 and Figure B-3 show the enantiomeric excess of the (S)-enantiomer for ATA-47 and ATA-82P, each free and co-lyophilized with both ILs. The enantiomeric excess shown was calculated from the samples drawn after 10 days of reaction time. It is clear that solvents significantly influence enantioselectivity. Solely cyclohexane is found to result in a constant e.e., regardless whether the enzyme is coated or free. Ethyl acetate, diethyl ether, and toluene led to relatively low e.e. The enantioselectivity in MTBE is strongly dependent on the preparation of the catalyst. Interestingly, in this study both enzymes showed quite similar enantioselectivity. However, according to non-published data by c-Lecta GmbH, ATA-47 shows in aqueous buffer much higher selectivity (>99.5 % e.e.) than ATA-82P (83 % e.e.). One could hypothesize that changes in enantioselectivity might be caused by the coating process. During the solidification while lyophilization the IL might influence the structural appearance of the enzyme leading to poor selectivity. Furthermore, the enzyme might lack flexibility in the solid IL-enzyme structure. The structure of the coating can also affect the selectivity of the enzyme by favoring the diffusion of one enantiomer. The impact of the solvent on the enantioselectivity has already been discussed by various researchers.⁴⁷⁻⁵² All the following

experiments were carried out using ATA-47 coated by means of co-lyophilization with EB in cyclohexane, because this reaction system proved to be the most active combination.

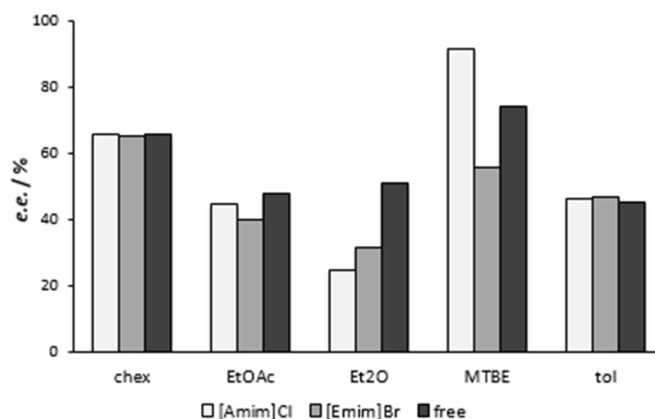


Figure B-2. Enantiomeric excess of (S)-methylbenzylamine of free ATA 47 and coated by co-lyophilization.

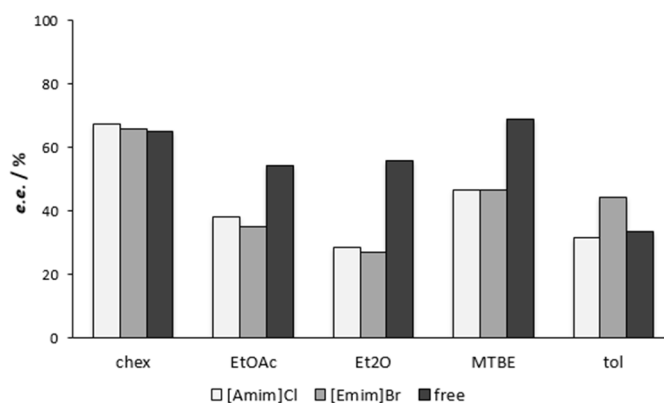


Figure B-3. Enantiomeric excess of (S)-methylbenzylamine of free ATA 82P and coated by co-lyophilization.

2.3 Coating Thickness

In order to identify the optimal coating thickness, so that maximal enzyme stability and reaction rate could be achieved while taking into consideration transport limitations caused by the additional barrier, various amounts of coating material were used for co-lyophilization. Figure B-4 shows the coated enzymes used for the experiments. After adding the organic solvent and with ongoing stirring of the mixture, the catalyst forms agglomerates (comparable with the coated enzyme in vial 6 in Figure B-4) due to the hydrophilic character of the enzyme and the IL. If the lyophilized enzyme is not broken down into pieces, the catalyst remains in a sponge-like structure throughout the whole reaction. (Figure B-5)



Figure B-4. ATA-47 co-lyophilized with various amount of EB: free enzyme (1), free enzyme lyophilized with PLP (2), 1:0.05 coating (3), 1:0.1 coating (4), 1:0.5 coating (5), and 1:1 coating (6).



Figure B-5. ATA-47 co-lyophilized with 1:0.5 IL (EB) after the reaction.

Figure B-6 shows the product formation over time for various amounts of coating material. The free enzyme was the least active. Lyophilization of the enzyme from buffer, in the same way as it was done for coating, let to some activation.²¹ Nevertheless, all the coated enzymes whether with 1:0.05 or 1:1 coating were more active than the free lyophilized enzyme. In the class of coated enzymes, a coating of 1:0.5 appeared to be the most active form.

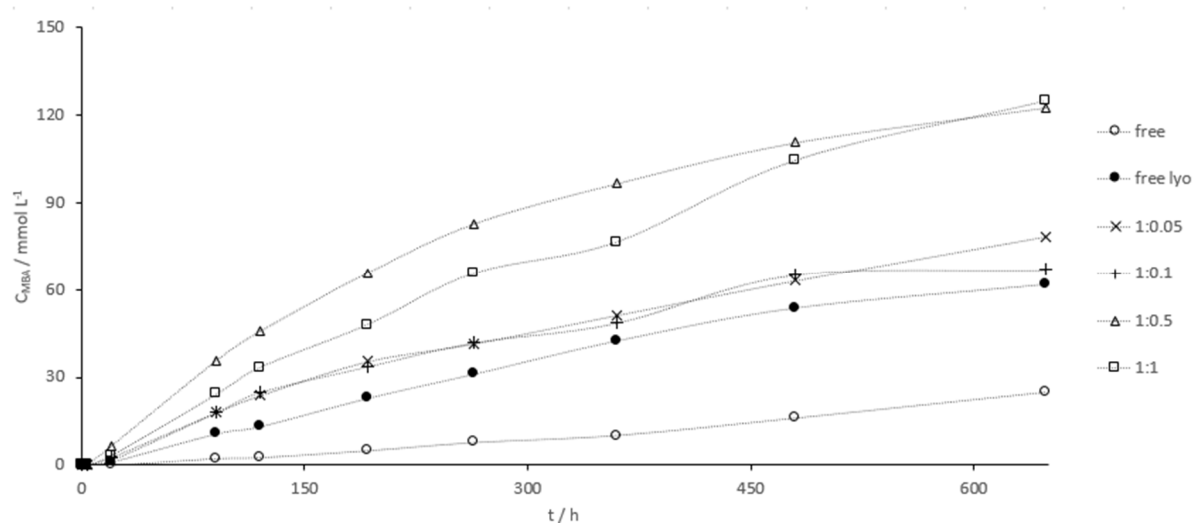


Figure B-6. Product formation over time for ATA-47 co-lyophilized with 1:0.05, 1:0.1, 1:0.5, 1:1 of IL (EB) and the free enzyme over 27 days.

2.4 Residual Water Content

Residual water in the co-lyophilized enzyme was determined for all six preparations by means of coulometric titration. The results show decreasing residual water content with increasing amount of IL (Table B-2). However, due to the increasing mass of the sample because of the increasing amount of coating material, the absolute amount of water in the prepared catalyst is constant. Thus, the coating does not affect the water content of the reaction mixture and, therefore, is not the driving force for the increasing activity of the coated enzyme.

Table B-2. Residual water content of the co-lyophilized enzyme with various coating thickness

entry	coating ratio	water [wt%]	water abs. [mg]
1	free lyo	0.49	0.38
2	1:0.05	0.49	0.40
3	1:0.1	0.46	0.39
4	1:0.5	0.22	0.32
5	1:1	0.19	0.36

2.5 Temperature Dependency

Furthermore, optimal reaction temperature was investigated in respect to kinetics. However, the reaction temperature was kept beneath the melting point of the IL (mp. 53 °C). Therefore, reactions were carried out at 25 °C, 30 °C, 35 °C, 40 °C and 45 °C. With rising temperature an increase in reaction rate could be observed. (Figure B-7)

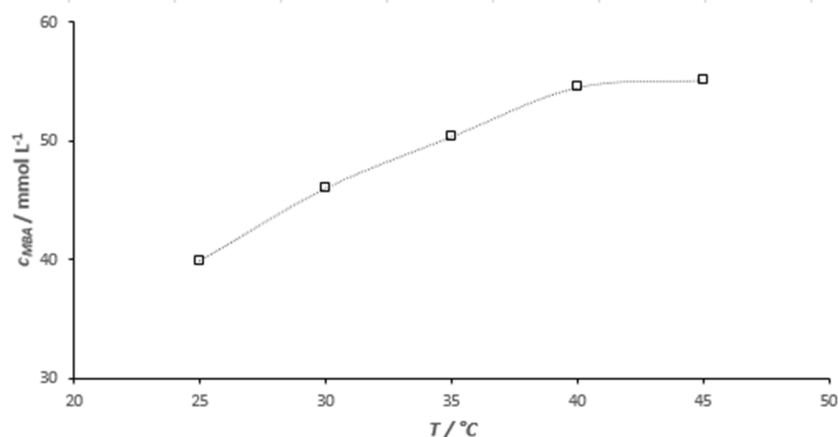


Figure B-7. Product concentration over after 5 days for ATA 47 co lyophilized with 1:0.5 EB for different reaction temperature.

2.6 Recyclability

To assess the potential of recycling the heterogeneous catalyst, the reusability of the enzyme was tested by refreshing the supernatant and hence the substrates after 5 days. This process was repeated four times. The recyclability of the co-lyophilized enzyme in cyclohexane was found to be excellent without any loss of activity (Figure B-8).

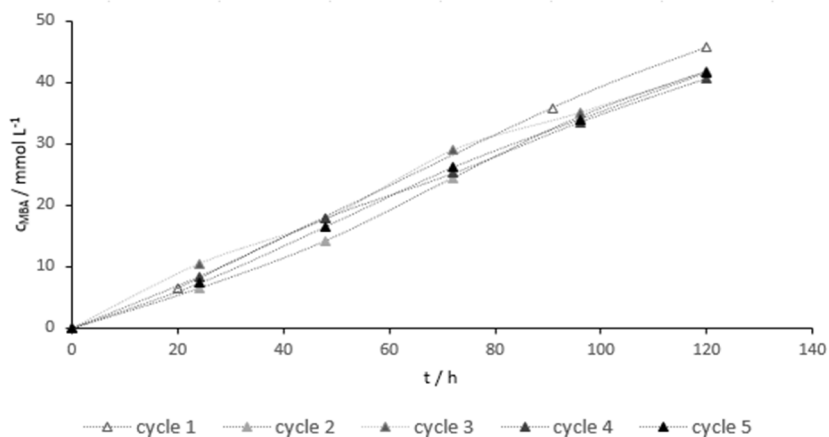
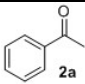
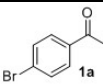
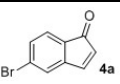
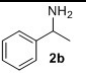
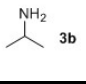
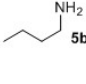


Figure B-8. Product concentration over time for recycled ATA 47 co lyophilized with 1:0.5 EB.

2.7 Substrate variation

In order to investigate the applicability of the IL coated transaminases for further substrates, three amino donors and three acceptors were tested giving a set of nine reaction systems.

Table B-3. Conversion of ketone [%] after 4 days for all screening reactions in cyclohexane with ATA 47 co-lyophilized 1:0.5 EB

donor	acceptor		
	 2a	 1a	 4a
 2b	-	<1	<1
 3b	23	<1	23
 5b	15	<1	86

The results of the screening are shown in Table B-3. ATA-47 shows hardly any acceptance for substrate **1a** independent from the donor. **2a** and **4a** are both substrates to ATA-47, however, the conversion strongly depends on the donor molecule. The best results are obtained from the amination of **4a** using butylamine as amino donor with 86 % conversion of the ketone after 4 days.

3 Conclusion

In this paper novel methods to coat cofactor dependent enzymes with ILs were explored. In conclusion, we have shown that the sensitive and cofactor-dependent transaminase (i) can be coated with RTSPIL and (ii) applied in different organic solvents it remained active. We were able to show improved stability and activity of ω -transaminase ATA-40, ATA-47, and ATA-82P by coating the lyophilized enzyme with RTSPILs. Melt coating and precipitation coating require more effort, although, this does not pay off, because the increase in activity does not exceed the activity of the free enzyme lyophilized in buffer with PLP. Co-lyophilization displays a simple and fast method to activate transaminases. ATA-47 showed 8-fold increased productivity compared to its free counterpart and twice the productivity of the free lyophilized enzyme. The amount of coating material has a significant influence on the reaction rate. For the co-lyophilized ATA-47 activity increased with increasing amount of coating up to 1:0.5, however, coating with 1:1 resulted in slightly reduced reaction rate compared to the 1:0.5 coating. Finally, the location of the cofactor was also found to be critical. If PLP is located together with the enzyme within the coating a reaction can occur. Placing the cofactor outside, i.e. in the solvent, prevents the reaction from taking place.

Our novel co-lyophilization method is not only a fast and simple method to activate enzymes but brings an important further advantage. Due to the broad range of ILs the system can be simply adopted to various process conditions, such as temperature and solvent. Furthermore, co-lyophilized enzymes possess all the benefits of heterogeneous catalysis, such as (i) easy and inexpensive separation from the reaction mixture, (ii) reduction of catalyst flushed into the product, and (iii) application in continuous reactors. In near future we will work with the aim of carrying out the co-lyophilization directly in a flow reactor, our in-house designed so-called Plug & Play reactor, in order to form the catalytically active stationary phase and apply it for continuous synthesis.⁵³

4 Experimental

General. The ionic liquids were kindly provided by Solvionic (France). [Emim]Br was provided in a 66.0 wt% aqueous solution and [Amim]Cl in 60.0 wt% aqueous solution. The enzymes were kindly provided by c-LEcta (Leipzig, Germany). ATA-47 and ATA-82P are both S-selective ω -transaminases. ATA-47 is an engineered, recombinant transaminase produced by microbial fermentation with *E. coli* with a molecular weight of 53.2 kDa and an activity of 690 U/g (One unit (U) forms 1 μ mol acetophenone per minute from α -methylbenzylamine (MBA) at 30 °C in 50 mM potassium phosphate buffer pH 7.4, 0.1 mM PLP, 10 mM sodium pyruvate, 10 mM racemic MBA). ATA-82P is an engineered, recombinant transaminase

produced by microbial fermentation with *E. coli* with an activity of 1100 U/g. ATA-82P was heat-purified and both enzymes were supplied as freeze-dried powder. ATA-40 was also from c-LEcta and already available in the lab, All the other chemicals (solvents, substrates) were purchased from Sigma Aldrich and used without further treatment.

Preliminary experiments. The prepared coated enzyme ATA-40 (melt coated, precipitations coated, free enzyme) (5 mg of enzyme, 1 mM PLP for final volume) were placed into a 1.5 mL Eppendorf tube. A total volume of 1 mL MTBE containing **1a** (10 mM) and a racemic mixture of **2b** (30 mM) was added. The reaction mixtures were shaken at 30 °C at 300 rpm. Samples were taken over time. For the samples 40 μ L of the supernatant were transferred in an Eppendorf tube and diluted with 260 μ L MTBE. After drying over Na₂SO₄ and spinning down the drying agent (75 s, 13,500 rpm), 150 μ L of the supernatant were transferred into a GC vial. 50 μ L of a 4 mM cyclohexylamine solution in MTBE were added as a standard. The amines were derivatized by adding 15 μ L triethylamine and 10 μ L acetic anhydride. Then the sample was analyzed by means of gas chromatography (Clarus 5000) with a CP-ChiralSil-DEX CB 25 x 0.25 column from Agilent Technologies, Santa Clara, CA, USA). Argon was used as carrier gas. The heating program started at 120°C. With a rate of 7.0°C/min the oven was heated to 170°C where it was held for 5.00 min. The heating continued with a rate of 12.0 °C/min to the final temperature of 200 °C. The whole method took 14.64 min.

Coating thickness. Coatings for the transamination in MTBE were prepared in various amounts of 1-ethyl-3-methyl-imidazolium bromide [Emim]Br. ATA-40 was coated with both coating methods with 1:1, 1:2, 1:5, 1:10 in terms of enzyme mass. Reactions were run under standard conditions with these coated enzymes and samples were taken over time to determine the influence of the coating thickness and method on reaction rate and enzyme stability.

Bradford Assay. The supernatant of the reactions with 1:1 coated enzyme was extracted with water. The samples were analyzed by the standard procedure.⁵⁴ There was no protein detected in the supernatant. In this studies enzyme leaching was tested by following the reaction progress in the supernatant after removing the enzyme after the first reaction cycle. No product was formed in the filtered reaction solution (data not shown).

Melt coating. The IL solution was placed in an Eppendorf tube, heated to 80 °C under reduced pressure to evaporate most of the water. The remaining clear liquid was mixed with ice cooled acetonitrile. The IL precipitates in white crystals. The solid IL was stored in acetonitrile in a tightly sealed container in the fridge. For the coating the necessary amount of solid IL was weighed out. The crystals were melted in a water bath at 60 °C. Enzyme and PLP were added and the mixture was stirred to a homogeneous mixture. The mixture was allowed to cool down

in the fridge. As the IL is very hydrophilic, all the steps carried out in air atmosphere must be done very fast. Otherwise, the IL soaks water from the air and forms a solution.

Precipitation coating. The required amount of aqueous IL solution was weighed into a 1.5 mL Eppendorf tube mixed with the enzyme and PLP (50 μ L of 20 mM stock, 1 mM for 1 mL reaction volume). The water was evaporated at 80 °C and reduced pressure. The remaining concentrated solution was mixed with 200 μ L ice cooled dried acetonitrile to precipitate the salt with the enzyme and cofactor in light yellow crystals. The supernatant was taken off and the residual solvent was evaporated before the catalyst was used.

Co-lyophilization. The co-lyophilized catalyst was manufactured by dissolving the enzyme, the IL and the cofactor in an aqueous buffer system (50 mM Tris/HCl buffer, pH 7). The solution was freeze dried overnight and the solid residue was used as catalyst without further treatment.

Free enzyme. For the free enzyme reaction, the biocatalyst was used as lyophilized powder with the cofactor added separately.

Lyophilized enzyme. The required amount of enzyme and PLP were dissolved in an aqueous buffer system (50 mM Tris/HCl buffer, pH 7). The solution was freeze dried overnight and the solid residue was used as catalyst without further treatment.

Screening for solvent and coating. For each screening reaction 5 mg of enzyme are weighed out and prepared in the appropriated way (melt coating, precipitation coating, co-lyophilization, free enzyme). The prepared enzyme was placed in a 2 mL HPLC vial. After adding a total volume of 1 mL organic solvent (cyclohexane (chex), methyl-*t*-butyl-ether (MTBE), toluene (tol), diethyl ether (Et₂O) or ethyl acetate (EtOAc)) containing the substrate **2a** (50 mM) and the donor **3b** (200 mM) the reaction mixture was shaken at 30 °C at 200 rpm. Samples were taken over time. For the samples 50 μ L of the supernatant were transferred into an HPLC vial and diluted with 450 μ L acetonitrile. After adding the standard 4'-bromoacetophenone (5 mM), the samples were analyzed by means of HPLC.

Analysis. Product formation was followed by achiral HPLC. All the samples were analyzed by means of reverse phase high performance liquid chromatography using an Agilent Instrument 1100 Series with a Poroshel 120 column (EC-C18 2.7 μ m, 50 mm x 4.6 mm). 0.5 μ L of the sample were injected. Eluent: 0-1.5 min 95 % H₂O:H₃PO₄ 300:1, 5 % ACN; 1.5-2.5 min gradient to 40 % H₂O:H₃PO₄ 300:1, 60 % ACN; keep this eluent for 1 min and then go back to the starting conditions 95 % H₂O:H₃PO₄ 300:1, 5 % ACN. The whole run takes 6 min. Flow

rate: 1 mL/min. Column temperature: 25 °C. For detection a UV detector was used, set at 210 nm. Retention times: **2a** 4.1 min, **2b** 2.5 min, **4a** 4.6 min, **5a** 4.6 min, **5b** 3.9 min. This method was adapted from literature.⁴⁵

The enantiomeric excess was determined by chiral HPLC using a Chiralcel OD-H (250 mm x 4.6 mm). 0.5 μ L of the sample were injected. Eluent: hexane:2-propanol 9:1. The whole run takes 8 min. Flow rate 0.8 mL/min. Column temperature: 25 °C. For detection a UV detector was used, set at 210 nm. Retention times: **2a** 4.5 min, **2b(R)** 6.35 min, **2b(S)** 6.54 min. This method was taken from literature.⁵⁵

Reference reaction in buffer. 5 mg of enzyme were weight out into a 2 mL vial and dissolved in 1 mL of buffer (50 mM Tris/HCl buffer, pH 7.0) containing 2 mM PLP and the substrates **2a** (50 mM) and **3b** (200 mM). The mixture was stirred with 200 rpm at 30 °C. Samples were taken over time. For the samples 50 μ L of reaction mixture were added to 500 μ L of acetonitrile to precipitate the enzyme. After centrifugation (2 min at 15,000 rpm) the supernatant was analyzed by means of RP-HPLC.

Coating thickness. To identify the optimal coating thickness, the enzyme (ATA-47) was co-lyophilized with various amounts of ionic liquid (EB). The amount of coating material was 1:0.05, 1:0.1, 1:0.5, 1:1 in terms of enzyme mass. 50 mg of enzyme, the required amount of IL in solution and PLP were dissolved in an aqueous buffer system (50 mM Tris/HCl buffer, pH 7.0). The solution was freeze dried overnight and the solid residue was employed to catalyse the amino transfer from donor **3b** (500 mM) to substrate **2a** (200 mM) in a total volume of 5 mL of cyclohexane. The mixture was stirred with 200 rpm at 30°C. Samples were taken over time. For the samples 50 μ L of the supernatant were transferred into an HPLC vial and diluted with 450 μ L acetonitrile. After adding an internal standard 4'-bromoacetophenone (5 mM) the samples were analyzed by means of HPLC.

Residual water content. Co-lyophilized enzyme was prepared by mixing 50 mg of enzyme (ATA-47) with the appropriate amount of IL (EB) and PLP with 1 mL 50 mM Tris/HCl buffer, pH 7.0. The mixture was lyophilized overnight. The obtained catalyst was suspended in Methanol and residual water content was determined by means of coulometric titration.

Effects of temperature. The reaction mixtures of the co-lyophilized enzyme with a coating of 1:0.5, respectively, were stirred at the required temperature (25 °C, 30 °C, 35 °C, 40 °C or 45 °C) with 200 rpm. The final product concentration after 5 days was determined by means of HPLC.

Recyclability. To investigate the recyclability of the co-lyophilized enzyme 50 mg of ATA-47 were coated by co-lyophilization with EB. The prepared enzyme was placed in a 2 mL HPLC vial. After adding a total volume of 1 mL cyclohexane containing the substrate **2a** (50 mM) and the donor **3b** (200 mM) the reaction mixture was shaken at 30°C at 200 rpm. Samples were taken over time. For the samples 50 μ L of the supernatant were transferred into an HPLC vial and diluted with 450 μ L acetonitrile. After adding an internal standard 4'-bromoacetophenone (5 mM) the samples were analyzed by means of HPLC. After 5 days the supernatant was taken off and replaced by fresh cyclohexane containing **2a** and **3b** in initial concentrations. This process was repeated 4 times.

Substrate variation. 50 mg of ATA-47 was coated with 1:0.5 EB by lyophilization. The solid catalyst was mixed with a total volume of 5 mL cyclohexane containing donor (500 mM) and acceptor (200 mM). The mixture was stirred with 200 rpm at 30°C. Samples were taken over time.

5 References

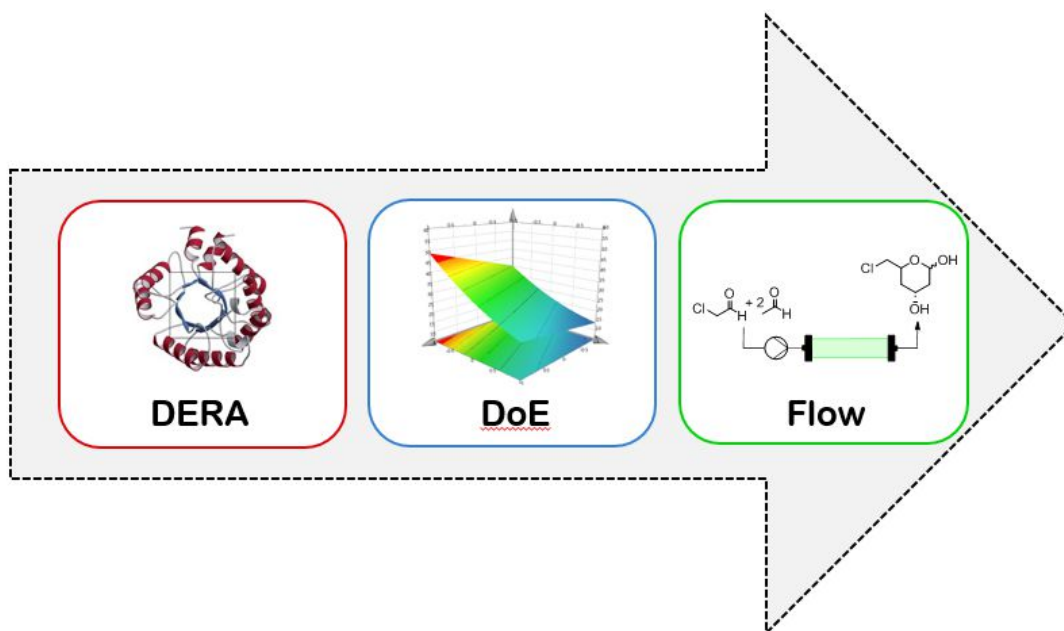
1. P. Clapés, W.-D. Fessner, G. A. Sprenger and A. K. Samland, *Curr. Opin. Chem. Biol.*, 2010, **14**(2), 154.
2. P. Tufvesson, J. Lima-Ramos, J. S. Jensen, N. Al-Haque, W. Neto and J. M. Woodley, *Biotechnol. Bioeng.*, 2011, **108**(7), 1479.
3. C. S. Fuchs, M. Hollauf, M. Meissner, R. C. Simon, T. Besset, J. N. H. Reek, W. Riethorst, F. Zepeck and W. Kroutil, *Adv. Synth. Catal.*, 2014, **356**(10), 2257.
4. M. Fuchs, J. E. Farnberger and W. Kroutil, *Eur. J. Org. Chem.*, 2015(32), 6965.
5. M. D. Truppo and N. J. Turner, *Org. Biomol. Chem.*, 2010, **8**(6), 1280.
6. H. Gruber-Woelfler, J. G. Khinast, M. Flock, R. C. Fischer, J. Sassmannshausen, T. Stanoeva and G. Gescheidt, *Organometallics*, 2009, **28**(8), 2546.
7. D. Ghislieri and N. J. Turner, *Top. Catal.*, 2014, **57**, 284.
8. C. K. Savile, J. M. Janey, E. C. Mundorff, J. C. Moore, S. Tam, W. R. Jarvis, J. C. Colbeck, A. Krebber, F. J. Fleitz, J. Brands, P. N. Devine, G. W. Huisman and G. J. Hughes, *Science*, 2010, **329**(5989), 305.
9. Food and Drug Administration, *Chemistry Review: Januvia Tablets*, 2010.
10. T. Loftsson and M. E. Brewster, *J. Pharm. Pharmacol.*, 2010, **62**(11), 1607.
11. S. Kalepu and V. Nekkanti, *Acta Pharm. Sin. B*, 2015, **5**(5), 442.
12. R. Lipp, *Am. Pharmac. Rev.*, 2013, **16**(3).
13. F. Hollmann and S. Kara, *Biospektrum*, 2014, **20**, 100.
14. F. G. Mutti and W. Kroutil, *Adv. Synth. Catal.*, 2012, **354**(18), 3409.
15. A. M. Klivanov, *Nature*, 2001, **409**.

16. V. Stepankova, S. Bidmanova, T. Koudelakova, Z. Prokop, R. Chaloupkova and J. Damborsky, *ACS Catal.*, 2013, **3**(12), 2823.
17. J. K. Lee and M.-J. Kim, *J. Org. Chem.*, 2002, **67**(19), 6845.
18. Y. Abe, K. Kude, S. Hayase, M. Kawatsura, K. Tsunashima and T. Itoh, *J. Mol. Catal. B-Enzym*, 2008, **51**(3-4), 81.
19. Y. Abe, K. Yoshiyama, Y. Yagi, S. Hayase, M. Kawatsura and T. Itoh, *Green Chem.*, 2010, **12**(11), 1976.
20. Y. Abe, Y. Yagi, S. Hayase, M. Kawatsura and T. Itoh, *Ind. Eng. Chem. Res.*, 2012, **51**(30), 9952.
21. J. Mutschler, T. Rausis, J.-M. Bourgeois, C. Bastian, D. Zufferey, I. V. Mohrenz and F. Fischer, *Green Chem.*, 2009, **11**(11), 1793.
22. T. Itoh, Y. Matsushita, Y. Abe, S.-h. Han, S. Wada, S. Hayase, M. Kawatsura, S. Takai, M. Morimoto and Y. Hirose, *Chem. Eur. J.*, 2006, **12**(36), 9228.
23. Y. Matsubara, S. Kadotani, T. Nishihara, Y. Hikino, Y. Fukaya, T. Nokami and T. Itoh, *Biotechnol. J.*, 2015, **10**(12), 1944.
24. F.-X. Dong, L. Zhang, X.-Z. Tong, H.-B. Chen, X.-L. Wang and Y.-Z. Wang, *J. Mol. Catal. B-Enzym*, 2012, **77**, 46.
25. M. B. Abdul Rahman, K. Jumbri, Mohd Ali Hanafiah, Nurul Ain, E. Abdulmalek, B. A. Tejo, M. Basri and A. B. Salleh, *J. Mol. Catal. B-Enzym*, 2012, **79**, 61.
26. D. T. Dang, S. H. Ha, S.-M. Lee, W.-J. Chang and Y.-M. Koo, *J. Mol. Catal. B-Enzym*, 2007, **45**(3-4), 118.
27. C. Wu, Z. Zhang, C. Chen, F. He and R. Zhuo, *Biotechnol. Lett.*, 2013, **35**(10), 1623.
28. X.-J. He, S.-Y. Chen, J.-P. Wu, L.-R. Yang and G. Xu, *Appl. Microbiol. Biotechnol.*, 2015, **99**(21), 8963.
29. B. Zou, C. Song, X. Xu, J. Xia, S. Huo and F. Cui, *Appl. Surf. Sci.*, 2014, **311**, 62.
30. D.-H. Zhang, H.-X. Xu, N. Chen and W.-C. Che, *Austin J. Biotechnol. Bioeng.*, 2016, **3**(2), 1060.
31. R. A. Sheldon, R. M. Lau, M. J. Sorgedraeger, F. van Rantwijk and K. R. Seddon, *Green Chem.*, 2002, **4**(2), 147.
32. P. Domínguez de María, *Angew. Chem. Int. Ed.*, 2008, **47**(37), 6960.
33. F. van Rantwijk, R. Madeira Lau and R. A. Sheldon, *Trends Biotechnol.*, 2003, **21**(3), 131.
34. S. Park and R. J. Kazlauskas, *Curr. Opin. Biotech.*, 2003, **14**(4), 432.
35. Z. Yang and W. Pan, *Enzyme Microb. Tech.*, 2005, **37**(1), 19.
36. M. Moniruzzaman, K. Nakashima, N. Kamiya and M. Goto, *Biochem. Eng. J.*, 2010, **48**(3), 295.
37. M. Erbedinger, A. J. Mesiano and A. J. Russell, *Biotechnol. Progr.*, 2000, **16**(6), 1129.
38. S. G. Cull, Holbrey J.D., V. Vargas-Mora and Seddon, K.R.: Lye, G.J., *Biotechnol. Bioeng.*, 2000, **69**(2), 227.
39. F. van Rantwijk and R. A. Sheldon, *Chem. Rev.*, 2007, **107**(6), 2757.
40. U. Kragl, M. Eckstein and N. Kaftzik, *Curr. Opin. Biotech.*, 2002(13), 565.
41. R. Madeira Lau, F. van Rantwijk, K. R. Seddon and R. A. Sheldon, *Org. Lett.*, 2000, **2**(26), 4189.
42. J. K. Lee and M.-J. Kim, *J. Mol. Catal. B-Enzym*, 2011, **68**(3-4), 275.

43. Y. He, J.-J. Li, Y.-K. Luo, F. Song, X.-L. Wang and Y.-Z. Wang, *RSC Adv.*, 2015, **5**(84), 68276.
44. N. Liu, L. Wang, Z. Wang, L. Jiang, Z. Wu, H. Yue and X. Xie, *Molecules*, 2015, **20**, 9949.
45. R. E. Meadows, K. R. Mulholland, M. Schürmann, M. Golden, H. Kierkels, E. Meulenbroeks, D. Mink, O. May, C. Squire, H. Straatman and A. S. Wells, *Org. Process Res. Dev.*, 2013, **17**(9), 1117.
46. L. H. Andrade, W. Kroutil and T. F. Jamison, *Org. Lett.*, 2014, **16**, 6092.
47. J. Broos, *Biocatal. Biotransfor.*, 2009, **20**(4), 291.
48. G. Carrea, ed., *Organic synthesis with enzymes in non-aqueous media*, Wiley-VCH, Weinheim, 2008.
49. T. Ke, C. R. Wescott and A. M. Klibanov, *J. Am. Chem. Soc.*, 1996, **118**(14), 3366.
50. A. M. Klibanov, *Acc. Chem. Res.*, 1990, **23**, 114.
51. H. Noritomi, Ö. Almarsson, G. L. Barletta and A. M. Klibanov, *Biotechnol. Bioeng.*, 1996, **51**, 95-99.
52. K. Faber, *Biotransformations in Organic Chemistry: A Textbook*, Springer, Heidelberg, 2011.
53. G. J. Lichtenegger, M. Maier, J. G. Khinast and H. Gruber-Wöfler, *J. Flow Chem.*, 2016, **6**(3), 244.
54. BioRad, *Quick Start Bradford Protein Assay - Instruction Manual*.
55. L. H. Andrade, W. Kroutil and T. F. Jamison, *Org. Lett.*, 2014, **16**(23), 6092.

C. DERA in flow: Synthesis of a statin side chain precursor in continuous flow employing DERA immobilized in alginate-luffa matrix*

Statins, cholesterol lowering drugs used for the treatment of coronary artery disease (CAD) are among the top 10 prescribed drugs worldwide. However, the synthesis of their characteristic side chain containing two chiral hydroxyl groups can be challenging. The application of deoxyribose-5-phosphate aldolase (DERA) is currently one of the most promising route for the synthesis of this side chain. In here, we describe the development of a continuous flow process for the biosynthesis of a side chain precursor. Design of Experiments (DoE) was used to optimize the reaction conditions (pH-value and temperature) in batch. A pH of 7.5 and a temperature of 32.5 °C were identified to be the optimal process settings within the reaction space considered. Additionally, an immobilization method was developed using the alginate-luffa matrix (ALM), which is a fast, simple, inexpensive method to for enzyme immobilization. Furthermore, it is non-toxic, biodegradable and from renewable resources. The final continuous process was operated stable for 4 h and can produce up to 4.5 g of product per day.



*The following chapter is taken from the journal article by Grabner *et al.*, published in *Catalysts* (Grabner, B., Pokhichuk, Y., Gruber-Woelfler, H., (2020). "DERA in flow – Synthesis of a statin side chain precursor in continuous flow employing DERA immobilized in alginate-luffa matrix".)

1 Introduction

Cardiovascular diseases (CVD) are the number one cause of death worldwide.¹ In Europe each year 3.9 million deaths (45 % of all deaths) are associated with CVD.² The primary reason for death among CVD patients is coronary artery disease (CAD). CAD is characterized by atherosclerosis – the formation of sedimentation (plaque) in the blood vessel that leads to reduced oxygen supply to the heart.³ Arterial plaque formation is often attributed to an increased level of low-density lipoprotein (LDL) cholesterol, which in western culture is often caused by unhealthy food and too little exercises. Besides a change in life-style being the first choice for lowering the cholesterol level in blood, one can choose between three medical mechanisms for the treatment of hypercholesterolemia - increase bile synthesis, decrease intestinal cholesterol absorption or inhibition of the 3-hydroxy-3-methylglutaryl coenzyme A (HMG-CoA) reductase, an essential enzyme in the synthetic route to cholesterol.^{4,5} Statins competitively inhibit HMG-CoA reductase and thus approach the reduction of LDL-cholesterol concentration by the latter of the above mentioned methods. One of the most prevalent statins is atorvastatin (Lipitor®), synthesized by Pfizer since 1996. It is known as the best-selling blockbuster in the past two decades. Despite the patent expiration in 2011, Lipitor was the third most commonly prescribed medication in the U.S. in 2016. An additional statin, simvastatin, was the 8th most prescribed medication; therefore, statins represent a significant share of the pharmaceutical market.⁶ Natural and semi-synthetic statins possess side chains in the form of lactones, which is in vivo hydrolyzed to the corresponding and biologically active hydroxyl acid. Synthetic statins, so-called super-statins such as rosuvastatin (Crestor®) are provided in the active form of dihydroxy heptanoic acid with two chiral alcohol groups attached to a heterocyclic core.^{7,8} The structures of the three above mentioned statins are depicted in Figure C-1.

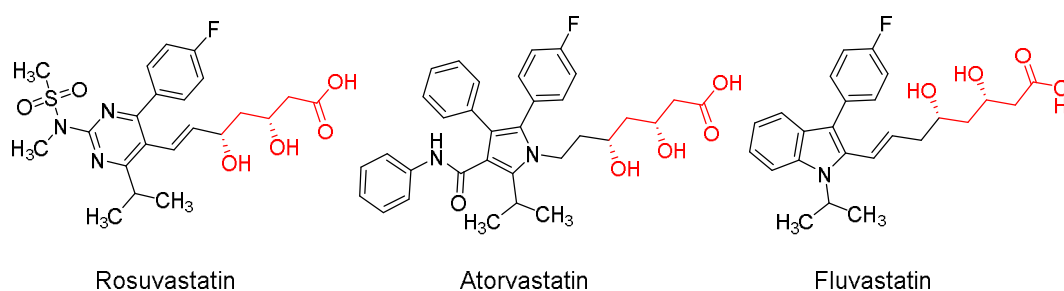


Figure C-1. Molecular structures of three statins, Simvastatin, Atorvastatin and Rosuvastatin. Dihydroxy heptanoic acid side-chain and its cyclic precursor are colored in red.

Only one of the enantiomers of the chiral side chain is active and needs to be provided in high purity for adequate activity. This is a major challenge for manufacturers.^{9,10} In the past decade numerous approaches for the enantiomerically pure synthesis of this side chain were

published.^{11–15} Chemical routes requiring harsh chemicals and numerous additional step for protection/de-protection of sensitive functional groups and by-product formation and waste generation are an issue. In contrast to that, it was shown by Tao *et al.* that biocatalysis could be a comparably sustainable approach.^{16,17} Besides numerous chemo-enzymatic routes the one employing deoxyribose-5-phosphate aldolase (DERA, EC 4.1.2.4) is very promising. DERA is a unique enzyme able to catalyze the aldol addition of two aldehydes resulting in an aldehyde product, which can again serve as substrate for another aldol addition. The product after two sequential addition reactions and spontaneous cyclization is the hemiacetal 2,4,6-trideoxyhexose **1c** (Figure C-2). This unique property of DERA was discovered by Gijzen *et al.* in 1994 and extensively studied around the millennium.^{18–23} Haridas *et al.* gives a great overview on this topic.²⁴ The product of this biotransformation can be further processed to the statin side chain via oxidation and subsequent ring-opening to **1e** (Figure C-2). The application of DERA on industrial scale is challenging as the enzyme is sensitive to high concentrations of acetaldehyde, its natural substrate. The active site of the wildtype DERA (DERA_{WT}) is irreversibly inhibited by the covalent binding of the side-product crotonaldehyde. In 2016 the group of Pietruszka at the Research Center Jülich GmbH tackled this issue and developed a mutant (C47M), which is resistant to acetaldehyde in a high degree.²⁵ This mutant showed outstanding catalytic activity in tests using acetaldehyde as donor molecule. Further implementation of the mutant was not reported by the group.

In the present work, a continuous process for the synthesis of a statin side chain precursor was developed. Continuous processes go hand in hand with a number of advantages such as reduced reaction time, constant product quality and cost reduction compared to batch mode. While continuous operations are well implemented in bulk industries such as paper and food, they have barely made their way into pharmaceutical drug synthesis.²⁶ Fortunately, numerous researchers are passionate about continuous flow synthesis and aim to accelerate the establishment of continuous processes in industry.^{27–30} In this manuscript we describe the process of developing a continuous biocatalytic synthesis employing the novel DERA mutant. Immobilized freeze-dried whole cells (*E. coli* hosting DERA (C47M)) in an alginate gel matrix on luffa sponge were used in a packed-bed reactor. This immobilization method was originally developed by Phisalaphong *et al.* and named alginate-loofa matrix (ALM).³¹ This method is simple, inexpensive and fast in preparation. Loofa sponge (*Luffa cylindrical*) as a support brings a number of advantages. The matrix originates from a renewable source, is a highly porous material and is fully biodegradable.^{32–34}

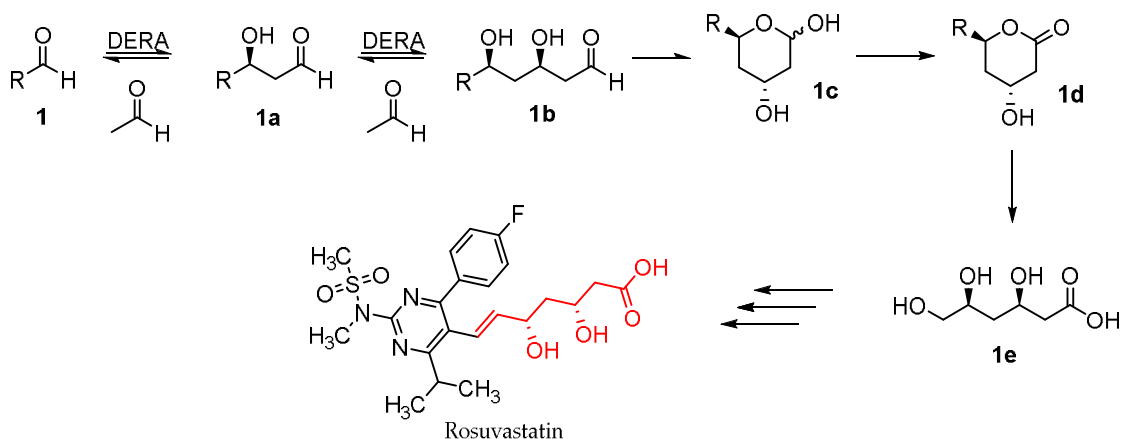


Figure C-2. DERA-catalyzed stereoselective aldol addition of three aldehydes to produce a lactol (**1c**), which can be further oxidized to a lactone results in the typical statin side chain after ring-opening.

In this work, Design of Experiments (DoE) was applied for the optimization of pH value and temperature for the enzymatic reaction and optimizing the flow conditions. DoE is a multivariate approach for parameter screening and optimization. In contrast to the original approach, where one factor is changed at a time, this method allows the identification of interaction between the individual parameters. DoE helps in gaining a maximum of information from a minimum number of experiments.^{35–37}

So far, no such development process using DoE for the optimization of a continuous enzymatic process was described in literature, to the best of our knowledge. Furthermore, this immobilization method and the application of DERA in continuous flow processes are barely found in literature.

2 Results

2.1 Design of Experiments for optimal batch conditions

In order to operate the continuous process under ideal conditions, the optimal parameters for the enzymatic reaction needed to be determined. For that, Design of Experiments (DoE) was used to evaluate the effect of the two crucial process parameters, temperature and pH value, on intermediate and product formation. In the first circuit of experiments a rough full-factorial lattice was designed. The temperature ranged between 28 °C and 37 °C in steps of 4.5 °C, pH ranged between 6.0 and 8.0 in steps of 0.5, in order to screen a wide range of process settings. For the second circuit a fine full-factorial lattice was laid in the optimum of the response surface of the first experimental circuit. Both designs are shown in Figure C-3.

For each point on the lattice an experiment was conducted. On a 500 µL scale 1.5 M acetaldehyde was dissolved in 0.1 M TEOA buffer set to the respective pH value via HCl.

Samples were collected over time and analyzed by means of GC-FID. The collected data (reaction rate for intermediate and product formation and enzyme stability) was evaluation using MatLab®. Details on the experimental design and parameters can be found in ESI (electronic supplementary information).

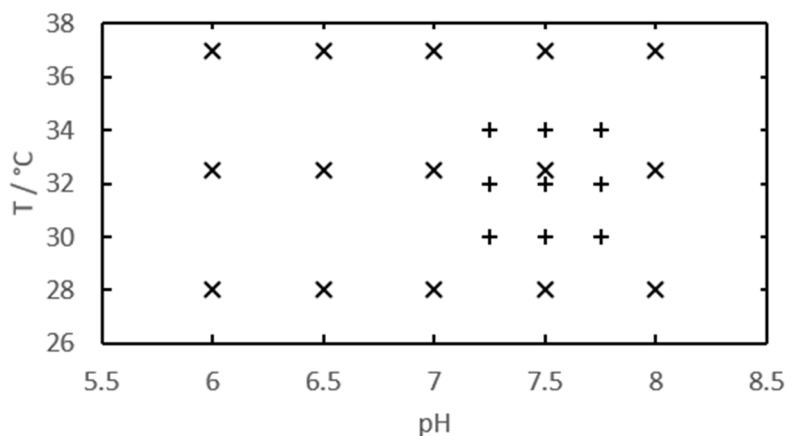


Figure C-3. Experimental design chosen for the two circuit of DoE (1st circuit: x, 2nd circuit: +)

The response surface for the rate for product formation is shown in Figure C-4 and Figure C-5. It shows an almost linear incline in enzyme activity with increasing reaction temperature. This correlation between the temperature and reaction rate is clearly visible in Figure S7 in ESI, which shows the data points without surface. The shape of this surface can be described by the Arrhenius law and the rate of inactivation, which is mathematically a logarithmic function. The productivity of the catalytic system grows until it reaches the point, where the inactivation rate is higher, than the reaction rate.³⁸ The highest activity is supposed to be at 34.5 °C. However, the deactivation rate due to denaturation is also high at this temperature. At 34 °C the activity was reduced by 30 % after 1 h of reaction time, while a reaction temperature of 32.5 °C retained more than 95 % of the initial activity after 1 h reaction time. Therefore, for all the following experiments 32.5 °C was the temperature of choice, as it constitutes the ideal compromise between the required reaction rate for a continuous application and stability for a steady state over several hours. The connection between pH value and reaction rate shows the typical Gaussian-like distribution, with an optimum at pH 7.5 (Figure C-5).

At $\text{pH} \leq 7.0$ no lactol was formed at all. Based on these results of the DoE, all the following experiments were conducted at 32.5°C and pH 7.5.

2.2 Substrate screening

Five substrates were tested under optimized batch conditions for their potential to serve as acceptor for aldol addition (Figure C-6). Acetaldehyde **1** and its chloro derivative **2** were converted to the desired products, while larger residues (benzaldehyde **4** and

cinnamaldehyde **5**) and acrolein **3** are not accepted. The major issue with aromatic substrates is the limited solubility in aqu. buffer systems, even in mixtures with DMSO.³⁹ These substrates would be especially interesting, as the direct addition of acetaldehyde to the molecule core would reduce the number process steps drastically. Acrolein was also tested as substrate. Although the mutant was successfully tested for its tolerance towards crotonaldehyde, acrolein still inhibits the enzyme.^{39,40} Further investigations were conducted using acetaldehyde **1** and chloroacetaldehyde **2**.

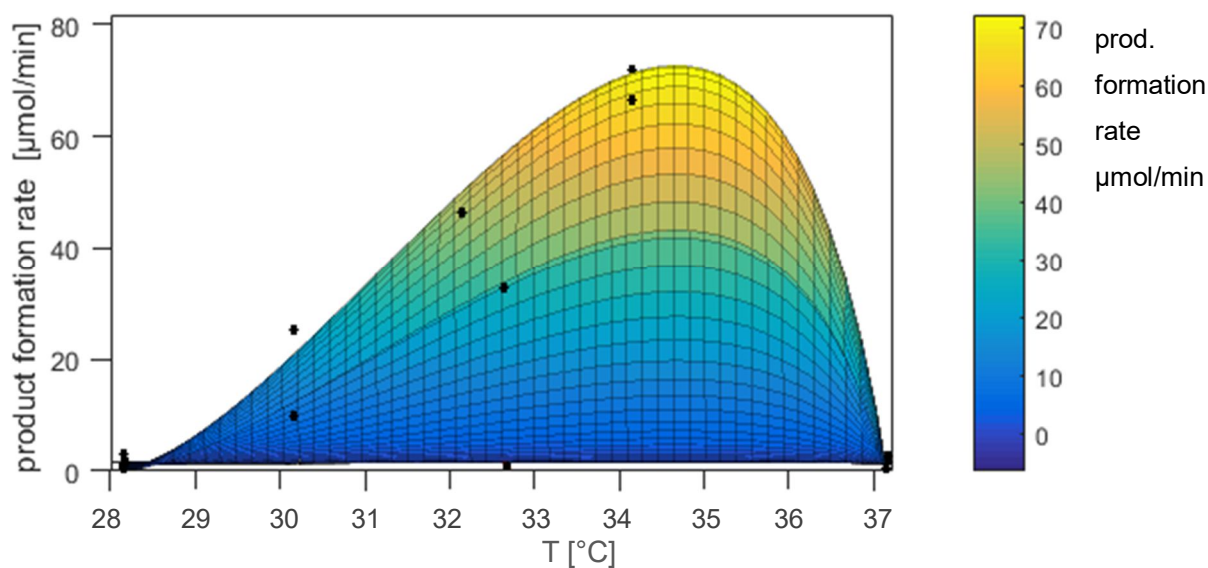


Figure C-4. Response surface for the experimental design over T. 1.5 M **1** in final volume 500 μL 0.1 M buffer ($6.0 \leq \text{pH} \leq 8.5$), 7 μL DMSO, 10 mg freeze-dried *E. coli* cells hosting DERA, $28\text{ }^\circ\text{C} \leq T \leq 37$

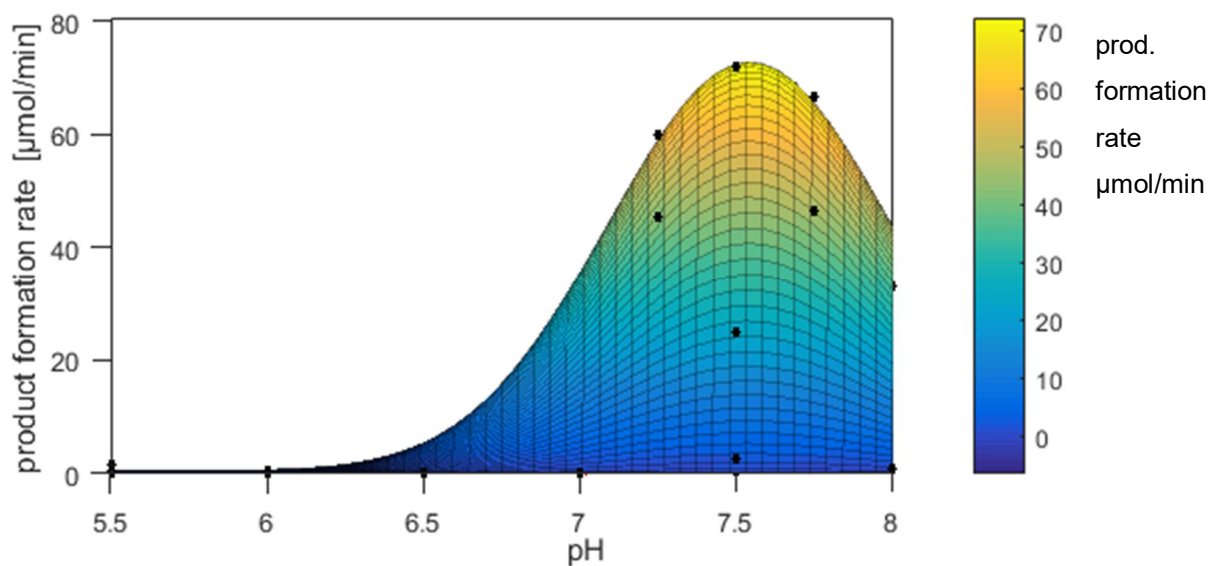


Figure C-5. Response surface for the experimental design over pH value. 1.5 M **1** in final volume 500 μL 0.1 M buffer ($6.0 \leq \text{pH} \leq 8.5$), 7 μL DMSO, 10 mg freeze-dried *E. coli* cells hosting DERA, $28\text{ }^\circ\text{C} \leq T \leq 37$

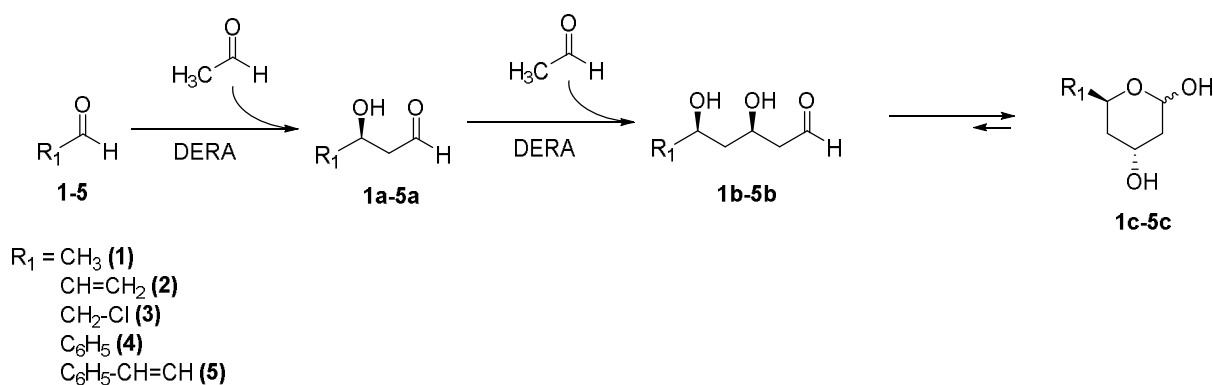


Figure C-6. Overview of tested substrates and corresponding products

2.3 Kinetics

After the optimal reaction conditions and accepted substrates were identified, it was of interest to investigate the kinetic behavior of the addition reaction. This reveals important information required for designing the continuous process. First, a batch experiment in which three molecules of acetaldehyde **1** are linked to the lactol **1c** was conducted. It shows that product formation is initiated as soon as intermediate concentration exceeds 100 mM (Figure C-7). After 3 h the conversion exceeded 95 % and the yield (determined by GC-FID) reached 88.5 %.

As **1** and thus **1c** does not host any functional groups that could serve in further coupling reactions to link the product to the core of the API, its chloro derivative **2** is of greater interest for industry. Fortunately, **2** proved to be converted faster than acetaldehyde. Most of the reaction progress can be observed within the first 60 min of the reaction, after which 75 % yield were detected (Figure C-8). After 3 h more than 90 % were reached. For the continuous flow application, **2** was chosen as aldehyde acceptor for the reasons mentioned above.

2.4 Immobilization of DERA in alginate-luffa matrix

Since the use of a packed-bed reactor brings along a number of advantages over the application of homogeneous catalysts, an appropriate immobilization method for the enzyme was required. Covalent binding to a solid support needs an additional purification step of the enzyme prior linking, which is a labor intense process. In order to keep catalyst preparation simple, adsorption and encapsulation were the remaining options. Adsorption bears the risk of enzyme leaching due to loose binding. Encapsulation into a matrix is a fast, inexpensive and simple technique to immobilize isolated biocatalysts or whole cells.

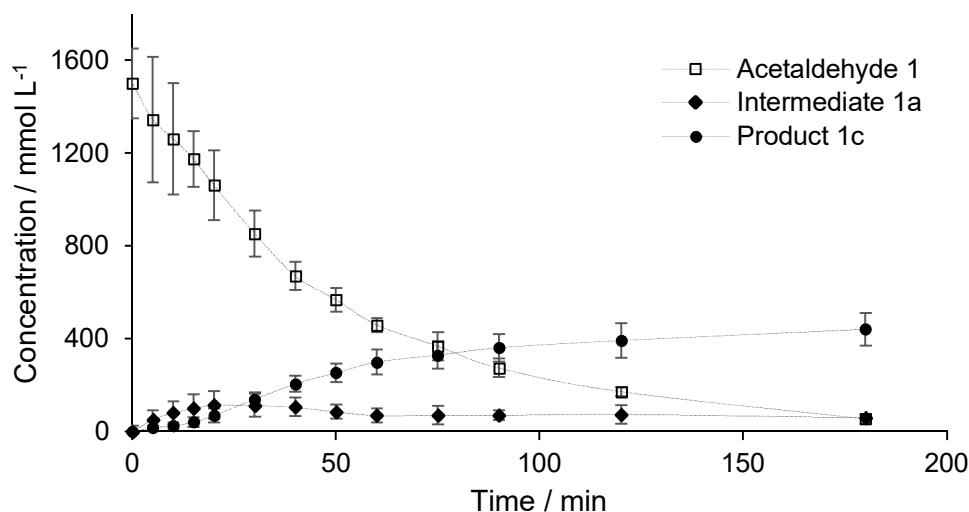


Figure C-7. Time course of conversion of acetaldehyde **1** with DERA to the dimer **1a** and subsequently to the lactol **1c** at the optimized reaction conditions (32 °C, pH 7.5) based on the DoE, 5 mL 0.1 M TEOA buffer, 1.5 M substrate concentration, 70 μ L DMSO, 100 mg DERA in freeze-dried *E. coli* cells.

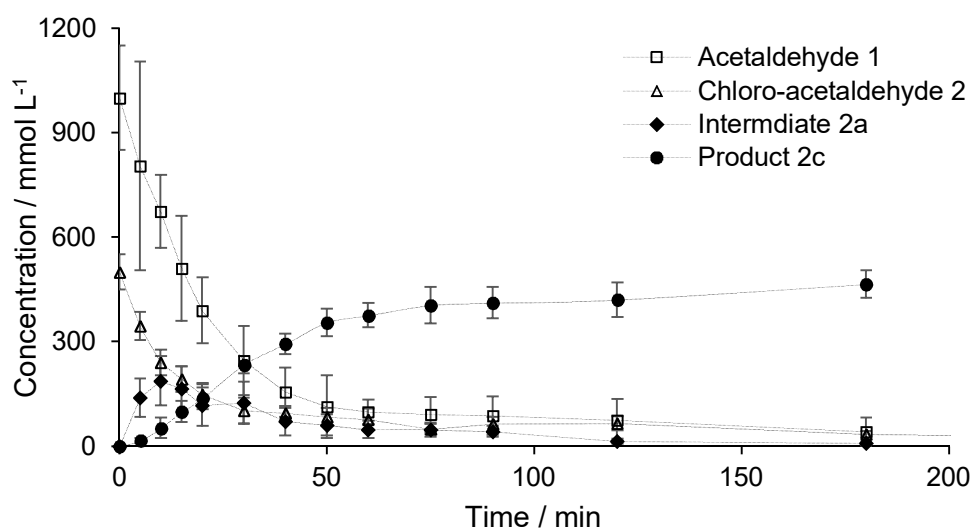


Figure C-8. Time course of batch bioconversion of chloroacetaldehyde **2** (0.5 M) and acetaldehyde **1** (1.0 M) to the dimer **2a** and subsequently to the lactol **2c** at the optimized reaction conditions (32 °C, pH 7.5) based on the DoE, 5 mL 0.1 M TEOA buffer, 70 μ L DMSO, 100 mg DERA in freeze-dried *E. coli* cells.

Alginate is non-toxic, biodegrade and made from a renewable feedstock (bacteria) and thus fulfills all requirements for a “green” matrix for biocatalyst encapsulation. Freeze-dried *E. coli* cells hosting overexpressed DERA were immobilized in two ways alginate beads and alginate of luffa sponge. The former of the two was prepared by dissolving 2 % (w/v) Na-alginate in 2 mL of a 0.9 % (w/v) NaCl-solution. After a clear solution was obtained, the biocatalyst was

suspended in the viscous liquid. To form spherical beads from the suspension, the mixture was dropwise added to a 2 % (w/v) solution of a bivalent cation for cross-linking, Ca^{2+} (CaCl_2) or Ba^{2+} (BaCl_2). Other tested cations (Zn^{2+} , Fe^{2+} and Mg^{2+}) did not lead to sufficient cross-linking to form a stable alginate matrix. Since the alginate matrix displays a barrier for the substrate, what results in a reduction of reaction rate, an increase in surface can be beneficial for the reaction rate. For that, porous material serving as support, which could be coated with the alginate matrix enclosing the enzyme was desired. Luffa sponge was chosen as support because it is a natural product of high porosity. This immobilization technique is called alginate-luffa matrix (ALM). In order to immobilize the same volume of alginate-enzyme mixture on luffa sponge a volume of 2.5 cm^3 (245 mg) as required. The sponge was soaked with the cell suspension and cross-linking was induced either by Ba^{2+} or Ca^{2+} (details in section 4). The results of the ALM were compared with cells immobilized in conventional alginate beads (I.D. 2 mm) (Figure C-9). The comparison shows that ALM is four times more active than the beads. The type of cross-linking cation has hardly any effect on the performance of the enzyme. ALM enclosing DERA was further employed for application in continuous flow.

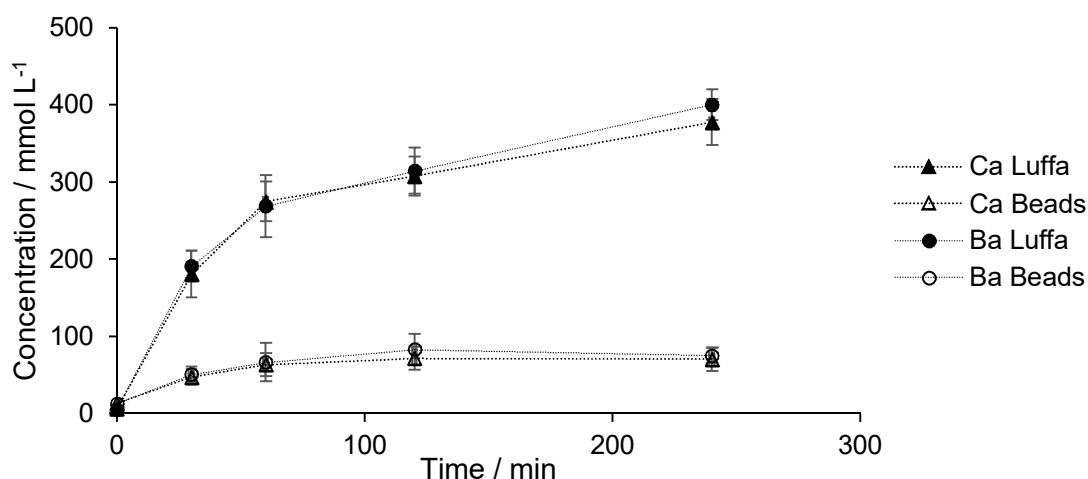


Figure C-9. Time course of lactol formation by immobilized DERA on Luffa or in beads, 5 mL final volume, 0.1 M TEOA buffer pH 7.5, 70 mL DMSO, 0.5 M **2**, 1.0 M **1**, 32.5 °C, 100 mg freeze-dried *E. coli* cells hosting DERA, 2 % (w/v) Na-alginate in 0.9 % (w/v) NaCl-solution, cross-linking induced by Ca^{2+} or Ba^{2+} , 2 % (w/v) respectively.

2.5 Flow application

Flow experiments were carried out in the so-called “Plug and Play” Reactor.⁴¹ It is a modular bench-top reactor (20 cm x 15 cm) equipped with heating/cooling shell and openings for reaction modules (commercially available HPLC columns). For catalyst immobilization a cylindrical piece of the sponge fitting into the column was cut manually to serve as solid support. 850 mg (10 cm^3) of luffa fitted into the column. Immobilized DERA on loofa sponge

was packed in an HPLC column (20 cm x 8 mm) (Figure C-10), which was placed in the reactor. After heating the catalyst to the respective temperature, the bed was flushed with buffer in order to remove residual chemicals from the immobilization process prior running the reaction.

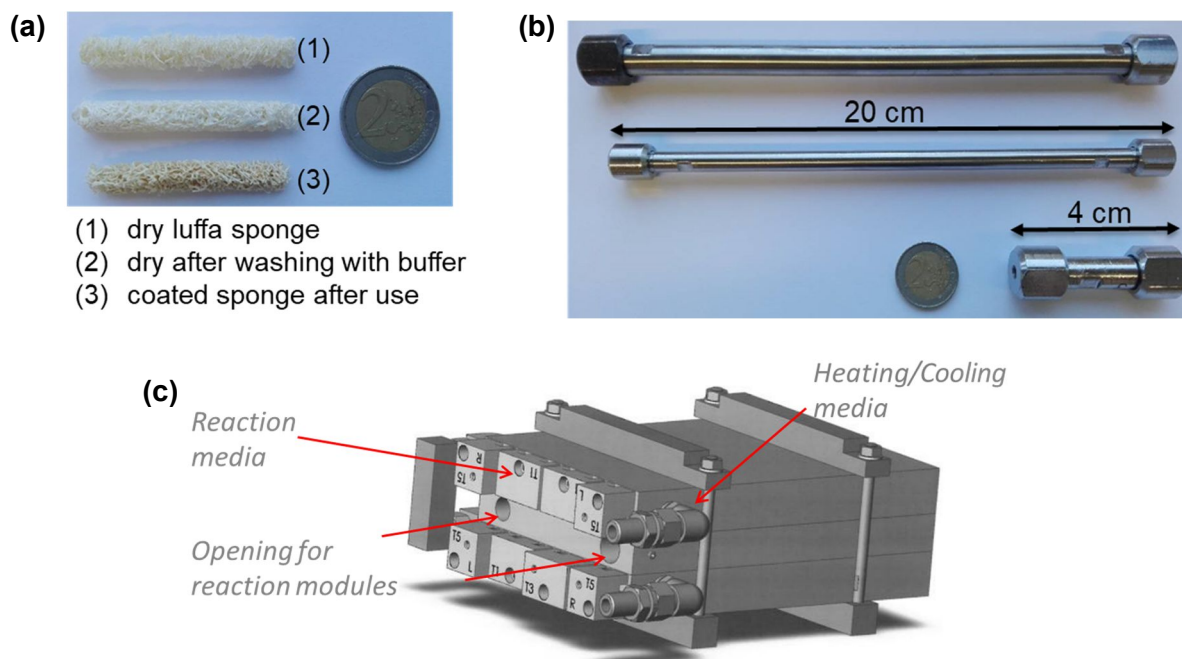


Figure C-10. Equipment used for continuous synthesis: luffa sponge (a), stainless steel tube (b), "Plug and Play" reactor (c)

2.5.1 Residence time distribution

Prior conducting experiments in flow the mean residence time in the reactor for various flow rates was determined. For that, the column was packed with luffa sponge and the mean residence time was determined (details in section 4). The results are summed up in Table C-1.

Table C-1. Theoretically and experimentally determined mean residence times and Bodenstein (Bo) numbers for the three test flow velocities going through an HPLC column (20 cm × 0.8 cm) packed with loofa sponge.

v [mL/min]	\bar{t}_{th} [min]	\bar{t}_{exp} [min]	Bo [–]
0.10	60.5	62.7	15.0
0.25	24.2	26.8	9.5
0.50	12.1	11.4	33.3

\bar{t}_{th} = theoretically calculated mean residence time, \bar{t}_{exp} = experimentally determined mean residence time. See section 4 for details

2.5.2 Design of Experiments for continuous flow application

For optimizing the flow process, the flow rate and substrate concentration were of interest. Furthermore, a potential effect of the cation used to induce cross-linking of alginate on the catalyst performance should be investigated. A full-factorial design for three parameters (flow rate, concentration, cation) was developed. Three levels were set for flow rate (0.1, 0.25 and 0.5 mL/min) and substrate concentration (0.25, 0.5 and 0.75 M **2a**). The influence of the chosen cross-coupling ion was investigated on two levels (Ba^{2+} and Ca^{2+}). The performance of the process was followed by collecting samples at the outlet of the reactor and determining the yield by means of GC-FID. The result was evaluated using MODDE® (Figure C-11 and Figure C-12). DERA immobilized in alginate cross-linked with Ba^{2+} showed stronger dependence on the flow rate and also on substrate concentration. At high substrate concentration this catalyst is less active. Also, high flow rate leads to low yield. Details on the results of the DoE can be found in section 4. Ca^{2+} cross-linked alginate was found to not immobilize the catalyst sufficiently, what led to enzyme leaching and rapid loss of catalyst activity within the reactor. Enzyme leaching was proved by not quenching the samples collected at the outlet of the reactor. The reaction proceeded, indicating the presence of active enzyme in the reaction mixture leaving the column. Ba^{2+} cross-linked alginate did not suffer from enzyme leaching. Therefore, this catalyst could also be applied for an increased period of time in a continuous process.

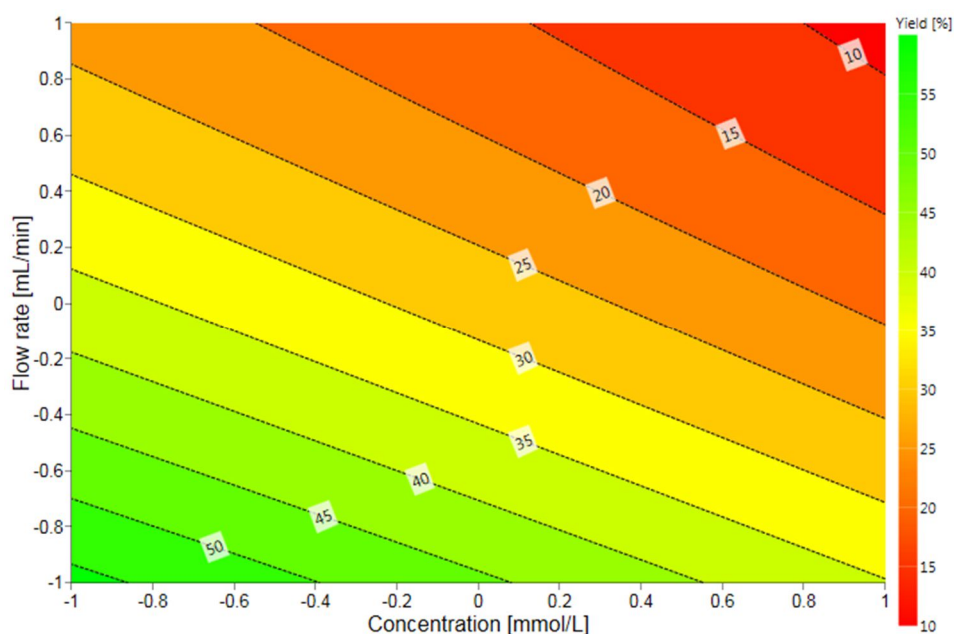


Figure C-11. Response surface for the performance of the continuous flow process for Ba^{2+} cross-linked alginate. Stock: 250 - 750 mM **2**, 500 -1500 mM (2 mol-eq.) **1** in 0.1 M TEOA buffer, pH 7.5 with 1.4 % DMSO, T = 32.5 °C, flow rate: 0.1 – 0.5 mL/min, 350 mg freeze-dried *E. coli* hosting DERA on 850 mg luffa sponge (10 mL of 2 % (w/v) Na-alginate solution), cross-linking by 2 % (w/v) BaCl_2 solution.

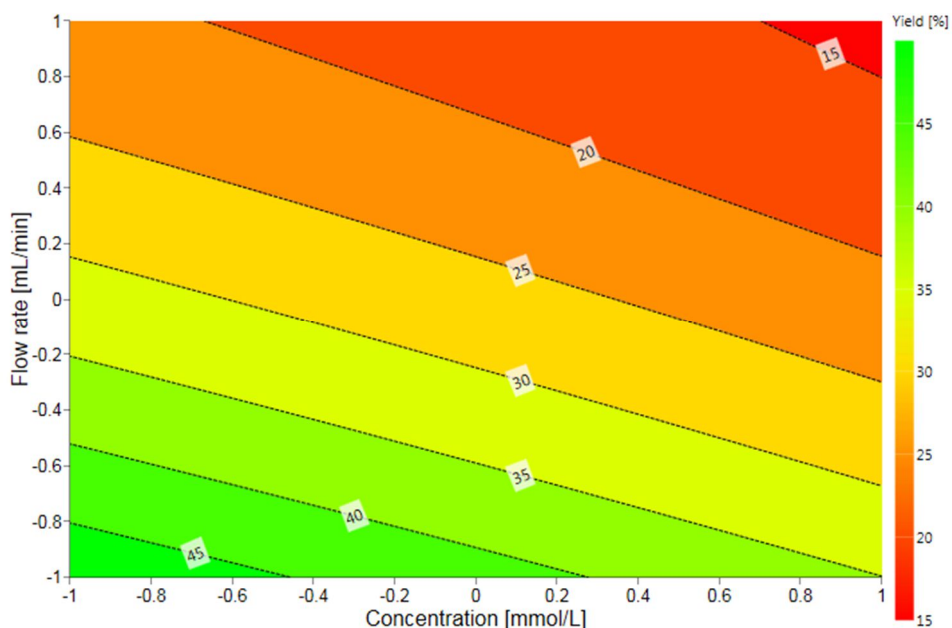


Figure C-12. Response surface for the performance of the continuous flow process for Ca^{2+} cross-linked alginate. Stock: 250 - 750 mM **2**, 500 -1500 mM (2 mol-eq.) **1** in 0.1 M TEOA buffer, pH 7.5 with 1.4 % DMSO, $T = 32.5\text{ }^{\circ}\text{C}$, flow rate: 0.1 – 0.5 mL/min, 350 mg freeze-dried *E. coli* hosting DERA on 850 mg luffa sponge (10 mL of 2 % (w/v) Na-alginate solution), cross-linking by 2 % (w/v) CaCl_2 solution.

2.5.3 Continuous synthesis

As a final step the ideal reaction conditions obtained from the DoE approach were applied for a continuous flow process for the synthesis of a statin side chain precursor. The time course for the process output is shown in Figure C-13. An increase in enzyme loading from 350 mg to 700 mg in the reactor lead to almost 80 % yield of **2c**. However, higher cell concentration in the alginate solution results in a highly viscous mixture, which made the handling and immobilization process more difficult.

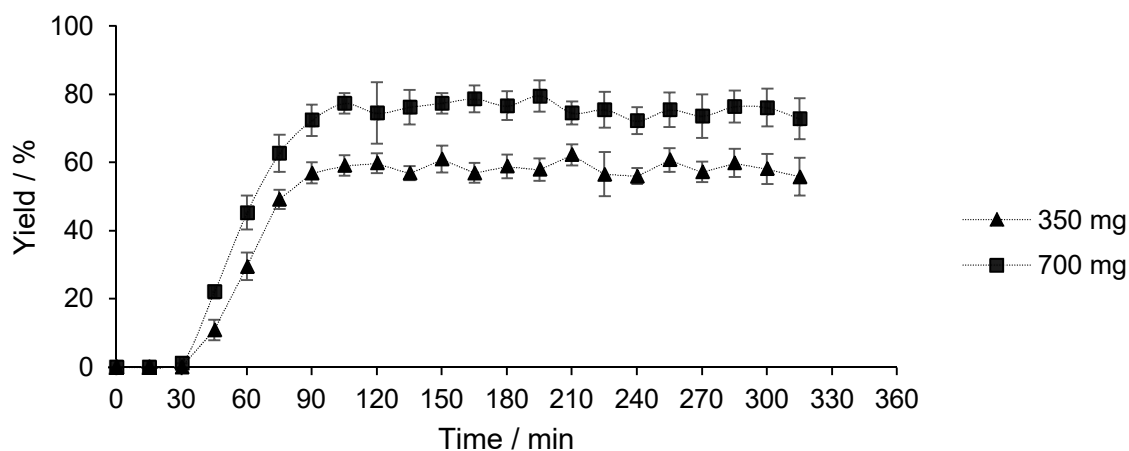


Figure C-13. Yield over time for continuous flow process using 350 mg and 700 mg of freeze-dried cells hosting DERA. $32.5\text{ }^{\circ}\text{C}$, 0.1 M TEOA buffer, pH 7.5, 0.1 mL/min flow rate, 0.25 M **2**, 0.5 M **1**.

3 Conclusion

We were able to develop an optimized continuous flow process for the synthesis of a statin side chain precursor by using a DoE approach. 32.5 °C and pH 7.5 turned out to be the ideal process parameters for DERA (C47M). A series of substrates was tested for its applicability as substrate, but only acetaldehyde **1** and chloroacetaldehyde **2** gave reasonable results. For immobilization alginate was chosen and tested as both alginate beads and alginate-luffa-matrix (ALM), of which the latter of them showed 4-fold higher reaction rate, most likely due to an increased surface area. After identifying ALM as a “green” technique for immobilizing biocatalysts, the enzyme was applied in continuous flow. While ALM cross-linked by Ca²⁺ suffered from enzyme leaching, Ba²⁺ led to sufficiently strong enclosing of the enzyme into the matrix. The usage of freeze-dried cells benefits from the size of the biocatalyst because it can be enclosed into the network more sufficient. ALM has the major advantage that it can be used for almost all biocatalysts to immobilize them in non-covalent encapsulation. The application is only restricted by the limited stability of alginate against harsh chemicals. However, these chemicals are in most cases not in the application field of biocatalysis. Finally, the optimized flow process (0.1 mL/min, 0.25 M chloroacetaldehyde and 0.5 M acetaldehyde) produced 4.5 g of product per day in a bench top reactor not bigger than a sheet of paper in area and 15 cm in height. The heterogeneous biocatalyst performed stable for 4 h and convinces by its simple, inexpensive and fast preparation. The mutant proved stability over the whole course of the continuous process and in the batch processes (homogeneous and heterogeneous). In addition, the whole catalytic system is biodegradable and made from renewable resources. In order to further increase the yield of the process, a longer reaction time could help. Also, an alternative immobilization method, which is not limited to a certain enzyme loading due to rapidly increasing viscosity can be a solution.

4 Experimental

General. All chemicals were purchased from Sigma Aldrich and used as received.

Enzyme expression and purification. 2 µL plasmid isolation and 100 µL of competent *Escherichia coli* cells (strain BL21(DE3)) were combined in a 0.2 cm electroporation cuvette and placed in the BioRad MicroPulser set to “Ec2”. The mixture was pulsed once. 1 mL of SOC medium (0.5 % (w/v) yeast extract, 2 % (w/v) tryptone, 10 mM NaCl, 2.5 mM KCl, 20 mM MgSO₄, pH 7.5) were added and the cells were suspended in the medium. After incubating for 1 h at 37°C the cells were applied on Agar plates containing the antibiotic Ampicillin and were grown over night at 37 °C. On the following day one culture spot was transferred into a shaking

flask together with 200 mL LB medium (5 g/L yeast extract, 10 g/L tryptone, 10 g/L NaCl) and 200 μ L of Ampicillin. The culture was incubated over night at 37 °C. The cells were harvested by centrifugation (15 min, 7000 g, 4 °C) and the obtained pellets were freeze-dried.

Optimization of reaction conditions in batch using Design of Experiments (DoE). In the first round a rough full-factorial lattice with two variables (temperature and pH) was designed. The temperature ranged between 28 and 36 °C in steps of 4.5 °C, while the pH was set to a value between 6.0 and 8.0 in steps of 0.5. Each reaction was carried out with 10 mg freeze-dried cells hosting DERA suspended in 500 μ L of buffer with 1.5 M acetaldehyde as substrate and 7 μ L of DMSO.²⁵ The mixture was stirred with 200 rpm at the respective temperature. Product formation was followed by taking samples after 30 and 60 min. For the samples 100 μ L of reaction suspension were mixed with 400 μ L acetonitrile to stop the reaction by precipitating the enzyme. After separating the inactivated enzyme by centrifugation (10 min, 15,000 rpm) the clear solution was transferred into a GC vial and analyzed by means of GC-FID. The results (yield of intermediate and product) were evaluated by surface fitting in MatLab® using the least square method. A Gaussian function was the result for the description of the activity over pH, while a combination of a polynomial function (increasing activity with rising temperature) and a logarithmic function (describing inactivation at elevated temperature) fitted the surface over temperature. From the response surface a new narrow full-factorial lattice was planned. This time the temperature ranged between 30 and 34 °C (steps 2 °C) and the pH was adjusted to 7.25, 7.5 or 7.75. Reactions and analysis were carried out the same way as for the first round.

GC analysis. Samples were analyzed by means of gas chromatography (GC) using a Perkin Elmer (USA) Clarus 500 equipped with an Optima 5-MS 0.25 μ m, 30 m x 0.32 mm ID capillary column and a flame ionization detector (FID) run on H₂ and synthetic air. N₂ was used as carrier gas. The heating program was set as follows: initial temperature 50 °C (5 min), gradient 10 °C min⁻¹ to 250 °C (5 min). Injection volume: 1 μ L. This method was adapted from literature.⁴² Retention times: **1** 1.6 min, **1a** 3.3 min, **1b** 10.2 min, **1c** 11.9 min, **2** 2.0 min, **2a** 7.9 min, **2c** 15.4 min.

Substrate screening. 100 mg of freeze-dried cells were suspended in 5 mL of 0.1 M triethanol amine (TEOA) buffer pH 7.5. After heating to 32.5 °C, 70 μ L DMSO, the substrates (500 mM acceptor 1-5, respectively and 1 M acetaldehyde 1) were added. The reaction mixture was stirred with 600 rpm. Samples were taken over time. For each sample 200 μ L of the reaction mixture were quenched with 800 μ L of acetonitrile. Centrifugation (10 min, 15,000 rpm) led to good separation of the precipitated catalyst. The supernatant was transferred into a GC vial and analyzed by means of GC-FID.

Immobilization in beads. A 2 % w/v sodium alginate solution was formulated by dissolving 40 mg of Na-alginate in 2 mL 0.9 % w/v aqueous NaCl solution. 100 mg of lyophilized *E. coli*

cells were added and the mixture was stirred to homogeneity. In order to form beads, the mixture was then added dropwise to a 2 % (w/v) solution of the cross-linking cation (CaCl₂, BaCl₂, ZnCl₂, MgCl₂ or FeCl₂) using a syringe and a needle. The beads were stirred in the cation solution for 60 min to let them solidify. The size of the beads could be varied by the diameter of the needle on the syringe. After filtering the beads were washed with 0.9 % (w/v) NaCl solution and kept under ambient conditions for 30 min to let the surface solidify and become more resistant to mechanical abrasion.

Immobilization in ALM for batch reaction. A 2 % w/v sodium alginate solution was formulated by dissolving 40 mg of Na-alginate in 2 mL 0.9 % w/v aqueous NaCl solution. 100 mg of lyophilized *E. coli* cells were added and the mixture was stirred to homogeneity. Afterwards, the carrier (Luffa sponge 245 mg cut into pieces, 2.5 cm³ volume) was soaked in the mixture and transferred to a 2 % (w/v) cation solution (CaCl₂, BaCl₂) where it was gently stirred for 60 min to solidify. The loaded carrier was then washed with 0.9 % NaCl solution, kept at ambient conditions for 30 min to solidify and stored in purified water at 4 °C until usage.

Immobilization in ALM for batch reaction. Loofa sponge was cut to completely be packed into the 20 cm × 0.8 cm HPLC column. The immobilization process is illustrated in Figure C-A11 in section 6. 350 mg or 700 mg, of freeze-dried *E. coli* cells were suspended in a 2 % (w/v) (200 mg) Na-alginate in 10 mL 0.9 % (w/v) NaCl-solution (Figure C-A11 (a)). 850 mg (10 cm³) of cylindrically cut luffa sponge was used to soak up the mixture. After completely soaking up the entire DERA-alginate solution, loofa sponge was submerged into 2 % w/v CaCl₂ or BaCl₂ for 1 h with stirring at room temperature for cross-linking, followed by 30 minutes of air-drying (Figure C-A11 (b)). The resultant loofa sponge carrying immobilized freeze-dried whole cells entrapped by alginate was used to pack the HPLC column for further use in continuous flow experiments

Design of Experiments for optimizing flow process. Continuous experiments were carried out in the so-called “Plug and Play” Reactor.⁴¹ 850 mg loofa sponge with the immobilized enzyme (350 mg cells) was packed in the stainless steel column (20 cm x 8 mm). The reaction medium consisting of 0.25, 0.5 or 0.75 M chloroacetaldehyde **2** and 2 mol eq. of acetaldehyde **1**, with respect to **2**, in 0.1 M TEOA buffer pH 7.5 was pumped through the column using an HPLC pump (Knauer, Azura P4.1 S) set to 0.10, 0.25 and 0.50 mL/min, respectively. The reaction temperature was 32.5 °C. A sample was taken every 15 min by collecting an aliquot of 200 µL of the product stream and diluting it with 800 µL of acetonitrile. After centrifugation (10 min, 15,000 rpm) the supernatant was transferred to a GC vial and analyzed by means of GC-FID. The results were evaluated by means of MODDE®. Details (table of experiments and results) are available in the section 6.

Continuous synthesis. 850 mg loofa sponge with the immobilized enzyme (350 mg cells) was packed in the stainless steel column (20 cm x 8 mm). The reaction medium consisting of 0.25 M **2** and 0.5 M **1** in 0.1 M TEOA buffer pH 7.5 was pumped through the column using an HPLC pump (Knauer, Azura P4.1 S) set to 0.10 mL/min. The reaction temperature was 32.5 °C. A sample was taken every 15 min by collecting an aliquot of 200 µL of the product stream and diluting it with 800 µL of acetonitrile. After centrifugation (10 min, 15,000 rpm) the supernatant was transferred to a GC vial and analyzed by means of GC-FID.

5 References

1. <https://www.who.int/news-room/fact-sheets/detail/the-top-10-causes-of-death> (last accessed January 2019).
2. E. Wilkins, L. Wilson, K. Wickramasinghe, P. Bhatnagar, J. Leal, R. Luengo-Fernandez, R. Burns, M. Rayner and N. Townsend, *European Cardiovascular Disease Statistics 2017*, Brussels, 2017.
3. <https://www.nhlbi.nih.gov/health-topics/ischemic-heart-disease> (last accessed September 2019).
4. E. J. Wald and M. R. Law, *BMJ*, 2003, **327**(7415).
5. K. R. Feingold and C. Grunfeld, *Endotext: Cholesterol Lowering Drugs*, South Dartmouth (MA), 2000.
6. E. S. Istvan and J. Deisenhofer, *Science*, 2001, **292**(5519), 1160.
7. P. Gazerro, M. C. Proto, G. Gangemi, A. M. Malfitano, E. Ciaglia, S. Pisanti, A. Santoro, C. Laezza and M. Bifulco, *Pharmacol. Rev.*, 2012, **64**(1), 102.
8. C. Stancu and A. Sima, *J. Cell. Mol. Med*, 2001, **5**(4), 378.
9. M. Müller, *Angew. Chem. Int. Ed.*, 2005, **44**(3), 362.
10. A. Liljeblad, A. Kallinen and L. Kanerva, *COS*, 2009, **6**(4), 362.
11. A. Ručigaj and M. Krajnc, *Org. Process Res. Dev.*, 2013, **17**(5), 854.
12. A. Ručigaj and M. Krajnc, *Chem. Eng. J.*, 2015, **259**, 11.
13. M. Wolberg, B. H. N. Dassen, M. Schürmann, S. Jennewein, M. G. Wubbolts, H. E. Schoemaker and D. Mink, *Adv. Synth. Catal.*, 2008, **350**(11-12), 1751.
14. S. Jennewein, M. Schürmann, M. Wolberg, I. Hilker, R. Luiten, M. Wubbolts and D. Mink, *Biotechnol. J.*, 2006, **1**(5), 537.
15. H. Fei, C.-c. Zheng, X.-y. Liu and Q. Li, *Process Biochem.*, 2017, **63**, 55.
16. J. Tao and J.-H. Xu, *Curr. Opin. Chem. Biol.*, 2009, **13**(1), 43.
17. J. Britton, S. Majumdar and G. A. Weiss, *Chem. Soc. Rev.*, 2018, **47**(15), 5891.
18. C. F. Barbas, Y.-F. Wang and C.-H. Wong, *J. Am. Chem. Soc.*, 1990, **112**, 2013.
19. H. J. M. Gijzen and C.-H. Wong, *J. Am. Chem. Soc.*, 1994, **116**(18), 8422.

20. H. J. M. Gijzen and C.-H. Wong, *J. Am. Chem. Soc.*, 1995, **117**(10), 2947.
21. H. J. M. Gijzen and C.-H. Wong, *J. Am. Chem. Soc.*, 1995, **117**(29), 7585.
22. H. Sakuraba, K. Yoneda, K. Yoshihara, K. Satoh, R. Kawakami, Y. Uto, H. Tsuge, K. Takahashi, H. Hori and T. Ohshima, *Appl. Environ. Microbiol.*, 2007, **73**(22), 7427.
23. C.-H. Wong, E. Garcia-Junceda, L. Chen, O. Blanco, H. J. M. Gijzen and D. H. Steensma, *J. Am. Chem. Soc.*, 1995, **117**(12), 3333.
24. M. Haridas, E. M. M. Abdelraheem and U. Hanefeld, *Appl. Microbiol. Biotechnol.*, 2018, **102**(23), 9959.
25. M. Dick, R. Hartmann, O. H. Weiergräber, C. Bisterfeld, T. Classen, M. Schwarten, P. Neudecker, D. Willbold and J. Pietruszka, *Chem. Sci.*, 2016(7), 4493.
26. B. Gutmann, D. Cantillo and C. O. Kappe, *Angew. Chem. Int. Ed.*, 2015, **54**(23), 6688.
27. M. B. Plutschack, B. Pieber, K. Gilmore and P. H. Seeberger, *Chem. Rev.*, 2017, **117**(18), 11796.
28. J. Steinreiber, M. Schurmann, M. Wolberg, F. van Assema, C. Reisinger, K. Fesko, D. Mink and H. Griengl, *Angew. Chem. Int. Ed.*, 2007, **46**(10), 1624.
29. M. Colella, C. Carlucci and R. Luisi, *Topics Curr. Chem.*, 2018, **376**(6), 46.
30. J. Britton and C. L. Raston, *Chem. Soc. Rev.*, 2017, **46**(5), 1250.
31. M. Phisalaphong, R. Budiraharjo, P. Bangrak, J. Mongkolkajit and S. Limtong, *J. Biosci. Bioeng.*, 2007, **104**(3), 214.
32. A. Dzionek, D. Wojcieszynska and U. Guzik, *EJB*, 2016, **23**, 28.
33. J. Shen, Y. Min Xie, X. Huang, S. Zhou and D. Ruan, *J. Mech. Behav. Biomed.*, 2012, **15**, 141.
34. J. C. Ogbonna, Y.-C. Liu, Y.-K. Liu and H. Tanaka, *J. Biosci. Bioeng.*, 1994, **78**(6), 437.
35. P. M. Murray, F. Bellany, L. Benhamou, D.-K. Bucar, A. B. Tabor and T. D. Sheppard, *Org. Biomol. Chem.*, 2016, **14**(8), 2373.
36. S. A. Weissman and N. G. Anderson, *Org. Process Res. Dev.*, 2015, **19**(11), 1605.
37. D. Lendrem, M. Owen and S. Godbert, *Org. Process Res. Dev.*, 2001, **5**(3), 324.
38. P. K. Robinson, *Essays Biochem.*, 2015, **59**, 1.
39. M. Dick, O. H. Weiergräber, T. Classen, C. Bisterfeld, J. Bramski, H. Gohlke and J. Pietruszka, *Sci. Rep.*, 2016, **6**.
40. D. C. Wilton, *Biochem. J.*, 1976, **153**, 495.
41. G. J. Lichtenegger, V. Tursic, H. Kitzler, K. Obermaier, J. G. Khinast and H. Gruber-Wöfler, *CIT*, 2016, **88**(10), 1518.
42. M. Ošljaj, J. Cluzeau, D. Orkić, G. Kopitar, P. Mrak and Z. Casar, *PloS one*, 2013, **8**(5), e62250.

6 Appendix

a. SDS-Page DERA

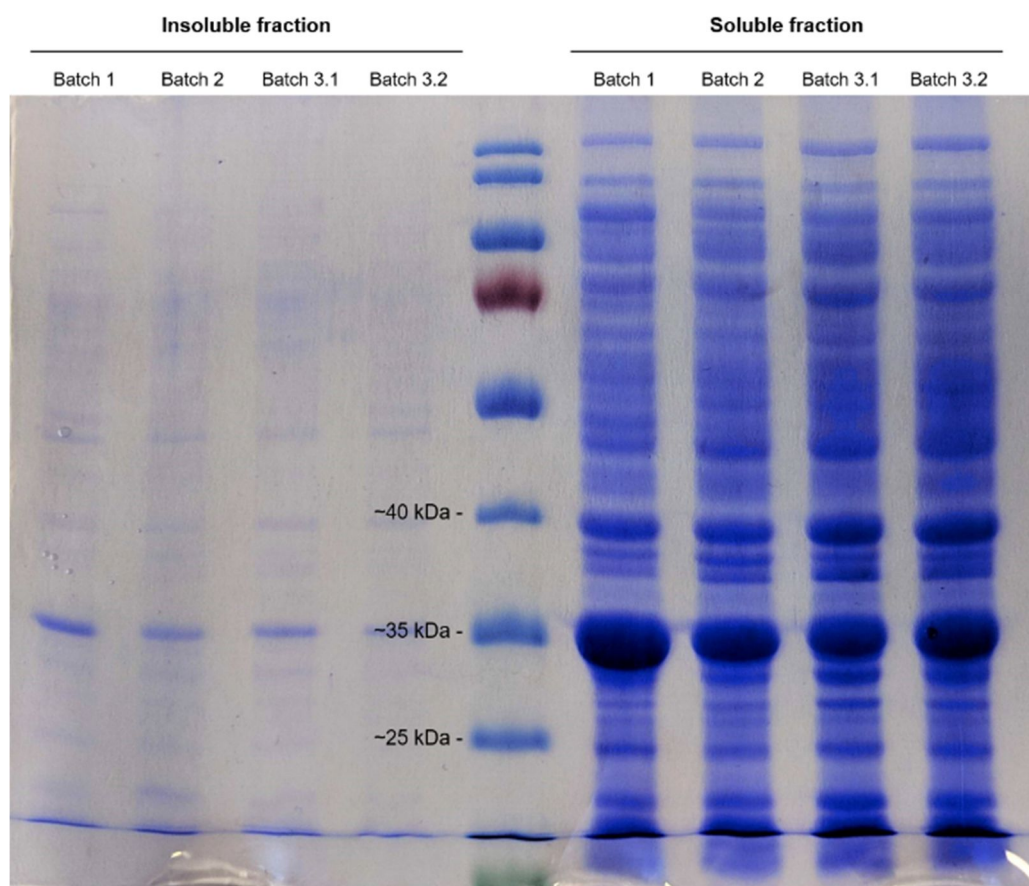


Figure C-A4. SDS-PAGE of freeze-dried *E. coli* BL21 (DE3), containing overexpressed DERA (27.7 kDa)

b. Experimental design for optimization of pH and temperature in batch

Table C-A2. Theoretically and experimentally determined mean residence time and dispersion number for the three test flow velocities going through an HPLC column (20 cm × 0.8 cm) packed with loofa sponge.

Entry	pH code	T code	pH	T / °C	$r_{\text{dimer}} / \mu\text{mol min}^{-1}$	$r_{\text{lactol}} / \mu\text{mol min}^{-1}$
1st circuit						
4	-1	-1	6.0	28.0	1.0	0.1
5	-1	0	6.0	32.5	21.9	0.1
6	-1	1	6.0	37.0	13.3	0.1
7	-0.5	-1	6.5	28.0	18.6	0.0
8	-0.5	0	6.5	32.5	1.0	0.1
9	-0.5	1	6.5	37.0	29.8	0.1
10	0	-1	7.0	28.0	6.4	0.0
11	0	0	7.0	32.5	16.0	1.1
12	0	1	7.0	37.0	5.1	0.0
13	0.5	-1	7.5	28.0	21.8	2.7
14	0.5	0	7.5	32.5	92.4	53.0
15	0.5	1	7.5	37.0	7.8	0.1
16	1	-1	8.0	28.0	24.5	0.7
17	1	0	8.0	32.5	74.5	32.8
18	1	1	8.0	37.0	50.9	0.5
2nd circuit						
19	0.25	0.44	7.25	30.0	150.1	9.4
20	0.25	0.89	7.25	32.0	40.4	45.3
21	0.25	1.33	7.25	34.0	88.2	59.6
22	0.5	0.44	7.50	30.0	154.6	24.8
23	0.5	0.89	7.50	32.0	88.6	46.0
24	0.5	1.33	7.50	34.0	102.4	71.5
25	0.75	0.44	7.75	30.0	15.8	0.0
26	0.75	0.89	7.75	32.0	66.0	46.1
27	0.75	1.33	7.75	34.0	75.2	66.3

Reaction conditions: 500 μL of 0.1 M TEOA buffer containing 1.5 M acetaldehyde, 7 μL DMSO, stir at 200 rpm for 1 h. Sampling: 200 μL of reaction mixture diluted with 800 μL of acetonitrile. Analysis by means of GC-FID

c. GC-Spectra

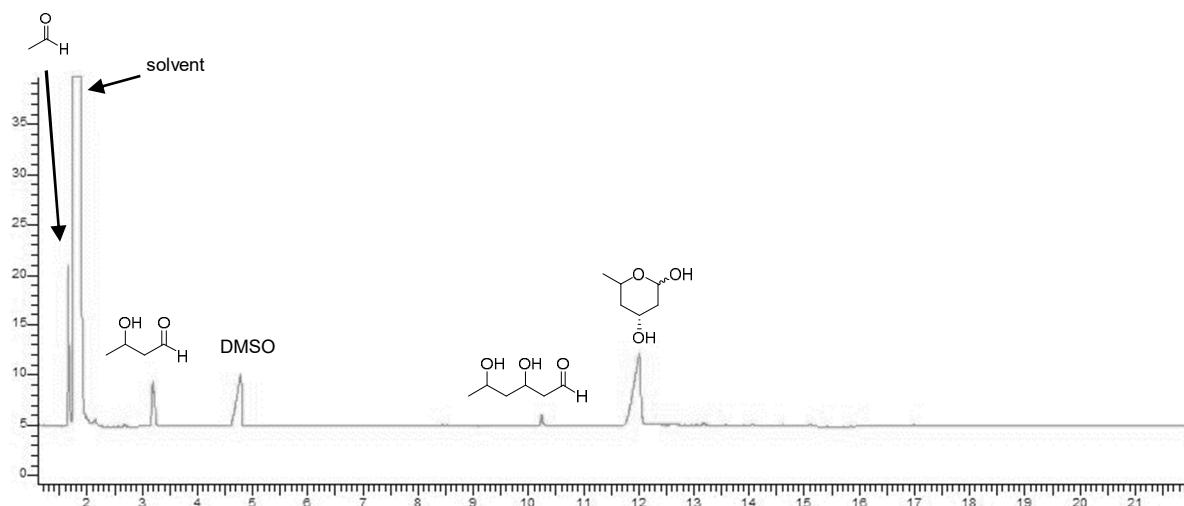


Figure C-A2. GC spectrum from a sample ($t = 120$ min) of a batch aldol addition of three molecules of acetaldehyde.

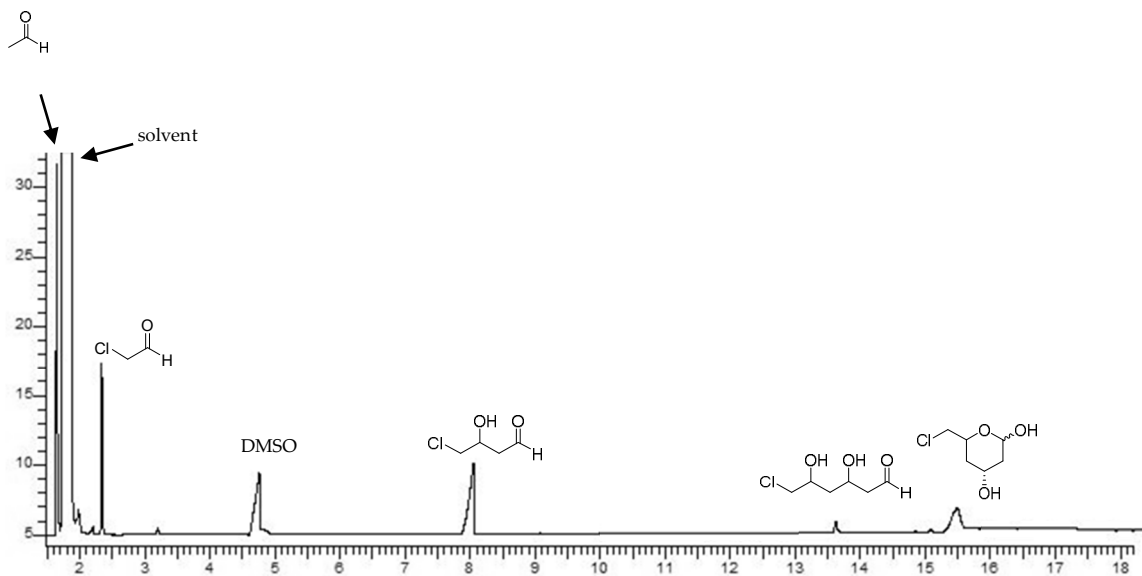


Figure C-A3. GC spectrum from a sample ($t = 30$ min) of a batch aldol addition of chloroacetaldehyde and two molecules of acetaldehyde.

d. GC-FID Spectra and selection of results

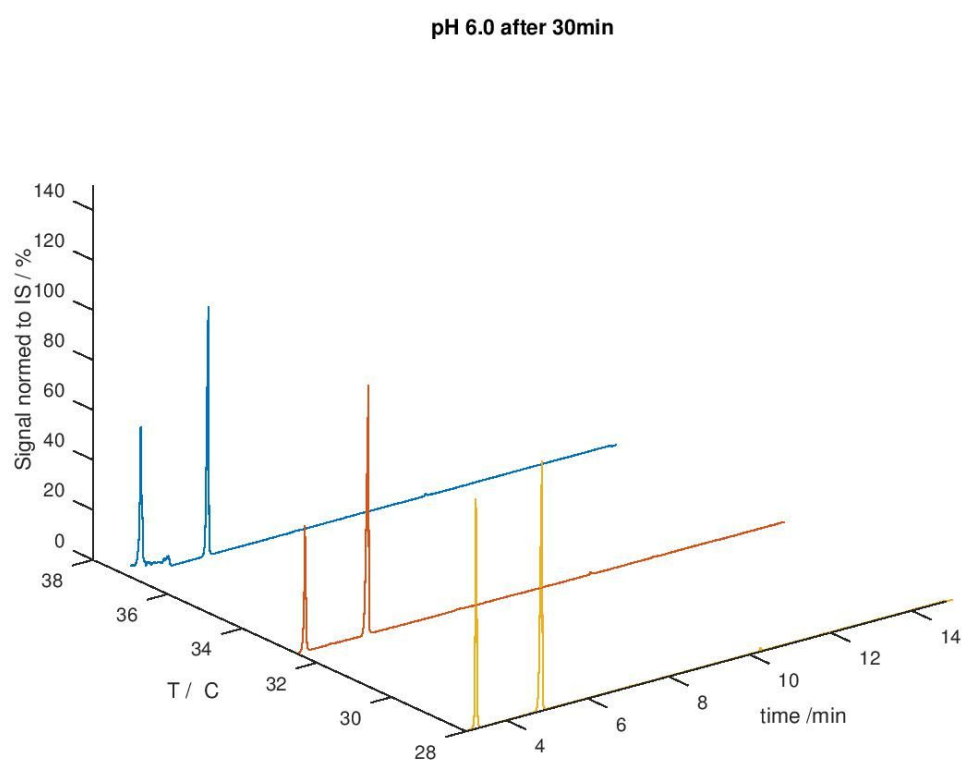


Figure C-A4. GC spectra for DoE runs at pH 6.0, T = 28 – 38 °C, t = 30 min

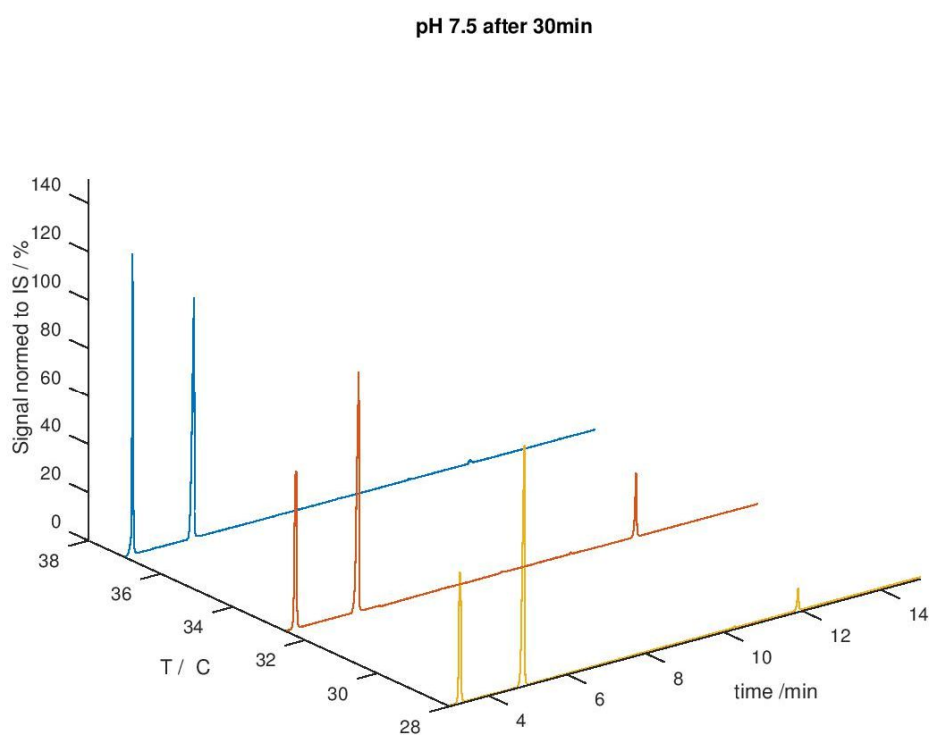


Figure C-A5. GC spectra for DoE runs at pH 7.5 T = 28 – 38 °C, t = 30 min

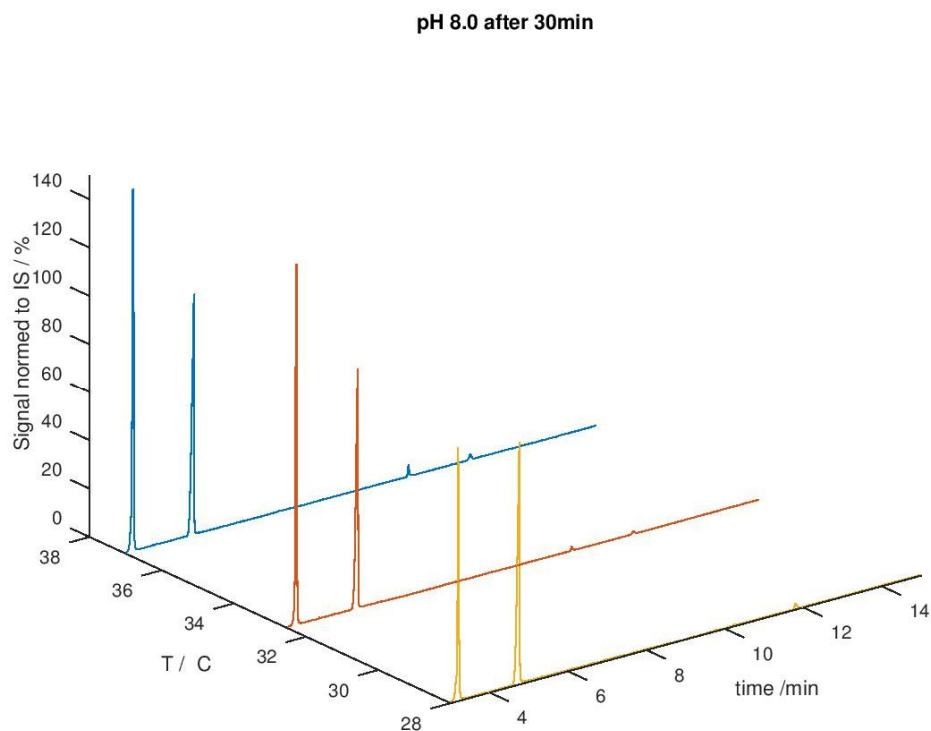


Figure C-A6. GC spectra for DoE runs at pH 8.0 T = 28 – 38 °C, t = 30 min

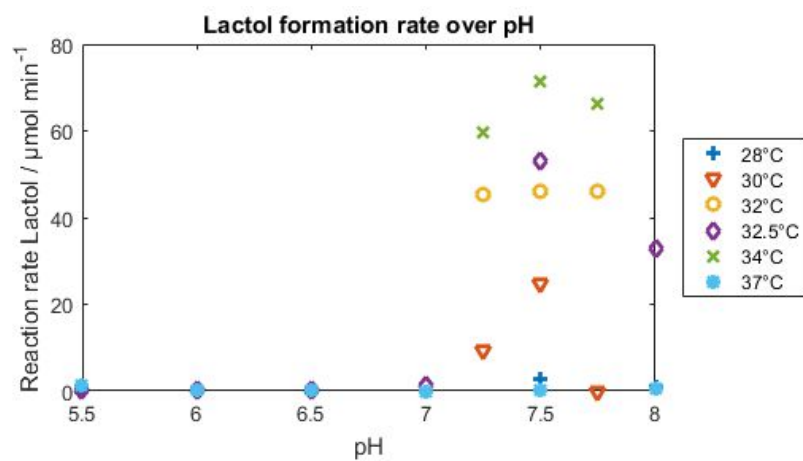


Figure C-A7. Result of DoE (product formation rate) for DoE over pH

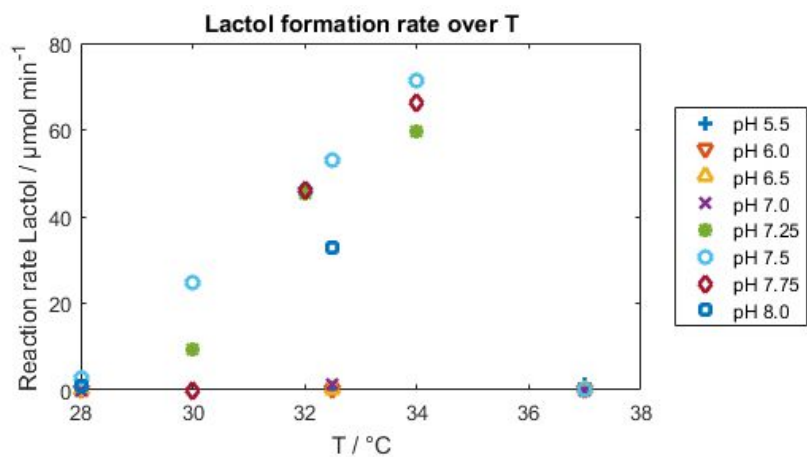


Figure C-A8. Result of DoE (product formation rate) for DoE over reaction temperature

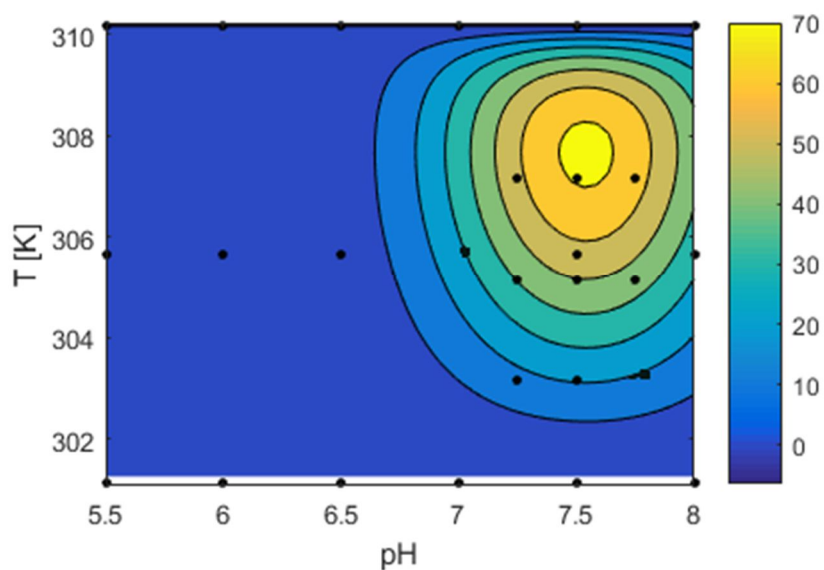


Figure C-A9. Response surface for the experimental design – view from top

e. Coating procedure

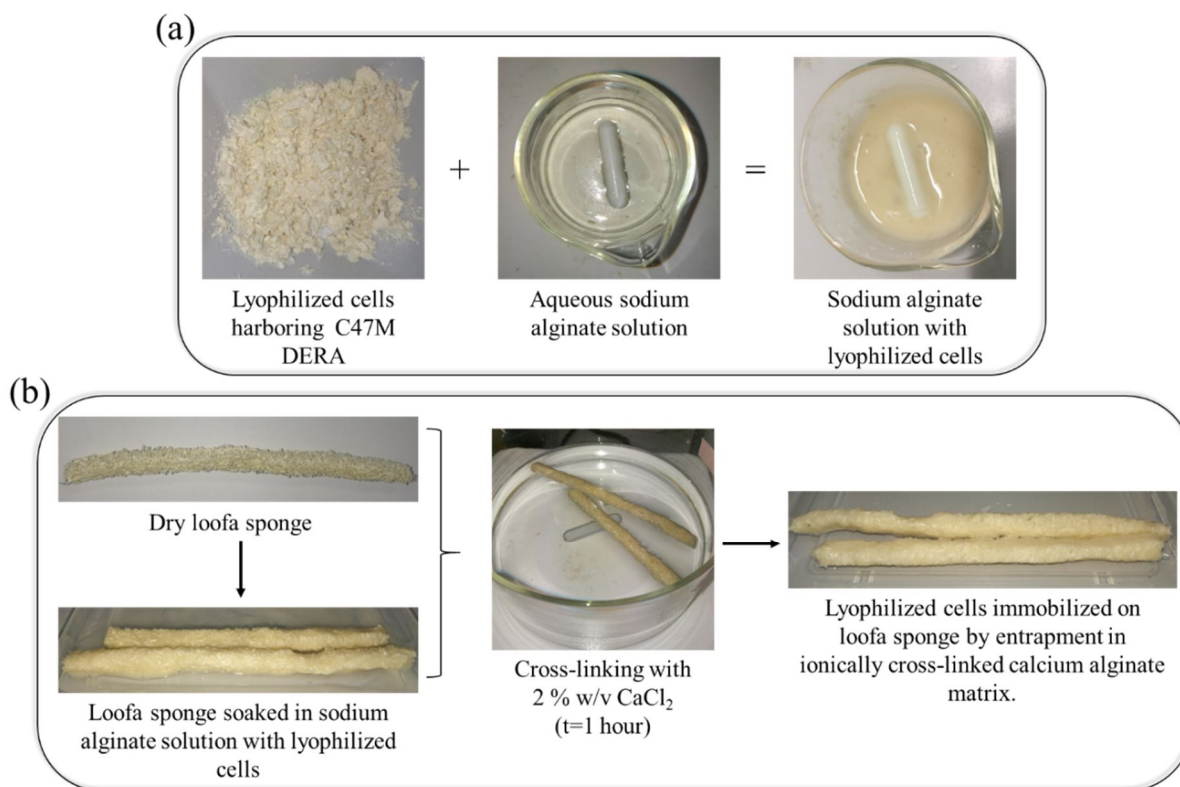


Figure C-A10. Immobilization of the lyophilized cells harboring C47M DERA mutant illustrating (a) preparation of the sodium alginate solution with the lyophilized cells and (b) cross-linking after soaking the sponge in the sodium alginate solution with the lyophilized cells and the final immobilized product.

f. Determination of the Residence Time Distribution (RTD) in the flow reactor

An HPLC (High Performance Liquid Chromatography) column (20 cm × 0.8 cm) packed with loofa sponge was connected to two HPLC pumps (Knauer, Azura P4.1 S) flushed with either solvent (ethanol:water 6:4 v/v) or tracer (0.4 % v/v anisole in ethanol:water 6:4 v/v). The outlets of the HPLC pumps and the inlet of the column were connected via a 6-port injection valve (IDEX Health & Science LLC, V-450) used for efficient solvent switching during a step input. The column was placed inside the plug & play reactor connected to a Lauda P18 Proline thermostat. The tracer signal was detected by an inline UV-vis flow cell (Avantes, Cell-Z-10) with 10 mm optical path length at the outlet of the reactor. UV-vis measurements were performed with an Avantes system equipped with a detector (Avantes, AvaSpec-ULS2048) and a deuterium lamp (Avantes, AvaLight-DS-DUV) light source. The RTD set-up is shown in Figure .

Loofa sponge was soaked in 0.9 % w/v NaCl buffer for one hour. The HPLC column was packed with the soaked loofa sponge and connected to an HPLC pump flushed with 60 % v/v EtOH in H₂O (RTD solvent). The column was flushed vertically with the RTD solvent to get rid of air bubbles. The column was placed inside the plug & play reactor and connected to the UV-vis flow cell with Avantes system. Both pumps were set to identical flowrates of either 0.5 mL/min, 0.25 mL/min, or 0.1 mL/min. After equilibration to a constant signal, a baseline correction was performed by measuring the absorption at 500 nm - 506 nm wavelength. The flow to the column was switched from RTD solvent to tracer (0.4 % v/v anisole in RTD solvent) manually with the 6-port injection valve for the step input. The tracer absorption was measured at 268 nm - 274 nm wavelength. Detected signal values were saved every 500 ms.

Theoretical mean residence time, \bar{t}_{th} , was calculated by the following equation:

$$\bar{t}_{th} = \frac{(V_R - V_S)}{v} \quad \text{Eq. 1}$$

where V_R is the empty reactor volume in mL, V_S is the volume of the loofa sponge soaked in RTD solvent (EtOH) in mL, and v is the flow velocity in mL/min. Volume of a loofa sponge was determined by applying the Archimedes' principle. A loofa sponge was placed in graduated cylinder filled with water and the volume of the displaced water was read from the graduated cylinder marks. Soaked loofa sponge was used to account for the sponge expansion.

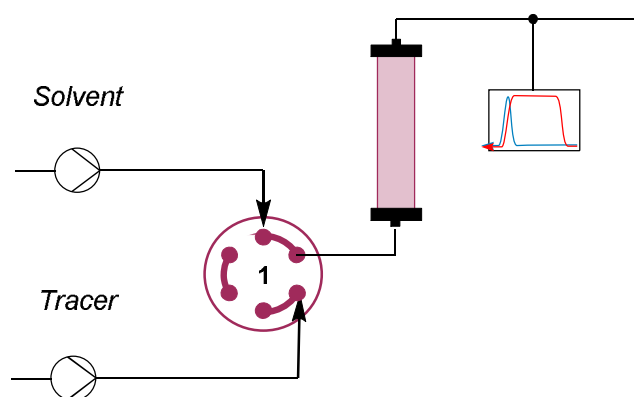


Figure C-A11. Experimental set-up for the RTD determination in flow. The step input is made by switching the manual 6-port injection valve from HPLC Pump 1 (Solvent) to HPLC Pump 2 (Tracer) position, allowing a constant flow of tracer through the column and subsequently the flow cell.

g. Product synthesis in Semi-Batch

Semi-batch reaction was performed based on the protocol described by Ručigaj A. and Krajnc M.¹¹ The enzyme suspension (0.1 M pH 7.5 TEOA buffer, 1.4 % v/v DMSO, and lyophilized cells) preparation and the reaction conditions were identical to the batch reaction. Chloroacetaldehyde (acceptor) and acetaldehyde (donor) were used as substrates for the semi-batch reaction. Both substrates were added to the enzyme suspension of 5 mL

initial volume continuously by the polyvalent programmable syringe pumps (Lambda Laboratory Instruments, VIT-FIT) at different rate. Each pump was equipped with one 20 mL syringe. The syringes were filled with either donor or acceptor in 0.1 M pH 7.5 TEOA buffer at an initial concentration of 2.8 M and 1.8 M, respectively.

For 120 minutes of the semi-batch reaction, chloroacetaldehyde and/or acetaldehyde were added to the enzyme suspension at various rates as described in Table C-A3. After feeding, the reaction was left to proceed for an additional hour. The total reaction time was 3 hours and the final volume of the reaction mixture was 9 mL.

Table C-A3. Semi-batch reaction regime of acetaldehyde (donor) and chloroacetaldehyde (acceptor) feeding.

Feeding Time [min]	Feeding Rate [mL/h]		Amount Fed [mmol]		Final Concentration [mol/L]	
	Donor	Acceptor	Donor	Acceptor	Donor	Acceptor
0-30	2.6	2.9	3.7	2.5	0.50	0.33
30-60	0.9	0.0	1.3	0.0	0.64	0.32
60-120	0.8	0.0	2.0	0.0	0.83	0.29

h. Product isolation and purification

The purification procedure steps were executed according to procedure outlined by Ošljaj et al.⁴² with slight modifications. The purification procedure was optimized and tailored to account for the differences between the reaction conditions.

Intermediate and product purified were synthesized by batch and semi-batch, respectively. After 180 minutes of semi-batch 3 vol. acetone was added to the reaction and left standing at room temperature for 30 minutes to precipitate the enzyme. The mixture was then filtered by gravity filtration using a fluted filter paper for enzyme capturing. Acetone was evaporated under reduced pressure and the enzyme-free reaction mixture was extracted 3 times with 2 vol. ethyl acetate (EtOAc). The organic EtOAc phases were combined, dried over MgSO₄, and filtered with fluted filter paper. After EtOAc evaporation under reduced pressure, intermediate and/or product were obtained as a light brown-yellow oil. The intermediate and product were purified by flash chromatography in silica gel (diethylether/hexane 1:1).

i. NMR

NMR-measurement was performed using a Bruker Avance III 300 MHz spectrometer (¹H: 300 MHz). The chemical shift (δ [ppm]) was reported relatively to the used solvent CDCl₃ (7.26, s).

Product (**2c**)¹⁹: ¹H NMR (CDCl₃): 1.50-2.05 (m, 4H); 3.50-3.60 (m, 2H); 4.10-4.15 (m, 2H); 4.31 (br, 1H); 4.58 (br, 1H); 5.18 (m, 1H);

j. Experimental design for optimization of the flow process

Table C-A4. Conducted experiments (process parameters: concentration of substrate 2, flow rate and cross-linking cation for ALM) for DoE to optimize the flow process.

Entry	Conc. code	Flow code	Conc. of 2 / mM	Flow rate / mL min ⁻¹	Cation	Yield / %
1	1	-1	250	0.10	Ba ²⁺	37.1
2	-1	-1	750	0.10	Ba ²⁺	57.6
3	0	-1	500	0.10	Ba ²⁺	43.3
4	1	1	250	0.10	Ba ²⁺	6.5
5	-1	1	750	0.10	Ba ²⁺	23.1
6	0	1	500	0.10	Ba ²⁺	18.6
7	1	0	250	0.25	Ba ²⁺	19.0
8	-1	0	750	0.25	Ba ²⁺	36.0
9	0	0	500	0.25	Ba ²⁺	28.2
10	1	-1	250	0.10	Ca ²⁺	35.2
11	-1	-1	750	0.10	Ca ²⁺	49.1
12	0	-1	500	0.10	Ca ²⁺	41.0
13	1	1	250	0.10	Ca ²⁺	15.1
14	-1	1	750	0.10	Ca ²⁺	20.2
15	0	1	500	0.10	Ca ²⁺	17.0
16	1	0	250	0.25	Ca ²⁺	21.5
17	-1	0	750	0.25	Ca ²⁺	33.9
18	0	0	500	0.25	Ca ²⁺	26.7
19	0	0	500	0.25	Ca ²⁺	25.9

Reaction conditions: 850 mg loofa sponge, 350 mg freeze-dried *E. coli* cells hosting DERA, 2 mol eq. of 1 with respect to 2. 0.1 M TEOA buffer pH 7.5, 1.4 vol% DMSO, T = 32.5 °C. total run time per experiment 120 min. Analysis by means of GC-FID

k. Details on DoE for optimizing flow process

MODDE supplies additional diagrams and information besides the contour plot of the response surface. The diagrams are shown in Figure C-A12 to Figure C-A17 and a brief explanation is given below.

a. Replicate Plot

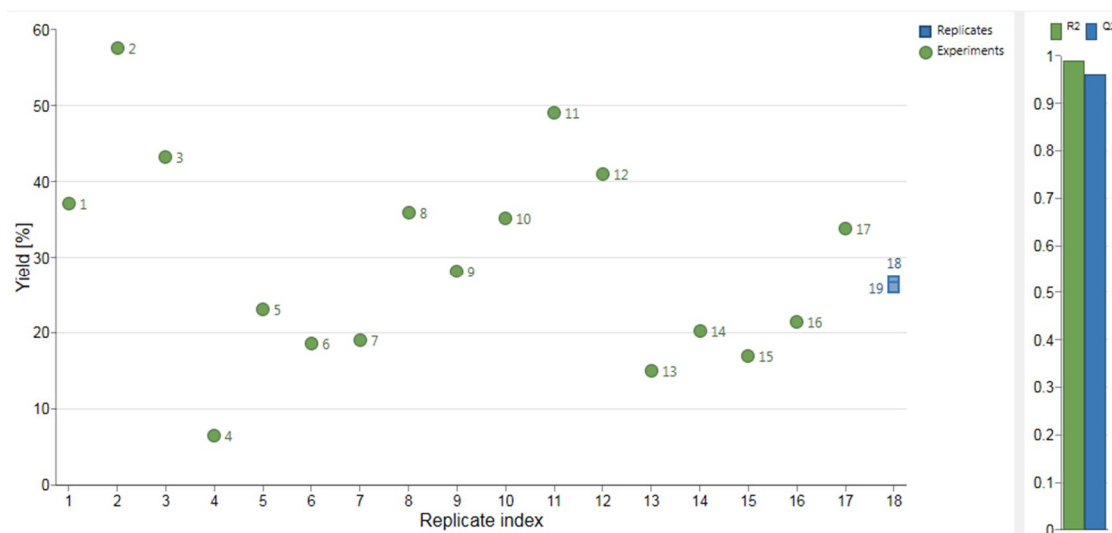


Figure C-A12. Replicate Plot of DoE for optimizing the flow process.

The replicate plot (Figure C-A12) sums up the response (yield) for all experiments conducted during DoE and the replicates. It shows that the variability of the replicates (18 and 19) is small in comparison to the variability of the other experiments. This is a hint that the resulting model will be very useful.

b. Histogram plot

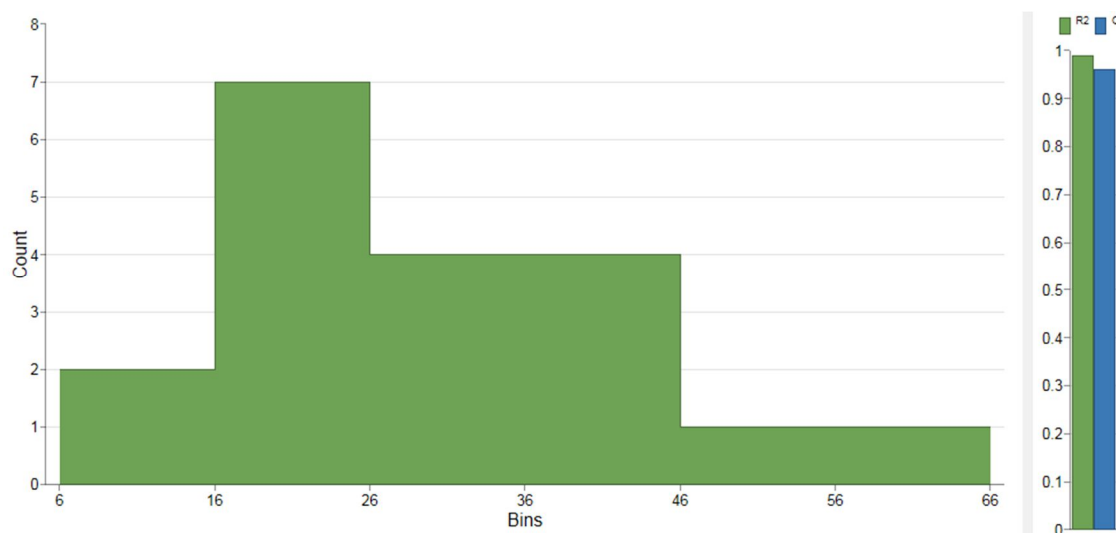


Figure C-A13. Histogram Plot of DoE for optimization of the flow process.

- a. The histogram (Figure C-A13) shows the shape of the response distribution and is used to determine whether a transformation is needed. Since the distribution already meets the requirement of being “bell shaped” no transformation is needed.

c. Coefficient plot

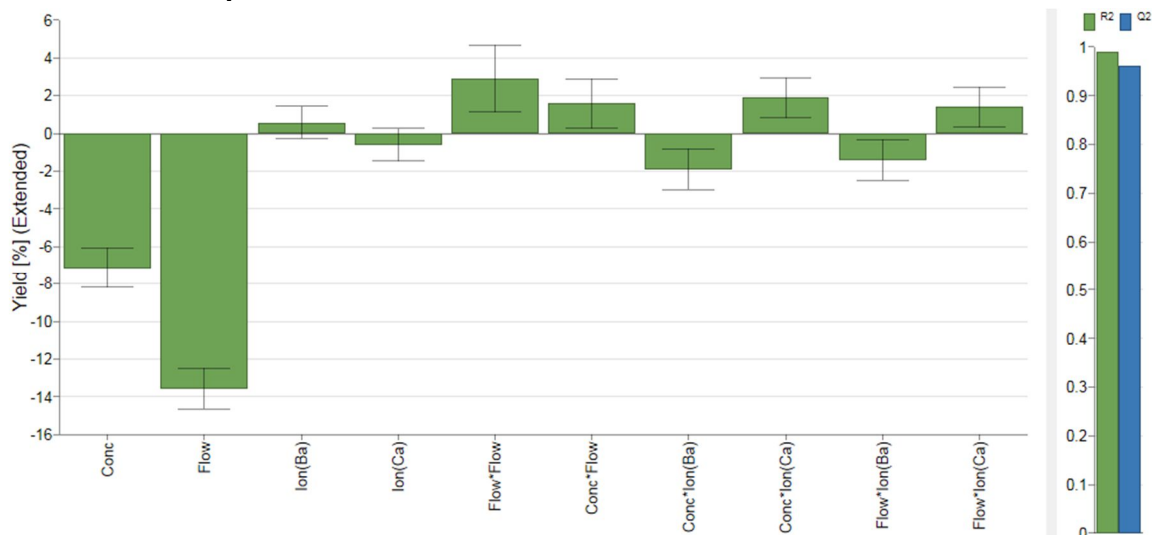


Figure C-A14. Coefficient plot of DoE for optimization of the flow process.

The diagram (Figure C-A14) shows the significance of the terms in the model. The concentration and flow rate have the biggest negative effect. With the value of these two parameters lead to a decrease in yield. The influence of the ion used for cross-linking so smaller than the variation of the experiments and thus does not need to be taken into account, when only looking at the performance of the flow set-up. There are slight interaction effects of the input parameter, but none of the them has a significant effect on the performance of the process as the variance of the experiments is almost as high as detected effect.

d. Summary plot

Figure C-A15. Summary plot of DoE for optimization of the flow process.

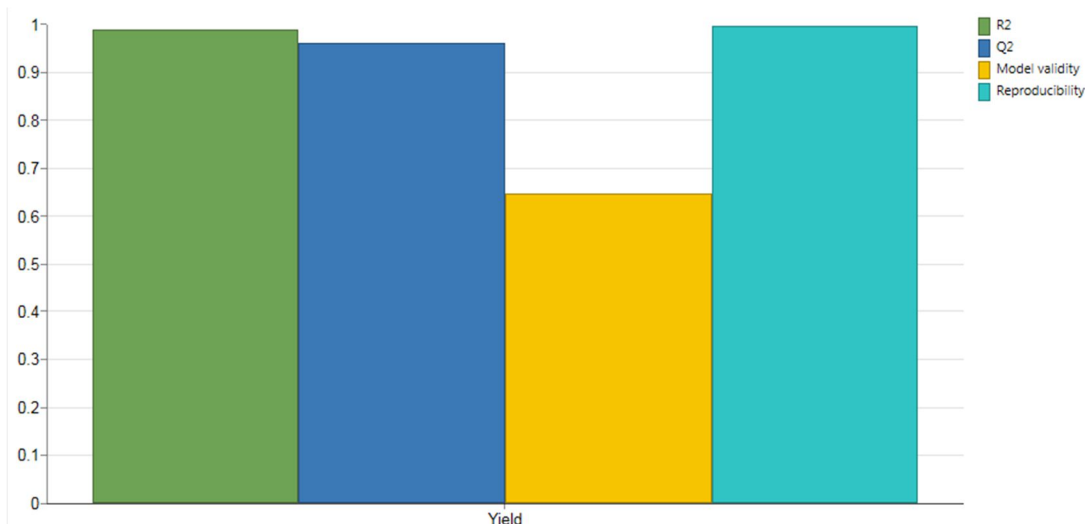


Figure C-A15, the summary plot, gives the model statistics in four parameters. The higher the value for the parameters the better (1 = 100 %). R2 shows the model fit. Q2 shows an estimate of the future prediction precision. A value greater than 0.5 indicates a good model. Model validity is a test of diverse model problems. If this value was lower than 0.25 would mean that statistically significant model problems, such as the presence of outliers, an incorrect model, or a transformation problem is present. Reproducibility is a variation of the replicates compared to the overall variability.

e. Residual Normal Probability plot

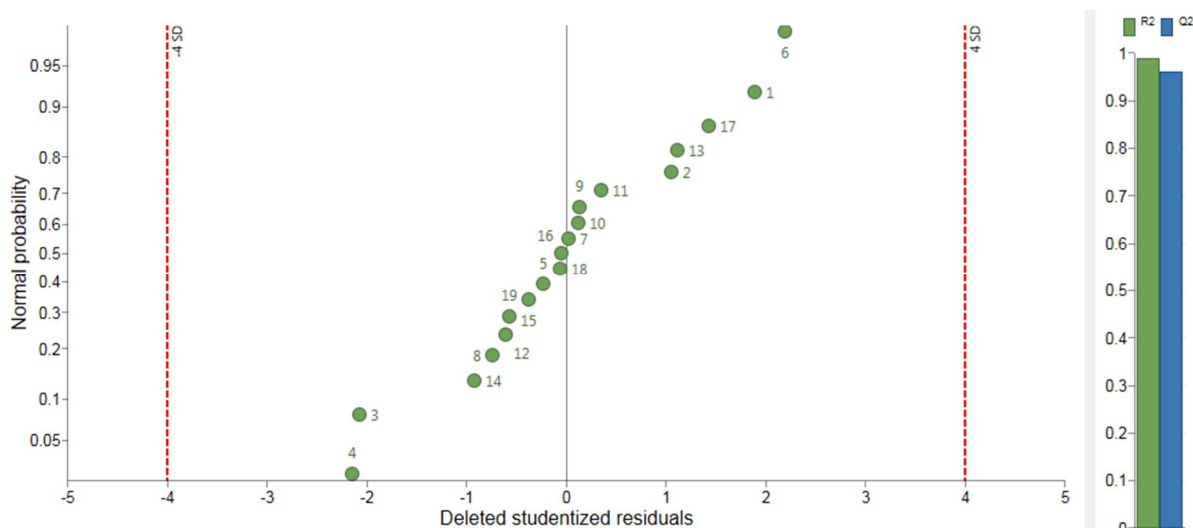


Figure C-A16. Residual normal probability plot of DoE for optimization of the flow process.

This plot (Figure C-A16) shows the residuals of a response vs. the normal probability of the distribution. Most points are on a straight line on the diagonal, indicating that the residuals are normally distributed noise. There are no points outside the red line, which would indicate outliers.

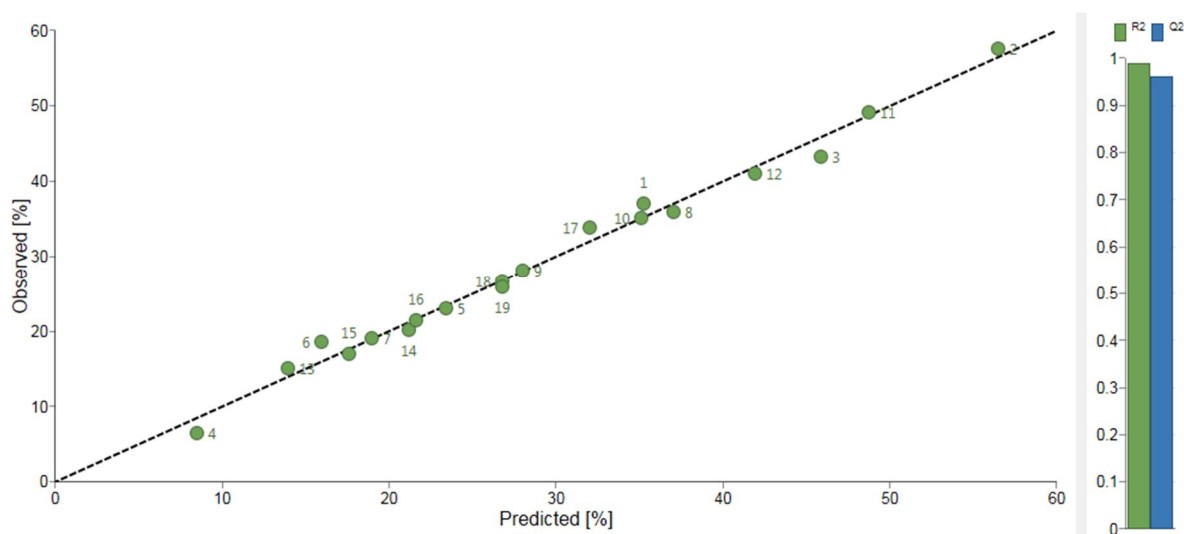
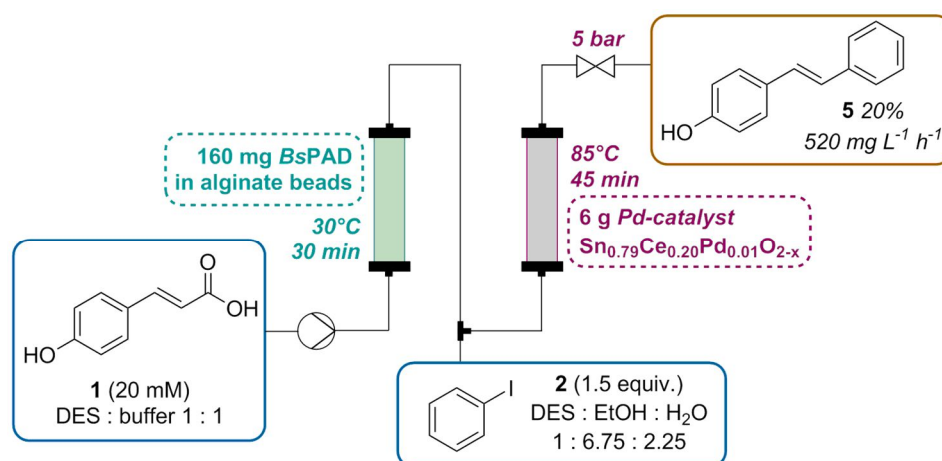
f. Observed vs. Predicted

Figure C-A17. Observed vs. predicted plot of DoE for optimization of the flow process.

This plot (Figure C-A17) displays observed response vs. predicted values. For a good model, the points should be close to a straight line, as it is in this diagram.

D. A chemo-enzymatic tandem reaction in a mixture of deep eutectic solvent and water in continuous flow*

The combination of metal- and biocatalysis is a challenging but forward-looking topic in synthetic chemistry. The unique selectivity of enzymes paired with the broad range of applications of chemical catalysts enables an undreamed-of number of novel processes. Herein, we describe the application of immobilized phenolic acid decarboxylase (PAD) for the decarboxylation of para-coumaric acid and subsequent Pd-catalyzed Heck cross-coupling with an aryl halide in a fully integrated two-step continuous flow process to synthesize (E)-4-hydroxy-stilbene. The application of a choline chloride-based deep eutectic solvent (DES) proved to be crucial to overcome the problem of solvent compatibility and enabled an increase in substrate concentration (from 5 mM in buffer to 20 mM in DES) as well as a process with a homogeneous starting solution. The two-step process was successfully operated for more than 16 h in continuous flow and full conversion was achieved. The results underline the usefulness of DES to overcome compatibility problems in tandem-catalytic processes. The system benefits from its simplicity due to increased substrate solubility, the possibility to conduct both reactions at their optimal temperatures and the elimination of isolating the reaction intermediate, which is prone to polymerization.

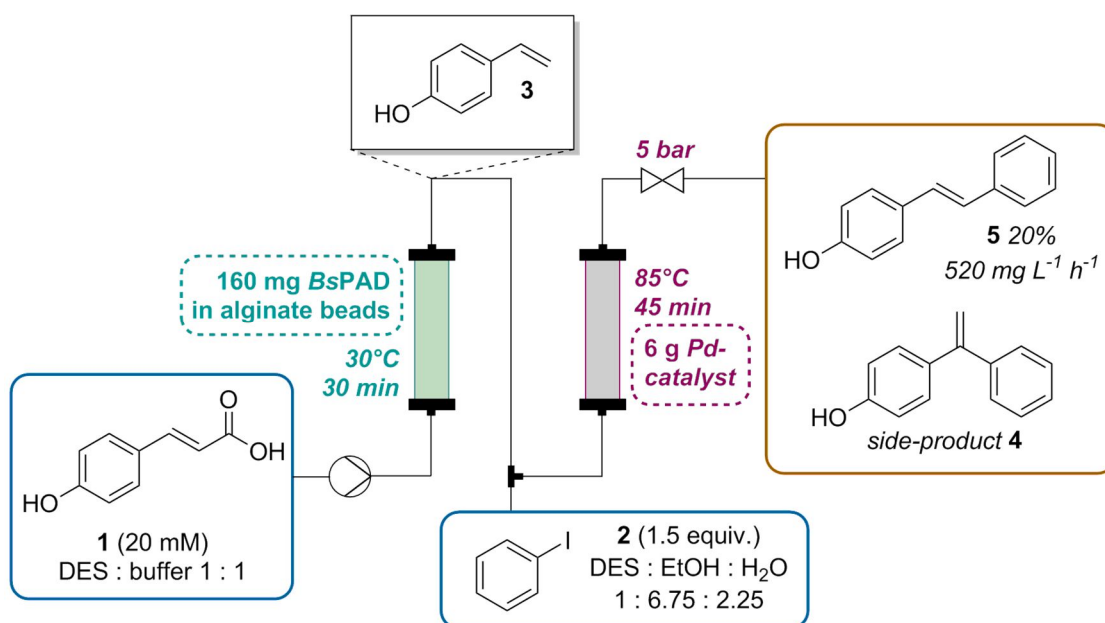


*Parts of the following chapter are published in a journal article by Grabner *et al.*, published in *Reaction Chemistry and Engineering* (Grabner B., Schweiger A. K., Gavric K., Kourist R., Gruber-Woelfler, H., (2020). "A chemo-enzymatic tandem reaction in a mixture of deep eutectic solvent and water in continuous flow".)

1 Introduction

Chemo-enzymatic one-pot syntheses have been attracting increasing attention of researchers in the past decade.¹⁻⁷ These tandem reactions offer the best of both worlds, the versatility of traditional chemical catalysis is replenished with the unbeatable selectivity and mild reaction conditions of enzymes. Nevertheless, besides numerous advantages these promising systems also pose several challenges. One obstacle is the compatibility of the considerable differences of ideal reaction conditions for the individual process steps.^{4,8} Especially, the choice of an appropriate solvent is crucial. Most enzymes show optimal activity in aqueous systems. However, low substrate solubility and the hydrolysis sensitivity of many chemo-catalysts are crucial arguments against the use of neat buffer systems. Alternative solvents, such as deep eutectic solvents (DESs) can help to overcome this obstacle of solvent compatibility.⁹⁻¹³ DESs are mixtures of two or more components which have a lower melting point than the individual compounds at a certain mixing ratio.¹⁴ In recent years these solvents have gained attention due to their simple preparation and tuneable properties. With lower intrinsic toxicity than ionic liquids, DESs have emerged as alternative solutions for issues such as low substrate solubility, enzyme activity and stability. Besides these advantages, DESs also bring along some drawbacks including occasional toxicity and high viscosity, depending on the starting materials. The latter is a challenge in the scale-up of processes, but can be tackled by mixing with water.¹⁵⁻¹⁸ Up to 50 % of water the characteristics of DESs is preserved. In mixtures containing a lower fraction of DES (in the second step in the process described in this work, after adding ethanol and water) their properties are comparable with salt solutions.¹⁹ This good miscibility with water becomes an issue, when the environmental compatibility is discussed. Therefore, a well thought-out process and post-process treatment of DESs and its mixtures with water is required in order to get DES into industrial application.^{20,21} Nevertheless, an impressive series of chemical^{22,23} and enzymatic²⁴⁻²⁶ reactions and also flow applications²⁷⁻²⁹ were successfully conducted in DESs. We have recently shown the feasibility to combine the enzymatic decarboxylation of hydroxycinnamic acids catalyzed by phenolic acid decarboxylase from *Bacillus subtilis* (BsPAD) in water and Ru-catalyzed homo-coupling in organic solvents in a one-pot reaction for the synthesis of a series of bio-based stilbene derivatives.³⁰ In order to expand the scope of the decarboxylation reaction towards the synthesis of asymmetric stilbenes, we envisioned a combination of enzymatic decarboxylation with the Heck reaction.³¹ The most prominent derivatives of stilbenes are resveratrol and its analogues. Due to their conjugated double bond system, many stilbenes possess anti-oxidant, anti-inflammatory, antidiabetic and antiaging properties^{32,33} and are under investigation as active pharmaceutical ingredients (APIs) for cancer preventive drugs.³⁴ For the synthesis of these important compounds, encapsulation proved to be a practical approach to achieve spatial and temporal

separation of the enzymatic in aqueous environment and the metal-catalyzed step in organic solvent.³⁰ Yet, biphasic systems are complex and difficult to scale. Therefore, the goal of this work is a continuous flow process using a solvent compatible for both catalysts and allowing high substrate loadings. Continuous flow synthesis yields a number of benefits over batch operation. Besides consistent product quality and reduced reaction time, the elimination of separation of the catalyst from the reaction solution is a major advantage.³⁵ Furthermore, splitting the two reaction steps into separate continuous flow reactors in a row made it possible to conduct the reaction at optimal reaction temperature for both catalysts (30 °C for enzymatic reaction, 85 °C for Heck reaction). Yet, the limited solubility of hydroxycinnamic acids in buffer of a few mM and the need to add additional 30 % ethanol for the Heck reaction would require to operate with very diluted substrate solutions in order to prevent reactor clogging. Recent findings showed that PAD is highly active in DES.³⁶ Experiments on interactions of the used DES and the biocatalyst were not conducted so far and are not scope of this work. A series of recently investigated DES-protein systems can be found in literature.³⁷ Encouraged by the fact that PAD is highly active in DES, we envisioned that this would be the appropriate solution for the transformation of the one-pot reactions to an integrated multi-step continuous flow process.



Scheme D-1. General reaction scheme for enzymatic decarboxylation with a phenolic acid decarboxylase from *Bacillus subtilis* (BsPAD) yielding 4-ethenylphenol **3**, which serves as substrate for a Pd-catalyzed cross-coupling reaction with aryl halide **2**, resulting in (*E*)-4-hydroxy-stilbene **5** and the side product (*para*-hydroxy-1,1-diphenylethylene **4**).

Furthermore, the combination of both reactions as cascade in flow lower the risks associated to the spontaneous polymerization of the intermediate hydroxystyrene. While conventional flow chemistry,^{38–43} also including C-C coupling reactions,^{39,44–47} and continuous biocatalysis^{48–50} are

currently in the focus of many researchers, examples for their successful combination are rare, which can also be attributed by the difficulties to find suitable reaction media.⁵¹ In this work we present a fully integrated two-step flow setup consisting of an enzymatic decarboxylation with a phenolic acid decarboxylase from *Bacillus subtilis* (*BsPAD*), followed by a Heck reaction catalyzed by a Pd-substituted Ce-Sn-oxide as shown in Scheme 1. For the proof of concept of the synthesis of asymmetric stilbenes, we chose the synthesis of (*E*)-4-hydroxy stilbene **5** from *para*-coumaric acid **1** and iodobenzene **2** because of the low price and good availability of these substrates.

2 Results

2.1 Decarboxylation in batch

We first started with batch experiments to investigate the compatibility of the systems. We recently showed the excellent compatibility of *BsPAD* with DESs.³⁶ Choline chloride (ChCl)-based eutectic mixtures were tested neat and in dilution with potassium phosphate buffer (50 mM, pH 6.0) for the decarboxylation of a variety of phenolic acid derivatives. Our results proved that not only the free enzyme, but also immobilized PAD shows excellent activity in deep eutectic solvents. The 1:1 (v/v) dilution of ChCl/glycerol 1:2 (mol/mol) with buffer gave the best results for PAD. Mixing DES with buffer has not only the advantage of increased enzyme activity and enhanced CO₂ release from the system, but also decreases the viscosity of the solvent system enabling its application in continuous flow.²⁹ With up to 50% water the properties of the DES are predominant and substrate solubility is significantly increased.¹⁹ Therefore, this solvent system was chosen for the first step in our two-step synthesis. As the final process requires a heterogeneous biocatalyst, PAD cell-free extract (CFE) was immobilized in 2 % alginate beads and tested in the DES:buffer mixture. The formation of the decarboxylation product **3** proceeded linearly (Figure D-1) and full conversion of **1** was reached after 6 h (70 mM) and a yield of **3** of 90 % was determined by HPLC. In order to test the heterogeneity of the biocatalyst, a “hot”-filtration test was conducted.⁵² Figure D-2 shows the formation of **3** in the reaction mixture until the beads were filtered off after 45 min reaction time, which stopped the reaction, thus indicating that no active enzyme leaches from the alginate beads under these reaction conditions (Details in section 4). Since the hot filtration test does not prove heterogeneity of a catalyst as a standalike method, further investigations regarding enzyme leaching were required in the flow experiment.

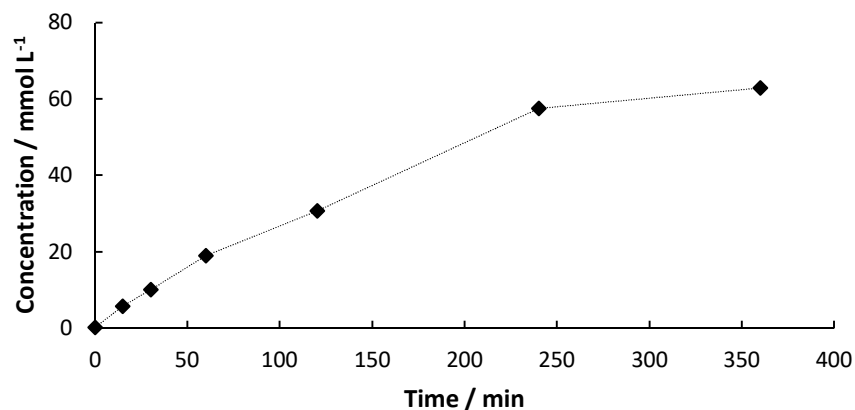


Figure D-1. Concentration of **3** from the decarboxylation of **1** (0.7 mmol) using *Bs*PAD immobilized in alginate beads (2 % (w/v) Na-alginate and 38.3 mg *Bs*PAD (CFE) in potassium phosphate buffer (1 mL, 50 mM, pH 6.0), cross-linking was induced by 2 % (w/v) BaCl₂ solution), 10 mL solvent (DES:buffer 1:1 (v/v)), 30 °C.

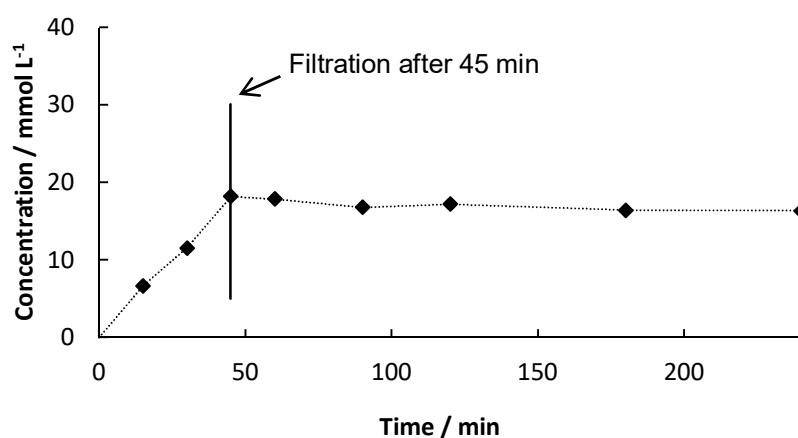


Figure D-2. Concentration of **3** from decarboxylation of **1** using *Bs*PAD immobilized in alginate beads (2 % (w/v) Na-alginate and 38.3 mg *Bs*PAD (CFE) in 1 mL potassium phosphate buffer (50 mM, pH 6.0)), 100 mM substrate in 10 mL solvent (DES:buffer 1:1 (v/v)), 30°C, catalyst beads filtered off after 45 min.

2.2 Heck coupling in batch

For the second step, the Heck coupling of **3** with **2**, an in-house developed heterogeneous Pd-catalyst^{45,53,54} (Pd-substituted cerium-tin-oxide with the molecular formula Sn_{0.79}Ce_{0.20}Pd_{0.01}O_{2.8}) was successfully tested for its activity in the novel solvent system. Full conversion of **3** was reached within 30 min (Figure D-3) with a mixture of DES:buffer 1:1 (v/v)

(from the first step in the continuous application) plus ethanol:water 1:1 (v/v) containing substrate **2** and the required base, K_2CO_3 , (both in 1.5 mol-eq. with respect to **3**).

Due to the similar reactivity of both sp^2 -atoms in the terminal olefin group, formation of two isomers (Scheme D-1) is expected during the Heck reaction, that can either be separated or applied as antioxidant mixture. Unfortunately, there is a number of potential side-reactions, such as homo-coupling of **2** or **3**, subsequent Heck reaction on the double-bond of the product or polymerization of **3**. These reactions led to a low isolated yield of the desired product **5** of 35 % in the batch reaction (for details see section 4).

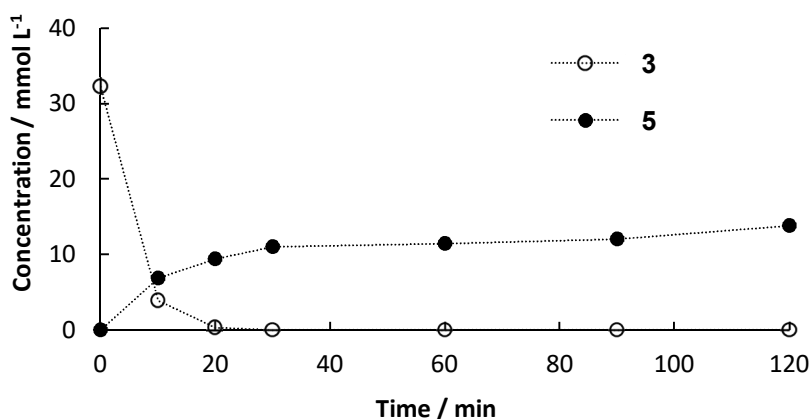


Figure D-3. Concentration of **3** (0.7 mmol) and **5** in a batch Heck coupling with **2** (1.5 mol-eq.) in the presence of a base (K_2CO_3 , 1.5 mol-eq.) using $Sn_{0.79}Ce_{0.20}Pd_{0.01}O_{2.5}$ as heterogeneous catalyst (0.05 mol%) in 20 mL solvent (DES:buffer:ethanol:water 1:1:1:1 (v/v/v/v)), 85 °C

2.3 Combined decarboxylation and Heck coupling in batch

A one-pot reaction was conducted to investigate potential negative impact of the first step on the second one (Figure D-4). A suspension of **1** (70 mM) was stirred together with 80 mg immobilized PAD alginate beads in DES:buffer 1:1 (v/v). After 180 min, the enzyme was filtered off and solvent, substrates and catalyst for the second step were added. Within 2 h all previously formed **3** was converted. Therefore, we can conclude that remaining **1**, which was not converted in the first step, does not negatively affect the performance of the catalyst in the second step and does also not serve as substrate leading to unwanted side-products. It was a very important finding that components from the immobilized CFE do not interfere with the Heck-reaction, which is a crucial requirement for a continuous approach.

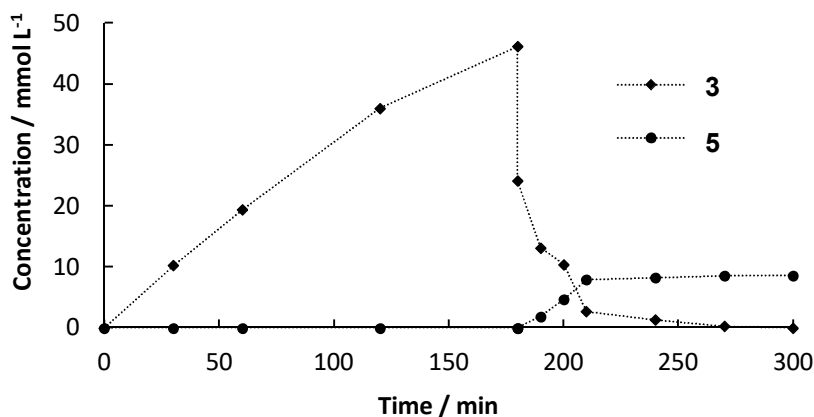


Figure D-4. Product formation over time in one-pot cascade reaction of **1** (0.7 mmol, 70 mM) in 10 mL DES:buffer 1:1 (v/v), 30 °C, 80 mg BsPAD immobilized in 2 % (w/v) alginate beads. Beads were filtered off after 180 min and add 10 mL ethanol:water 1:1 (v/v) containing **2** and K₂CO₃ (1.05 mmol, 1.5 mol-eq. to **1**), 25.2 mg (0.05 mol% Pd loading) of Pd-catalyst, 85 °C

2.4 Individual steps in flow

Before both reactions were combined in a two-step flow process, each reaction was tested in continuous mode. Immobilization of PAD in alginate beads with an average diameter of 2 mm proved to be a straightforward method using cell-free extract, thus avoiding any steps for enzyme purification. The beads were packed into two stainless steel columns (40 mm x 8 mm i.d.) connected in a series with a total volume of 4 mL. This “packed bed reactor” was heated to 30 °C in a water bath. The reactor was filled and flushed with solvent (DES:buffer 1:1 (v/v)) for 1 h before switching to the feed solution containing **1** (20 mM). This lower concentration was chosen to guarantee complete solubility of the substrate (substrate crystals need to be avoided in order to prevent clogging of the capillaries in the continuous setup). The feed stock was pumped with a syringe pump equipped with a 20 mL stainless steel syringe at a flow rate of 45.5 $\mu\text{L min}^{-1}$ resulting in a residence time of 75 min in the whole set-up, of which 30 min was

the residence time within the reactor. Product formation was followed by taking samples of the product stream in 15 min intervals (Figure D-5). The progress of this step could be followed visually as CO₂ bubbles left the reactor as soon a full conversion of the substrate was achieved and no back pressure regulator was used. Details on the flow set-up are available in section 4. In order to investigate the heterogeneity of the immobilized biocatalyst, samples were taken and not quenched, but additional substrate was added. No further product formation was observed, indicating that there is no active enzyme leaching into to product stream.

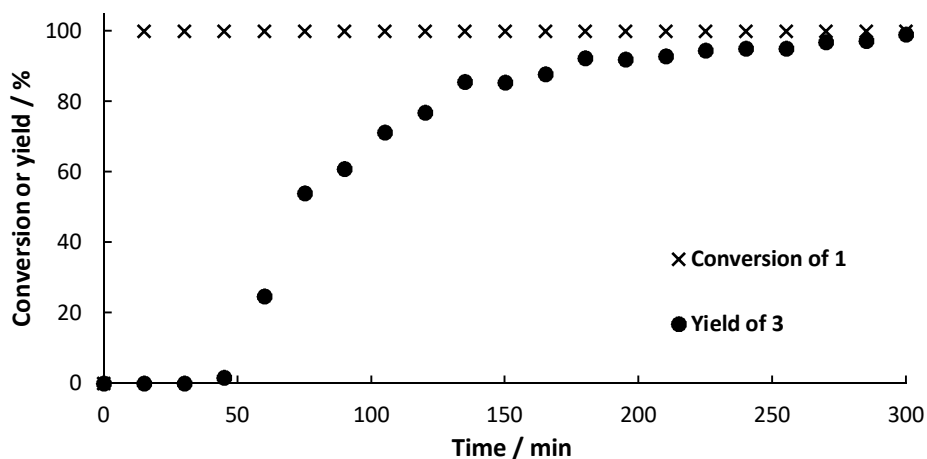


Figure D-5. Conversion⁵⁴ of **1** and yield⁵⁴ (determined by HPLC) of **3** for the continuous flow synthesis. 160 mg *BsPAD* immobilized in alginate beads (4 mL beads volume), 20 mM substrate in DES:buffer 1:1 (v/v), 30°C, flow rate: 45.5 $\mu\text{L min}^{-1}$

Continuous Heck coupling was conducted by packing the catalyst powder (2 g, $\text{Sn}_{0.79}\text{Ce}_{0.20}\text{Pd}_{0.01}\text{O}_{2.6}$) in a stainless steel column (40 mm x 8 mm i.d.).⁵⁵ This packed bed reactor was heated to 85 °C in a water bath. The reactor was flushed with solvent (aqueous solution of DES:buffer:ethanol:water 1:1:1:1 (v/v/v/v)) for 1 h before switching to the feed stock, which contained **3** (10 mM, simulating the product stream from the first step) as well as 1.5 mol-eq. of **2** and K_2CO_3 , respectively, dissolved in DES:buffer:ethanol:water 1:1:1:1 (v/v/v/v). The feed solution was pumped with a syringe pump equipped with a 20 mL stainless steel syringe at a flow rate of 91 $\mu\text{L min}^{-1}$. Samples were taken from the product stream in 15 min intervals and analysed with HPLC. After a start-up time of 200 min a approximate steady-state with an average conversion of 90 % of **3** was reached. The residence time within the reactor was determined to be 45 min. More information can be found in section 4.

2.5 Combined decarboxylation and Heck coupling in flow

Since the outcome of both continuous processes was satisfactory for us, the combination of them was the next goal. For the first step, all the preparations were similar to the single step continuous flow. To improve the performance of the second step, some changes needed to be done. In order to achieve complete dissolution of the substrates, the solvent composition of the feed stock for the second step was adapted to DES:ethanol:H₂O 1:6.75:2.25. Therefore, the final solvent composition for the Heck reaction was 30 vol% DES, 25 vol% buffer, 34 vol% ethanol and 11 vol% water. Furthermore, the amount of catalyst was increased. Instead of a column of 40 mm in length a column with the dimensions 120 mm x 8 mm i.d. was used (6 g of catalyst). The flow rate was set to 45.5 $\mu\text{L/min}$ for both pumps (90 $\mu\text{L/min}$ in sum). Samples of 100 μL were collected every 15 min at the outlet of the reactor. As soon as decarboxylation

product was detected at the outlet of the a column packed with PAD, both steps were connected. CO₂ initially leaving the decarboxylation in bubbles, were not observed after connecting the reactors, because the pressure increased to 5 bar and CO₂ dissolved in the reaction solvent. In a first attempt, some leaching of the enzyme led to channel clogging in the pre-heating tube before the Pd-packed reactor after 11 h (see Figure-D9 in section 4). Blocking of the capillary reduced the supply of intermediate **3** for the second column, which led to increased formation of biphenyl by homo-coupling of the excess **2**. Leaching could easily be overcome by a thorough overnight flushing of loosely bound enzyme from the surface prior to the continuous experiment. In addition to that, a filter (HPLC pre-column filter) was installed after the pre-heating channel, catching the denaturated enzyme. The filter could easily be changed and hence the continuous process could proceed for 16 h in a steady-state with full conversion of both **1** in the first step and **3** in the second step yielding an average of 20 % of desired product **5** (Figure D-6). The yield in the batch process was higher than in the continuous setup, because after full conversion we observed isomerization of **4** to the more stable and desired product **5**. The ratio of both products was determined to be 3:1 (mol/mol) and shift towards **5** with increasing reaction time. However, the rate of isomerization is too small to be considered as a way to synthesize **5**. The product could easily be isolated by evaporation of ethanol followed by extraction in MTBE. The residence time in the reactors was determined to be 30 min for the decarboxylation and 45 min for the Heck coupling resulting in a space-time yield of 4.8 g L⁻¹ h⁻¹ for decarboxylation and 0.52 g L⁻¹ h⁻¹ for Heck coupling. Since constant feed of **3** could be achieved this time, side-product formation due to homo coupling of **2** could be limited to a maximum of 0.8 mM (see Figure D-6). Other potential side reactions are polymerization of **3** resulting in high conversion, but not leading to any detectable product.

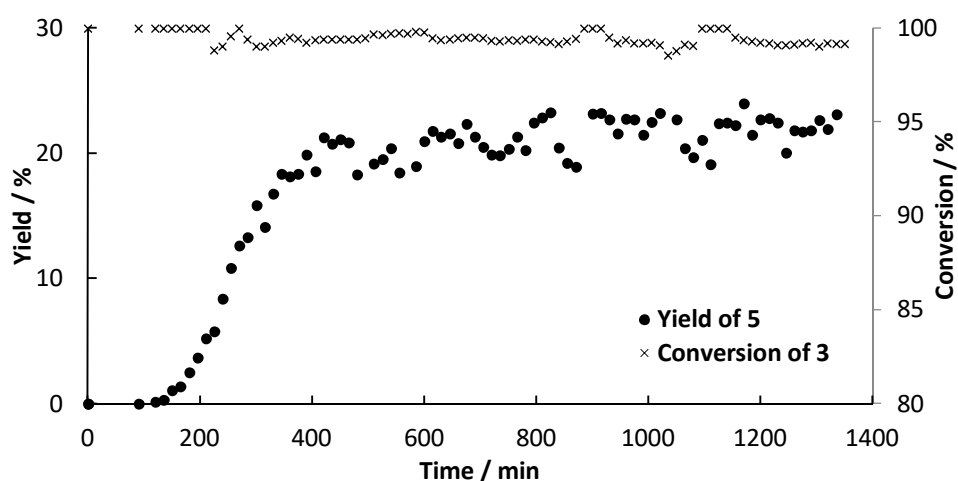


Figure D-6. Yield⁵⁴ (determined by HPLC) of **5** and conversion⁵⁴ of **3** over time for the continuous synthesis by enzymatic decarboxylation by *Bs*PAD and subsequent Pd-catalyzed Heck reaction using Sn_{0.79}Ce_{0.20}Pd_{0.01}O_{2-δ} to couple **2** and **3**.

3 Conclusion

In conclusion, we were able to develop a fully integrated flow process combining an enzymatic decarboxylation by encapsulation of the enzyme and subsequent Heck coupling via a heterogeneous Pd-catalyst. To our knowledge, this is the first example of a chemo-enzymatic cascade in flow using a non-conventional solvent system of DES with water. The outstanding potential of DES to overcome obstacles like substrate solubility and solvent compatibility is a major step towards broad application of continuous flow chemo-enzymatic reactions. In comparison to the one-pot setup, continuous flow requires a reduction in substrate concentration. However, long-term usage of catalysts in continuous flow is economically and ecologically more favourable. Admittedly, the complex chemistry of the chosen reaction leads to a number of side reactions and thus a low yield of the desired product. Nevertheless, due to the elimination of the isolation of the highly reactive intermediate, the use of bio-based, cheap substrates and the reuse of the expensive Pd-catalyst, this proof-of-concept can be the first step on the path to establish flow reactions in aqueous DES mixtures.

In near future further substrates will be tested for their potential to serve as bio-based substrates for the decarboxylation in order to extend the scope of this setup. Furthermore, experiments regarding catalyst and enzyme activity, stability and heterogeneity are planned. Additionally, optimization of process parameters and product ratio are currently under investigation.

4 Experimental

General. All chemicals and starting materials were purchased from Sigma Aldrich and used as received.

Expression of BsPAD and variants. The recombinant pET28a expression plasmid, containing the *padC* gene (Gene ID: 398579 encoding for PAD from *Bacillus subtilis*, was constructed as described elsewhere.¹ Both recombinant plasmids pET28a_BsPAD_WT were provided by the authors. Chemo-competent *E. coli* BL21 (DE3) cells were transformed with the expression plasmids and single colonies were used to inoculate overnight cultures (5 mL LB-Kan, 40 µg/µL kanamycin), which were incubated at 37 °C and 130 rpm. The complete overnight culture was used to inoculate 200 mL TB-Kan medium in 1 L baffled flasks. Cultures were incubated at 37 °C and 130 rpm, until OD₆₀₀ reached 0.5-0.7 and protein expression was induced by addition of IPTG to a final concentration of 0.1 mM. After incubation at 20 °C and 120 rpm for 20-24 h the cells were harvested by centrifugation (15 min, 4500 rpm, 4 °C) and

the cell pellet was washed once with 50 mM KPi buffer (pH 6). Cells were either stored at -20 °C or directly used for the preparation of cell-free extract.

Preparation of cell-free extract and freeze-drying. Cell pellets were resuspended in 50 mM KPi buffer (pH 6) to a concentration of 100 mg_{cww} mL⁻¹ and lysed by sonication (Branson sonifier 250; 5 min, Duty cycle 5, Output control 50 %). The cell-free extract obtained after centrifugation (20 min, 11000 rpm, 4 °C) was sterilized by filtration, shock-frozen in liquid nitrogen and directly used for freeze-drying (AdVantage Pro Lyophilizer, SP Scientific). The lyophilized cell-free extract was stored at -20 °C until further use.

Enzyme immobilization. Cell-free extract (CFE) was dissolved in 2 % (w/v) sodium alginate solution in 50 mM potassium phosphate buffer (pH 6.0) in a concentration of 38.8 mg/mL. The mixture was then dropwise added to a 2 % (w/v) BaCl₂-solution in purified water using a syringe and a needle (0.8 mm ID) in order to form uniform beads of approximately 2-3 mm diameter. The beads were gently stirred in BaCl₂-solution for 1 h to solidify and turned from almost clear to opaque. The beads were washed with 0.9 % (w/v) NaCl-solution and dried in ambient conditions for 30 min in order to solidify the surface of the beads and make them more resistant to shear forces. In the case more enzyme needed to be immobilized, the amount of potassium phosphate buffer was adjusted to the amount of cell-free extract. All the other parameters and concentrations were kept constant.

Preparation of DES. For the preparation of the deep eutectic solvent (DES), the components choline chloride (ChCl) and glycerol were weighed out in a ratio of 1:2 (mol/mol) and mixed together. The mixture was heated to 80 °C and stirred for 1 h. After cooling down, the prepared clear viscous liquid could be used as reaction solvent.

Preparative synthesis of 4-Vinylphenol. *Para*-coumaric acid **1** (5 mmol) was mixed with 500 mL potassium phosphate buffer (50 mM, pH 6.0 (final concentration: 10 mM)) in a 1 L round bottom flask (Substrate does not completely dissolve in buffer!). 100 mg of lyophilized cell free extract (CFE) of PAD WT were added and the reaction mixture was stirred at 30 °C. The reaction was monitored by thin layer chromatography (TLC) on silica coated aluminium plates (Merck, silica gel 60, F254) and spots were visualized with UV light (254 nm) (cyclohexane/ethyl acetate = 1:1, R_f (**1**) = 0.36, R_f (**3**) = 0.78). When full conversion was detected by TLC, the reaction mixture was extracted with methyl-*tert*-butyl ether (MTBE) (2 x 300 mL). The enzyme precipitating in this step was filtered off. To ensure quantitative extraction of the product, TLC analysis of the aqueous layer was performed after extraction. The combined organic layers were washed with brine (1 x 300 mL) and dried over anhydrous Na₂SO₄. Parts of the solvent were removed to obtain the product as a 50 mM solution in MTBE. The solution was stored at 4 °C until further use.

Decarboxylation Batch Experiments. The prepared alginate beads (38.8 mg CFE in 1 mL KPi buffer) were suspended in the solvent mixture of 5 mL DES (choline chloride/glycerol 1:2 (mol/mol)) and 5 mL potassium phosphate buffer (50 mM, pH 6.0) in a round bottom flask and heated to 30 °C. 115 mg (0.7 mmol) of *para*-coumaric acid were added (did not dissolve!) and samples were taken after 0, 15, 30, 60, 120 and 240 min. For each sample 100 µL of the reaction mixture were diluted with 1 mL of HPLC solvent (methanol: HPLC buffer 7:3, HPLC buffer = water:H₃PO₄ 300:1)). The sample was filtered through cotton to remove particles from non-dissolved *para*-coumaric acid.

Hot-filtration test. A hot-filtration test was conducted to investigate the heterogeneity of the biocatalyst. The reaction was set up similar to the batch decarboxylation. Samples were taken after 0, 15, 30 and 45 min. After the 45 min sample the alginate beads were removed by filtering the reaction mixture through a preheated filter (30 °C). The remaining solution was further heated and stirred until the whole reaction time of 240 min was reached. Samples were taken after 60, 90, 120, 180 and 240 min of the overall reaction time.

Synthesis of the Pd-catalyst. The catalyst synthesis was adopted from the procedure described by Lichtenegger *et al.*² All the starting materials ((NH₄)₂Ce(NO₃)₆ (2.124 g), SnC₂O₄ (3.162 g), PdCl₂ (0.034 g) and glycine (3.345 g) were weight out in a mortar and well mixed with a pestle. The mixture is then dispersed in 3 mL of water in a 600 mL beaker. The dispersion was treated with ultrasound until a homogeneous solution is obtained. The redox mixture was heated to 350 °C in a furnace, where a self-propagating combustion reaction takes place. The product, a light yellow-brown porous solid, was ground and again heated in the furnace to 350 °C for another 5 h. The obtained yellow-brown powder was used as catalyst without further treatment.

Heck Batch Experiments. MTBE of the storage solution (avoid polymerization) needed to be removed from the starting material under reduced pressure prior the reaction because MTBE was found to inhibit the reaction. In order to avoid polymerization of the reactive styrene substrate the solution was cooled in an ice bath. The concentration of the starting solution was 50 mM. 14.0 mL of solution was evaporated to obtain 84.1 mg (0.7 mmol) of 4-vinylphenol. The remaining substrate (colorless oil) was dissolved in the reaction solvent consisting of 5 mL DES (choline chloride/glycerol 1:2 (mol/mol)), 5 mL potassium phosphate buffer (50 mM, pH 6.0), 5 mL ethanol and 5 mL purified water. The second substrate (iodobenzene) (1.05 mmol) and K₂CO₃ (1.05 mmol) were added and the mixture was heated to 85 °C. Afterwards the reaction was started by adding 5 mg of catalyst. Samples were taken after 0, 10, 20, 30, 60, 90, 120 and 240 min and analyzed by means of HPLC. For each sample 100 µL of the reaction mixture were diluted with 1 mL of HPLC solvent (methanol: HPLC buffer 7:3, HPLC buffer = water:H₃PO₄ 300:1)). After 24 h ethanol was evaporated under reduced pressure and the

product was extracted in MTBE (3x 30 mL). The organic phases were combined, washed with brine and MTBE was removed under reduced pressure. The crude product (yellow oil) was purified by column flash chromatography on silica gel using hexane/ethyl acetate 3:1 (v/v). Isolated yield: 35 %

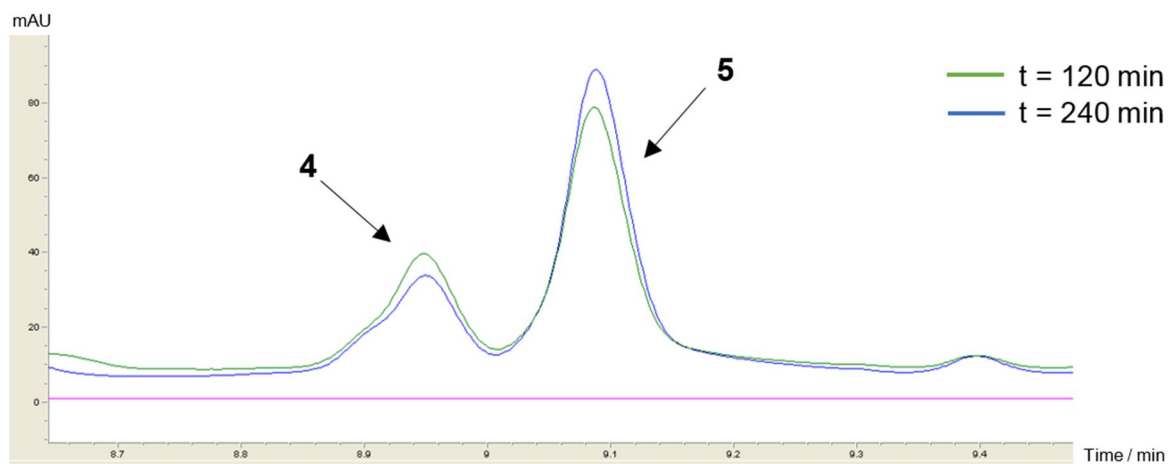


Figure D-7. Isomerization of products in Heck reaction in batch over time. Comparison of HPLC peaks of product **5** and side-product **4** at two different time points during Heck coupling in batch, $t = 120$ min (green) and $t = 240$ min (blue)

One-pot experiment. For the one-pot reaction the enzymatic decarboxylation was conducted as described previously but with increased catalyst loading (80 mg). After 180 min the alginate beads with PAD was removed from the reaction mixture by filtration. 10 mL of solvent (5 mL ethanol and 5 mL water) were added containing the substrates iodobenzene (1.05 mmol, 1.5 mol-eq. with respect to *para*-coumaric acid, 214.2 mg) and K_2CO_3 (1.05 mmol, 1.5 mol-eq., 145.1 mg). After heating the solution to 85 °C the catalyst (25.2 mg) were added to start the reaction. Samples were taken over time and analyzed by means of HPLC.

Decarboxylation flow experiment. 160 mg of CFE PAD was immobilized as described previously in 4 mL final bead volume in 2 % (w/v) alginate beads. The immobilized biocatalyst was packed in a stainless steel column (120 mm x 8 mm ID). The remaining free volume of the column was filled with glass beads. The used capillaries, fittings and syringe adapters were standard HPLC equipment (1/16 inch OD. x 0.03 inch ID, PEEK). The column was heated to 30 °C in a water bath and flushed with solvent (DES:buffer 1:1 (v/v)) at a flow rate of 45.5 μ L/min from a syringe pump (Lambda VIT-FIT, Syringe pump equipped with 20 mL stainless steel syringe, Lambda Instruments). After 1 of flushing the reaction was started by switched to the feed stock containing 20 mM *para*-coumaric acid **1**. Samples were collected at the outlet in 15 min intervals. From the product stream 50 μ L were diluted with 500 μ L of HPLC solvent (methanol:HPLC buffer 7:3, HPLC buffer = water:H₃PO₄ 300:1). To test enzyme leaching, samples were collected at the outlet of the reactor at $t = 40, 80, 120, 190$ and 250 min.

Additional substrate was added and the samples were kept at ambient conditions overnight. The next day 50 μL of the sample were diluted and analyzed as usual. No further product formation was observed.

Heck flow experiment. The prepared catalyst powder was packed in a stainless steel column (40 mm x 8 mm ID) (2 g). The used capillaries, fittings and syringe adapters were standard HPLC equipment (1/16 inch OD. x 0.03 inch ID, PEEK). The packed-bed reactor was heated to 85 $^{\circ}\text{C}$ in a water bath and flushed with solvent (DES:buffer:ethanol:water 1:1:1:1 (v/v/v/v)) at a flow rate of 45.5 $\mu\text{L}/\text{min}$ from a syringe pump (Lambda VIT-FIT, Syringe pump equipped with 20 mL stainless steel syringe, Lambda Instruments). After 1 of flushing the reaction was started by switched to the feed stock containing 10 mM 4-vinylphenol, 15 mM iodobenzene and 15 mM K_2CO_3 . Samples were collected at the outlet in 15 min intervals. From the product stream 50 μL were diluted with 500 μL of HPLC solvent (methanol:HPLC buffer 7:3, HPLC buffer = water:H₃PO₄ 300:1)).

Two-step flow experiment. Two stock solutions were prepared. Stock A served as feed for the enzymatic decarboxylation consisting of DES:potassium phosphate buffer (50 mM, pH 6.0) in a ratio of 1:1 (v/v) and **1** (20 mM.) Stock B was the feed for the Heck coupling and was mixed with the outlet of the decarboxylation before entering the Pd-packed column. Stock B contained 30 mM (1.5 mol-eq. with respect to **1**) **3** and 30 mM (1.5 mol-eq.) K_2CO_3 dissolved in DES:ethanol:water in a ratio of 1:6.75:2.25. The used capillaries, fittings and syringe adapters were standard HPLC equipment (1/16 inch OD. x 0.03 inch ID, PEEK). A T-mixing element (Advantage™ Stainless Steel Tee, 0.25 mm Thru-hole for 1/16 inch OD tubing) was used to mix the product stream of the first reactor with the substrate feed for the second reactor.

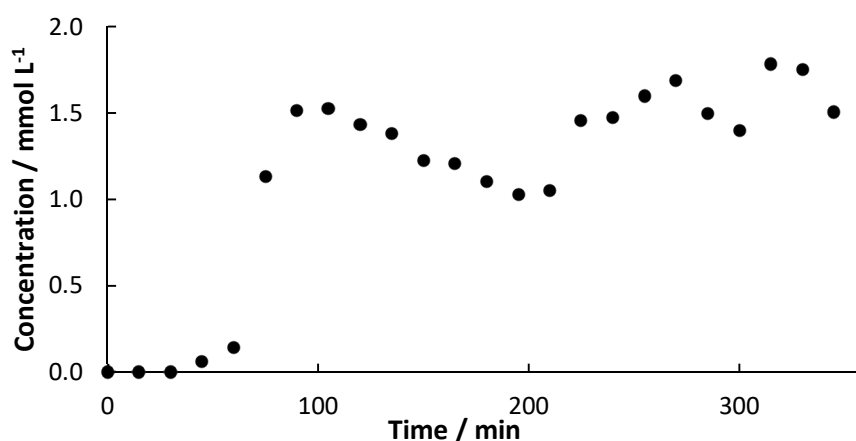


Figure D-8. Concentration of 4-hydroxystilbene from 4-vinylphenol (10 mM) in a continuous flow Heck cross coupling with iodobenzene (1.5 mol-eq.) in the presents of K_2CO_3 (1.5 mol-eq.) using $\text{Sn}_{0.79}\text{Ce}_{0.20}\text{Pd}_{0.01}\text{O}_{2.5}$ as heterogeneous catalyst. 85 $^{\circ}\text{C}$, solvent: DES:buffer:ethanol:water 1:1:1:1 (v/v/v/v), flow rate: 91 $\mu\text{L min}^{-1}$

The packed columns were heated in water baths of 30 °C for the decarboxylation (160 mg PAD immobilized in alginate bead of a total volume of 4 mL in two stainless steel columns in a series (each 40 mm x 8 mm ID) were flushed with solvent with 45.5 $\mu\text{L}/\text{min}$ overnight to remove loosely bound enzyme and non-linked alginate) and 85 °C for the Heck reaction (6 g of catalyst powder in a stainless steel column 120 mm x 8 mm ID). After flushing the system with solvent for 1 h, the feed was switched to the stock solutions (Lambda VIT-FIT, Syringe pump equipped with 20 mL stainless steel syringe, Lambda Instruments, flow rate: 45.5 $\mu\text{L}/\text{min}$, respectively). The pressure in the system was kept at 5 bar (IDEX BPR Cartridge 75 psi Gold Coat). Samples were collected at the outlet in 15 min intervals. From the product stream 50 μL were diluted with 500 μL of HPLC solvent (methanol: HPLC buffer 7:3, HPLC buffer = water:H₃PO₄ 300:1).

HPLC Analysis. Samples were collected and analysed in singlets (no error bars shown). However, repetition of the experiments led to similar outcomes and hence proved reproducibility of the results. The samples were analyzed by reversed phase high performance liquid chromatography (RP-HPLC) using an Agilent Instrument 1100 Series equipped with a ThermoFischer Scientific Accucore™ C18 reversed phase column (50 x 4.6 mm ID; 2.6 μm). 2.0 μL of the sample was injected. Eluent: 0-1 min 60 % H₂O:H₃PO₄ 300:1, 40 % methanol; 1-12 min gradient to 10 % H₂O:H₃PO₄ 300:1, 90 % methanol; 12-14 min gradient to 60 % H₂O:H₃PO₄ 300:1, 40 % methanol. Sample analysis lasted 16 min. Flow rate: 1 mL/min. Column temperature: 25 °C. For detection of the analyts, a UV detector was used. Retention times: *para*-coumaric acid **1** 1.1 min (282.4 nm), 4-vinylphenol **3** 3.4 min (237.4 nm), iodobenzene **2** 8.7 min (237.4 nm), *para*-hydroxy-1,1-diphenylethylene **4** 8.9 min (237.4 nm), 4-hydroxystilbene **5** 9.1 min (282.4 nm).

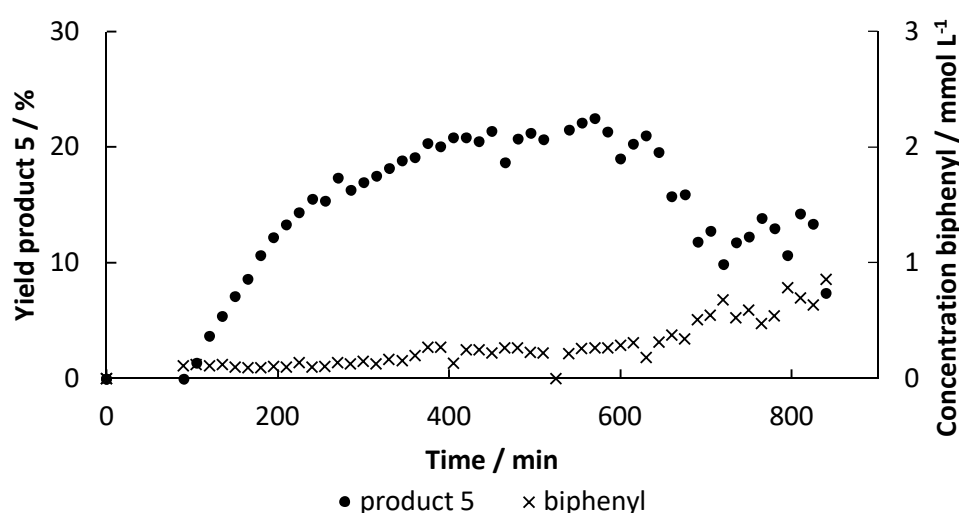


Figure D-9. Yield⁵⁴ of **5** and concentration of the side-product biphenyl due to homo-coupling to **2** over time for the first attempt of continuous synthesis of **3** by enzymatic decarboxylation by BsPAD and

subsequent Pd-catalyzed Heck reaction using $\text{Sn}_{0.79}\text{Ce}_{0.20}\text{Pd}_{0.01}\text{O}_{2.5}$ to couple **3** and **2**, yield determined by HPLC.

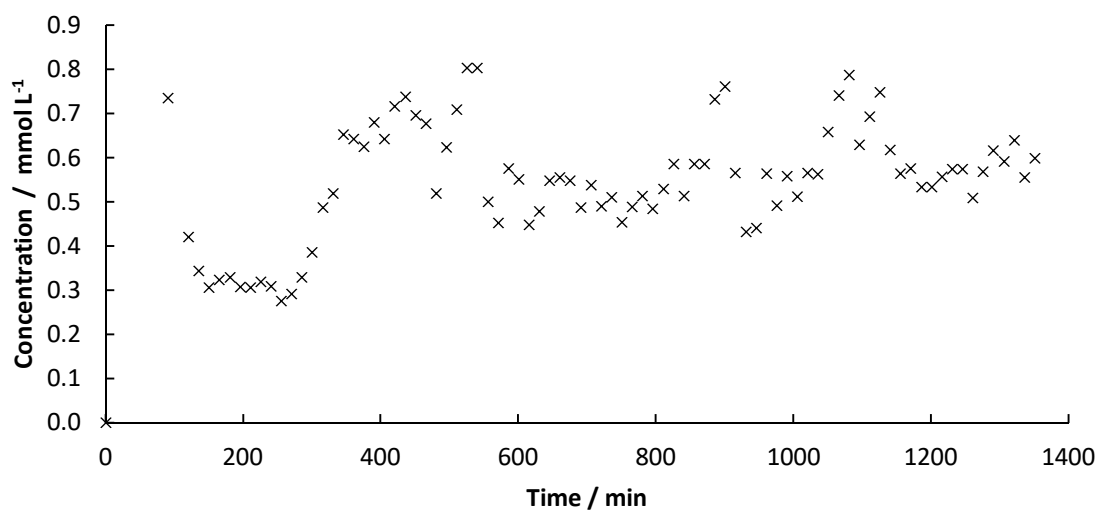


Figure D-10. Concentration of side-product biphenyl due to homo-coupling of **2** over time for the flow process for continuous synthesis of **3** by enzymatic decarboxylation by BsPAD and subsequent Pd-catalyzed Heck reaction to couple **3** and **2**, concentration determined by HPLC.

NMR. NMR-measurements were recorded using a Bruker Avance III 300 MHz spectrometer in CDCl_3 . $^1\text{H-NMR}$ of product **5** and side-product **4** are shown in Figure D-11 and D-12.

para-Hydroxystilbene (5)⁵⁶: $^1\text{H-NMR}$: 7.50 – 7.48 (d, 2H, Ar-H), 7.43 - 7.40 (d, 2H, Ar-H), 7.37 - 7.32 (t, 2H, Ar-H), 7.26 - 7.22 (t, 1H, Ar-H), 7.09 - 6.94 (dd, 2H, H-C=C-H), 6.85 – 6.82 (d, 2H, Ar-H), 4.77 (s, 1H, O-H) ppm.

para-Hydroxy-1,1-diphenylethylene (4): $^1\text{H-NMR}$: 7.31 – 7.28 (m, 5H, Ar-H), 7.25 - 7.20 (d, 2H, Ar-H), 6.81 - 6.78 (d, 2H, Ar-H), 5.39 (s, 1H, C=C-H), 5.35 (s, 1H, C=C-H), 4.74 (s, 1H, O-H) ppm.

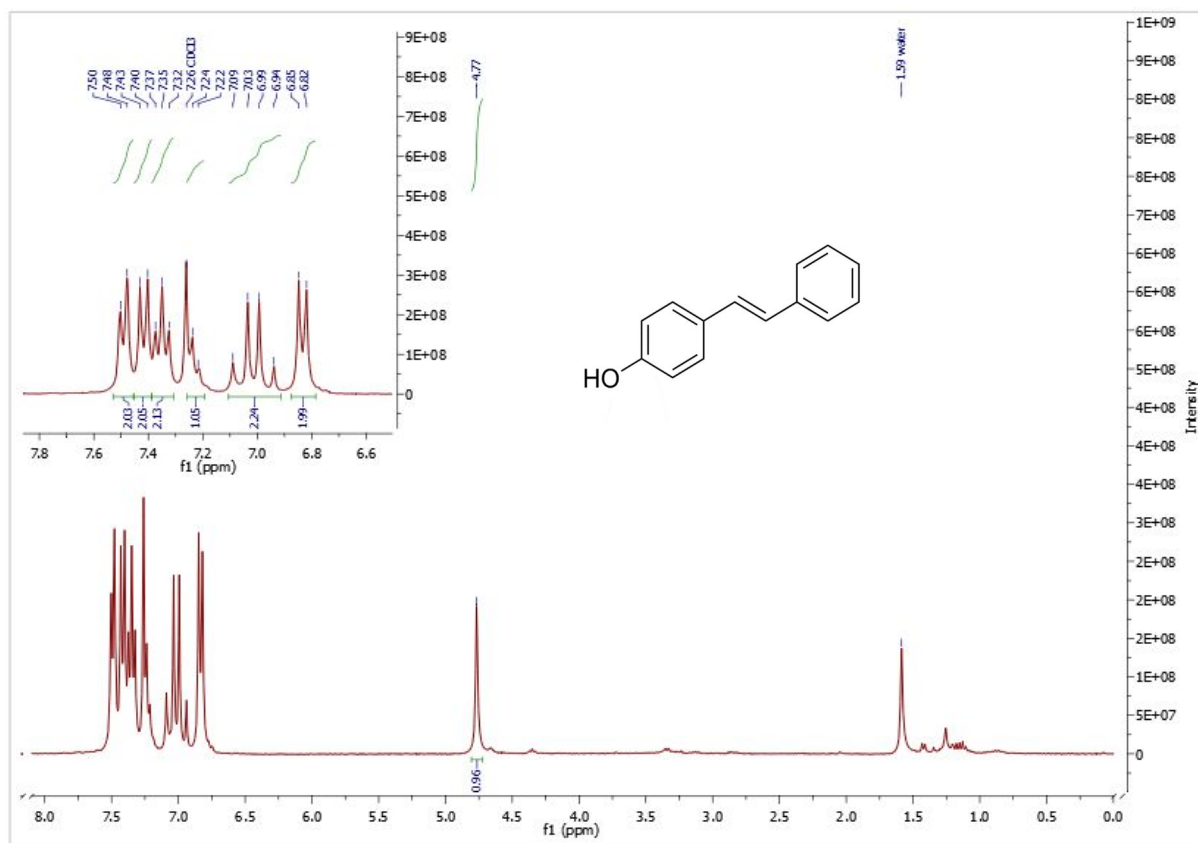


Figure D-11. $^1\text{H-NMR}$ of product **5**

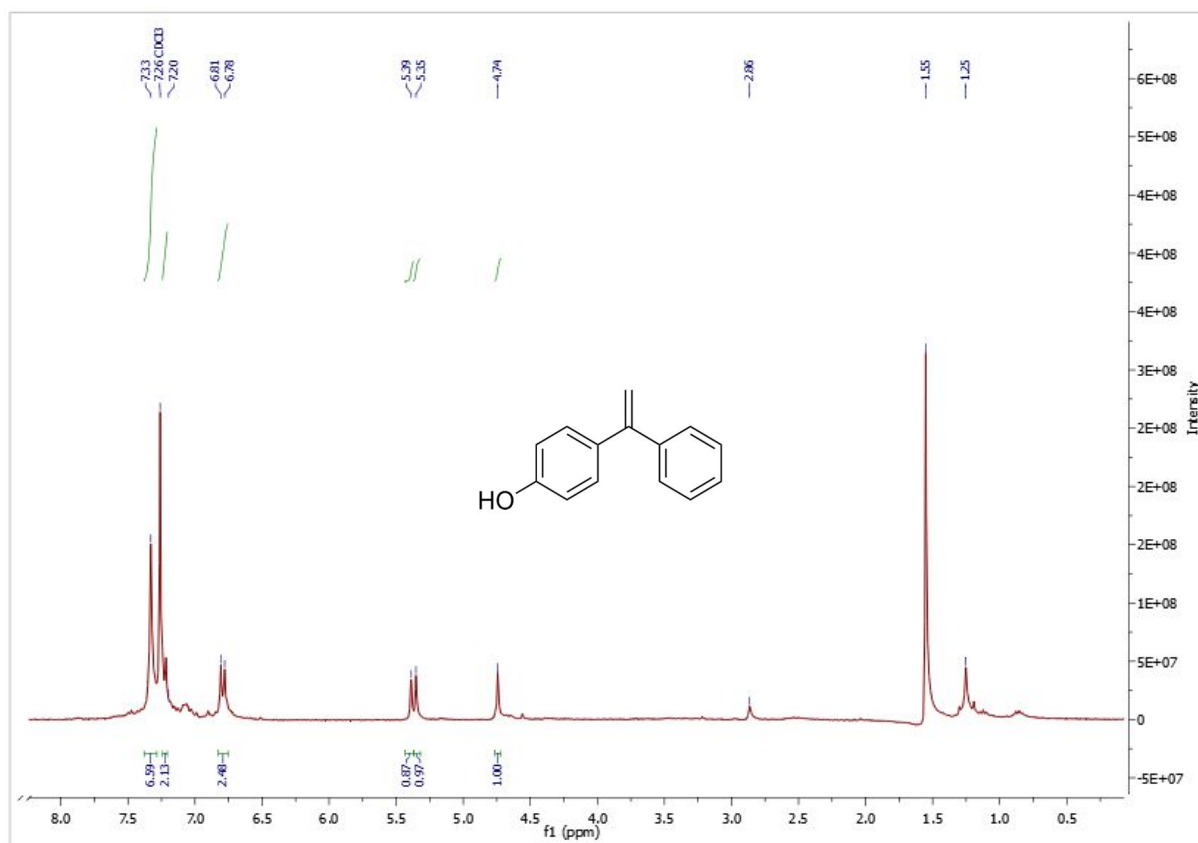


Figure D-12. $^1\text{H-NMR}$ of side-product

5 References

1. E. Liardo, N. Ríos-Lombardía, F. Morís, F. Rebolledo and J. González-Sabín, *ACS Catal.*, 2017, **7**(7), 4768.
2. N. Ríos-Lombardía, J. García-Álvarez and J. González-Sabín, *Catalysts*, 2018, **8**(2), 75.
3. F. Rudroff, M. D. Mihovilovic, H. Gröger, R. Snajdrova, H. Iding and U. T. Bomscheuer, *Nat. Catal.*, 2018, **1**(1), 12.
4. S. Schmidt, K. Castiglione and R. Kourist, *Chem. Eur. J.*, 2018, **24**(8), 1755.
5. J. Enoki, C. Mügge, D. Tischler, K. Miyamoto and R. Kourist, *Chemistry*, 2019, **25**(19), 5071.
6. T. Himiyama, M. Waki, Y. Maegawa and S. Inagaki, *Angew. Chem. Int. Ed.*, 2019, **58**(27), 9150.
7. H. Gröger and W. Hummel, *Curr. Opin. Chem. Biol.*, 2014, **19**, 171.
8. J. M. Sperl, J. M. Carsten, J.-K. Guterl, P. Lommès and V. Sieber, *ACS Catal.*, 2016, **6**(10), 6329.
9. J. Paris, N. Ríos - Lombardía, F. Morís, H. Gröger and J. González - Sabín, *ChemCatChem*, 2018, **10**(19), 4417.
10. L. Cicco, N. Ríos-Lombardía, M. J. Rodríguez-Álvarez, F. Morís, F. M. Perna, V. Capriati, J. García-Álvarez and J. González-Sabín, *Green Chem.*, 2018, **20**(15), 3468.
11. V. Gotor-Fernández and C. E. Paul, *J. Biotechnol.*, 2019, **293**, 24.
12. N. Guajardo, C. R. Müller, R. Schrebler, C. Carlesi and P. Domínguez de María, *ChemCatChem*, 2016, **8**(6), 1020.
13. Z. Maugeri and P. Domínguez de María, *ChemCatChem*, 2014, **6**(6), 1535.
14. E. L. Smith, A. P. Abbott and K. S. Ryder, *Chem. Rev.*, 2014, **114**(21), 11060.
15. E. E. L. Tanner, K. M. Piston, H. Ma, K. N. Ibsen, S. Nangia and S. Mitragotri, *ACS Biomater. Sci. Eng.*, 2019, **5**(7), 3645.
16. C. Ma, A. Laaksonen, C. Liu, X. Lu and X. Ji, *Chem. Soc. Rev.*, 2018, **47**(23), 8685.
17. M. Kuddushi, G. S. Nangala, S. Rajput, S. P. Ijardar and N. I. Malek, *J. Mol. Liq.*, 2019, **278**, 607.
18. F. Gabriele, M. Chiarini, R. Germani, M. Tiecco and N. Spreti, *J. Mol. Liq.*, 2019, **291**, 111301.
19. O. S. Hammond, D. T. Bowron and K. J. Edler, *Angew. Chem. Int. Ed.*, 2017, **56**(33), 9782.
20. P. Xu, G.-W. Zheng, M.-H. Zong, N. Li and W.-Y. Lou, *Bioresour. Bioprocess.*, 2017, **4**(1), 34.
21. A. Paiva, A. A. Matias and A. R. C. Duarte, *Curr. Opin. Green Sustain. Chem.*, 2018, **11**, 81.
22. D. A. Alonso, A. Baeza, R. Chinchilla, G. Guillena, I. M. Pastor and D. J. Ramón, *Eur. J. Org. Chem.*, 2016, **2016**(4), 612.
23. X. Marset, A. Khoshnood, L. Sotorríos, E. Gómez-Bengoa, D. A. Alonso and D. J. Ramón, *ChemCatChem*, 2017, **9**(7), 1269.
24. Z.-L. Huang, B.-P. Wu, Q. Wen, T.-X. Yang and Z. Yang, *J. Chem. Technol. Biotechnol.*, 2014, **89**(12), 1975.

25. I. Wazeer, M. Hayyan and M. K. Hadj-Kali, *J. Chem. Technol. Biotechnol.*, 2018, **93**(4), 945.
26. I. Juneidi, M. Hayyan and M. A. Hashim, *Process Biochem.*, 2018, **66**, 33.
27. X. Liu, X.-Y. Meng, Y. Xu, T. Dong, D.-Y. Zhang, H.-X. Guan, Y. Zhuang and J. Wang, *Biochem. Eng. J.*, 2019, **142**, 41.
28. N. Guajardo, R. A. Schrebler and P. Domínguez de María, *Bioresour. Technol.*, 2019, **273**, 320.
29. N. Guajardo, P. Domínguez de María, K. Ahumada, R. A. Schrebler, R. Ramírez-Tagle, F. A. Crespo and C. Carlesi, *ChemCatChem*, 2017, **9**(8), 1393.
30. Á. Gómez Baraibar, D. Reichert, C. Mügge, S. Seger, H. Gröger and R. Kourist, *Angew. Chem. Int. Ed.*, 2016, **55**(47), 14823.
31. S. E. Payer, K. Faber and S. M. Glueck, *Adv. Synth. Catal.*, 2019, **361**(11), 2402.
32. W. Nawaz, Z. Zhou, S. Deng, X. Ma, X. Ma, C. Li and X. Shu, *Nutrients*, 2017, **9**(11), 1188.
33. H.-Y. Tsai, C.-T. Ho and Y.-K. Chen, *J. Food. Drug. Anal.*, 2017, **25**(1), 134.
34. M. Savio, D. Ferraro, C. Maccario, R. Vaccarone, L. D. Jensen, F. Corana, B. Mannucci, L. Bianchi, Y. Cao and L. A. Stivala, *Sci. Rep.*, 2016, **6**, 19973.
35. D. Webb and T. F. Jamison, *Chem. Sci.*, 2010, **1**(6), 675.
36. A. K. Schweiger, N. Ríos-Lombardía, C. K. Winkler, S. Schmidt, F. Morís, W. Kroutil, J. González-Sabín and R. Kourist, *ACS Sustainable Chem. Eng.*, 2019, **7**(19), 16364.
37. T. El Achkar, S. Fourmentin and H. Greige-Gerges, *J. Mol. Liq.*, 2019, **288**, 111028.
38. M. B. Plutschack, B. Pieber, K. Gilmore and P. H. Seeberger, *Chem. Rev.*, 2017, **117**(18), 11796.
39. T. Noël and S. L. Buchwald, *Chem. Soc. Rev.*, 2011, **40**(10), 5010.
40. B. Gutmann, D. Cantillo and C. O. Kappe, *Angew. Chem. Int. Ed.*, 2015, **54**(23), 6688.
41. R. Porta, M. Benaglia and A. Puglisi, *Org. Process Res. Dev.*, 2016, **20**(1), 2.
42. M. Baumann and I. R. Baxendale, *Beilstein J. Org. Chem.*, 2015, **11**, 1194.
43. J. Britton and C. L. Raston, *Chem. Soc. Rev.*, 2017, **46**(5), 1250.
44. P. L. Lau, R. W. K. Allen and P. Styring, *Beilstein J. Org. Chem.*, 2013, **9**, 2886.
45. G. J. Lichtenegger, M. Maier, J. G. Khinast and H. Gruber-Wöfler, *J. Flow Chem.*, 2016, **6**(3), 244.
46. N. Nikbin, M. Ladlow and S. V. Ley, *Org. Process Res. Dev.*, 2007, **11**(3), 458.
47. K. Hiebler, S. Soritz, K. Gavric, S. Birrer, M. C. Maier, B. Grabner and H. Gruber-Woelfler, *J. Flow Chem.*, 2019, **116**, 1074.
48. J. Britton, S. Majumdar and G. A. Weiss, *Chem. Soc. Rev.*, 2018, **47**(15), 5891.
49. N. Guajardo and P. Domínguez de María, *ChemCatChem*, 2019, **11**(14), 3128.
50. Y. Zhu, Q. Chen, L. Shao, Y. Jia and X. Zhang, *React. Chem. Eng.*, 2019, **36**, 73.
51. C. A. Denard, H. Huang, M. J. Bartlett, L. Lu, Y. Tan, H. Zhao and J. F. Hartwig, *Angew. Chem. Int. Ed.*, 2014, **53**(2), 465.
52. G. J. Lichtenegger and H. Gruber-Woelfler, *Chimica Oggi*, 2015, **33**(4), 12.
53. G. J. Lichtenegger, M. Maier, M. Hackl, J. G. Khinast, W. Gössler, T. Griesser, V.S.P. Kumar, H. Gruber-Woelfler and P. A. Deshpande, *J. Mol. Catal. A-Chem*, 2017, **426**, 39.

- 54 $A_{(\text{limiting})} + B \rightarrow P$; Yield $Y [\%] = (C_{P,t}/C_{A,0}) * 100$; Conversion $X [\%] = (C_{A,0} - C_{A,t}) / C_{A,0} * 100$, Yield and conversion determined by HPLC after calibration
- 55 Leaching of the inorganic catalyst was not investigated in this work, but will be topic of future investigations. Leaching data of the catalyst under similar conditions can be found in Ref. 45 and 47
- 56 J. F. Civicos, D. A. Alonso and C. Nájera, *Adv. Synth. Catal.* 2011, **353**, 1683

E. Outlook

This thesis focussed on three novel approaches for alternative processes in chemical and pharmaceutical synthesis. On the one hand, ideas outside of the box and the comfort zone of classical chemistry were given the opportunity to show their performance. On the other hand, ancient sustainable concepts, such as the alginate-luffa matrix (ALM) were tested for modern processes with the favour of making them more valued again.

In the future, further development of all the presented approaches should be considered. Especially, the very early-stage concept of ionic liquid coated enzymes (ILCE) would be interesting. Due to the huge number of potential anion-cation combinations, an almost unconceivable number of ILs can be prepared with properties tuned to meet the requirement of the enzymatic process. However, this method is not limited to the application in biocatalysis, but can also serve as immobilization technique for other catalysts. Thanks to the sponge-like structure and high porosity of the IL emerging from the lyophilisation process, the resulting heterogeneous catalyst could also be implemented in a continuous flow setup.

The concept of ALM could be an interesting method for immobilizing other enzymes than DERA (deoxyribose-5-phosphate aldolase). However, transferring the alginate matrix onto another carrier be favourable because luffa as a natural product varies in its structure from crop to crop, but also within the sponge, making it difficult to prepare the support reproducibly. One option would be the use of 3D-printed designed structures. Direct printing of the alginate harbouring the catalyst into designed structures for packed bed reactors is another possibility. For the process employing the alternative heterogeneous biocatalyst re-optimization is required. This should again be done by design of experiments (DoE), as DoE is of great value, also in a chemical laboratory, and its application in process development and optimization should be promoted.

Further investigation of the chemo-enzymatic flow process is planned in the near future. Besides testing additional substrates and enzyme immobilization methods, process understanding should be developed by investigations such as leaching tests and long-term stability tests of the (bio-)catalyst in the flow process. Chemo-enzymatic flow processes are challenging tasks, but by extending the chemical resources to less conventional ones, such as deep eutectic solvent (DES) or even ILs, some issues like solvent compatibility and substrates solubility can become less hindering.

In conclusion it should be mentioned that these concepts are just a small number of ideas in the “crazy toolbox” of biocatalysts, heterogeneous catalysis and flow applications. More researchers should be encouraged to investigate and elaborate their coffee break ideas.